

United States
Department of Interior
Geological Survey

Surface and near-surface geology, Navarin basin province:
results of the 1980-81 field seasons

Herman A. Karl and Paul R. Carlson

Open-File Report 84-89

This report is preliminary and has not
been reviewed for conformity with U.S.
Geological Survey editorial standards.

Any use of trade names is for descriptive
purposes only and does not constitute
endorsement by U.S. Geological Survey.

Menlo Park, California

1984

Table of Contents

Chapter

Introduction

1. Reports pertaining to Navarin Basin province published as of January 1983
2. Geologic hazards
3. Textural variations of surficial bottom sediment
4. Rates of sediment accumulation
5. Pre-Quaternary rocks and semi-consolidated sediment from the Navarin continental margin
6. Isopach map of seismic Unit A, youngest sedimentary sequence in Navarin Basin
7. Summary of geotechnical characteristics
8. Hydrocarbon gases in sediments - results from 1981 field season
9. Benthic foraminifers
10. Diatom analysis of surface samples recovered from Pervenets Canyon
11. Aspartic acid geochronology of molluscs

INTRODUCTION

Navarin Basin province is located on the outer continental shelf and upper slope in the northwestern Bering Sea (Fig. 1). This promising petroleum region is bounded on the northwest by the U.S.-U.S.S.R. Convention Line of 1867, on the southwest by the base of the continental slope and extends to within 100 km of St. Matthew Island to the northeast and St. Paul Island to the southeast. Navarin Basin (Marlow and others, 1976) consists of a thick (>12 km) section of Mesozoic and Cenozoic sedimentary material on the northwestern portion of the Bering continental shelf (Fig. 1).

The Navarin basin province includes a very wide, flat (0.02°) continental shelf, a rugged moderately steep (3°-8°) slope between 150 and 3000 m of water depth that is deeply cut by five large submarine canyons, and a broad gently sloping (1°) rise that consists of coalescing deep-sea fans. A detailed bathymetric map of the study area is included in Figure 2; a report by Fischer and others (1982) provides a large format copy of this map and discusses in some detail the morphology of the Navarin continental margin.

The principal sources of data for this study have been the seismic reflection profiles and sediment samples collected on the 1980 and 1981 R/V DISCOVERER cruises (Carlson and Karl, 1981, 1982; Karl and Carlson, 1982). Some additional data were collected in 1980 from the USCG POLAR STAR and in 1980 and 1982 from the R/V S.P. LEE. We are also incorporating into our data base seismic reflection records that were collected over the past fifteen years by the U.S.G.S. for resource evaluation (Marlow and others, 1981). Other sources of data include studies by the University of Washington and Alaska, Russian, and Japanese scientists (e.g., Knebel, 1972; Sharma, 1979; Lisitsyn, 1966; Takenouti and Ohtani, 1974).

State of the art high-resolution geophysical equipment (air gun, minisparker, 3.5 kHz), and bottom samplers (gravity corer, grab, dredge, and near-bottom suspended sediment samplers) were used to collect data on the two cruises. Navigation system used included Satellite and Loran C. Spacing between tracklines was approximately 30 km, with more closely spaced lines in selected areas. Geologic samples (principally gravity cores) were collected at the intersections of tracklines and at selected locations. The geophysical systems used on the Navarin Basin cruises were as follows:

<u>System</u>	<u>Resolution</u>
1. Air gun (up to 80 in ³)	5 - 10 m
2. Minisparker (800 J)	1 - 3 m
3. 3.5 kHz	1 m

We acknowledge the assistance provided by the officers and crew of the NOAA ship DISCOVERER during the two cruises which comprise the principal source of data for this report. During DISCOVERER cruises DC 4/5-80-BS/NB (July 2 - August 17, 1980) the scientific party collected 6700 line km of seismic reflection profiles, 104 gravity cores, 10 grab samples, and 1 dredge sample (Fig. 3, 5); 8050 line km of seismic reflection profiles, 88 gravity cores, 10 grab samples, 6 box cores and 5 vibracores were collected during DISCOVERER cruise DC 2/3-81-BS/NB (Fig. 4, 5). NOAA officers and survey

technicians provided navigational control using LORAN C and satellite fixes. We acknowledge also the assistance of the officers and crew of the USCG POLAR STAR and USGS S.P. LEE and the scientific personnel on these supplemental cruises.

This report supplements and updates Open-File Report 81-1217 (Carlson and Karl, 1981), and the reader is referred to that report for additional information.

REFERENCES

- Carlson, P. R. and Karl, H. A., 1981, High-resolution seismic reflection profiles: Navarin Basin province, northern Bering Sea, 1980: U.S. Geological Survey Open-File Report 82-1221, 4 p., 1 map, scale 1:1,000,000.
- Carlson, P. R. and Karl, H. A., (eds.), 1981, Seafloor geologic hazards, sedimentology, and bathymetry: Navarin basin province, northwestern Bering Sea: U.S. Geol. Survey Open-File Report 81-1217, 149.
- Carlson, P. R. and Karl, H. A., 1982, High-resolution seismic reflection profiles: Navarin Basin province, northern Bering Sea, 1981: U.S. Geological Survey Open-File Report 82-786, 5 p., 1 map, scale 1:1,000,000.
- Fischer, J. M., Carlson, P. R., and Karl, H. A., 1982, Bathymetric map of Navarin basin province, northern Bering Sea: U.S. Geological Survey Open-File Report 82-1038, 11 p., 1 map, scale 1:1,000,000.
- Karl, H. A. and Carlson, P. R., 1982, Location and description of sediment samples: Navarin Basin province, Bering Sea, 1980-81: U.S. Geological Survey Open-File Report 82-958, 5 p., 2 maps, scale 1:1,000,000.
- Knebel, H. J., 1972, Holocene sedimentary framework of the east-central Bering Sea continental shelf: Ph.D. thesis, Univ. Washington, Seattle, 186 p.
- Marlow, M. S., Scholl, D. W., Cooper, A. K., and Buffington, E. C., 1976, Structure and evolution of Bering Sea shelf south of St. Lawrence Island: American Association of Petroleum Geologists Bulletin, v. 60, p. 161-163.
- Marlow, M. S., Carlson, P. R., Cooper, A. K., Karl, H. A., McLean, H., McMullin, R., and Lynch, M. B., 1981, Resource report for proposed OCS sale 83 Navarin Basin, Alaska: U.S. Geological Survey Open-File Report 81-252, 83 p.
- Lisitsyn, A. P., 1966, Protessy Sovremennogo Osodko' obrazovaniya v Beringovom More: Akad. Nauk SSR Inst. Okeal., Moskva, 574 p. (Recent sedimentation in the Bering Sea: Israel Program for Sci. Translations, 1969, Jerusalem; U.S. Dept. of Commerce, Clearinghouse for Federal Sci. Tech. Info., Springfield, VA, 614 p.).
- Sharma, G. D., Naidu, A. S., and Hood, D. W., 1972, Bristol Bay: model contemporary graded shelf: Am. Assoc. Petroleum Geologists, v. 56, p. 2000-2012.
- Takenouti, A. Y. and Ohtani, K., 1974, Currents and water masses in the Bering Sea: a review of Japanese work: in Hood, D. W. and Kelley, E. J., eds., Oceanography of the Bering Sea, Univ. Alaska, Inst. Marine Science, Occas. Publ. 2, p. 39-57.

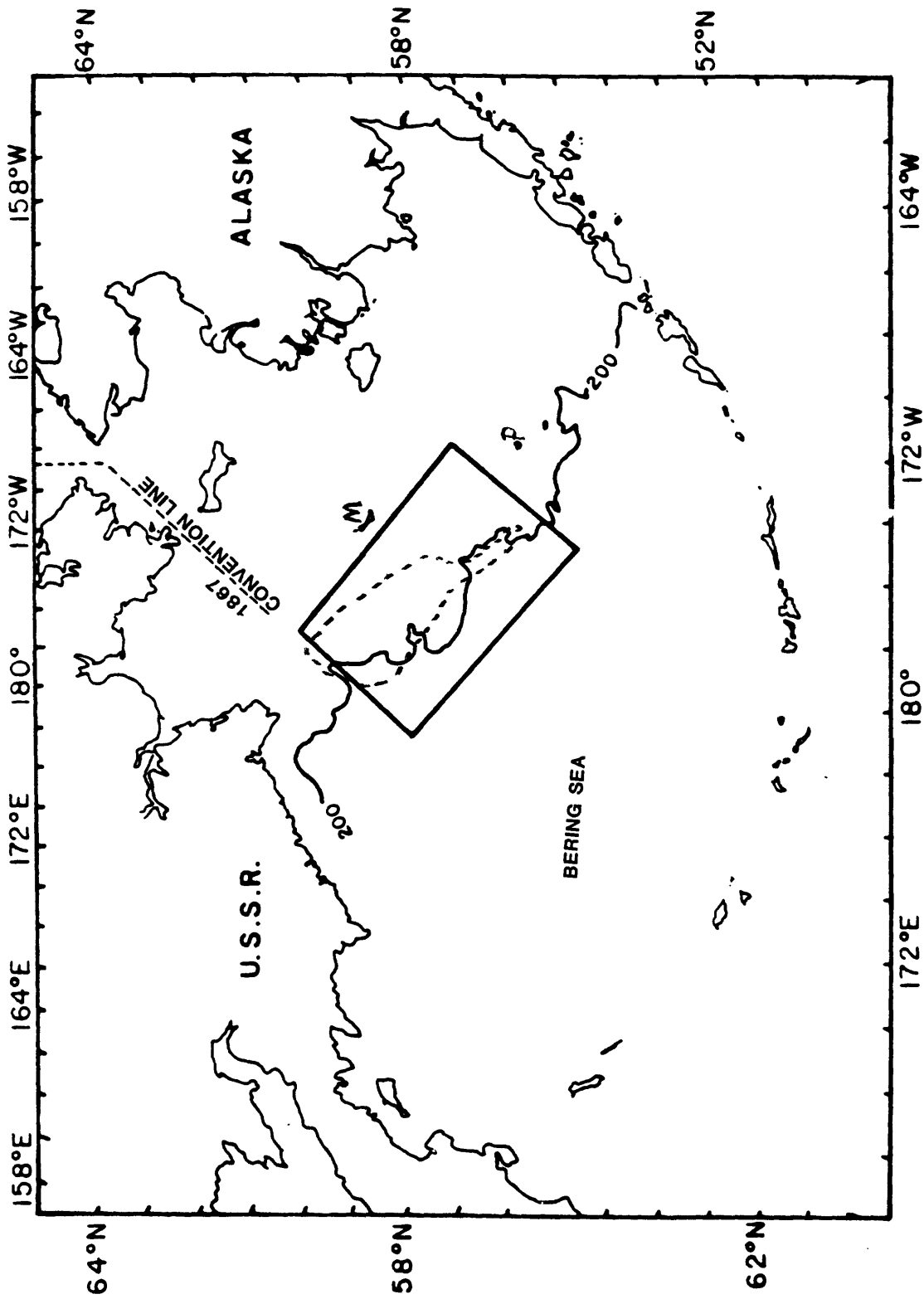


Figure 1. Location map of Navarin Basin province. Dotted line indicates >2 km sediment thickness delineating Navarin basin (from Marlow et al., 1981). 200 m bathymetric contour from Fischer et al. (1982). (M = St. Matthew Island; P = St. Paul Island).

DEPARTMENT OF THE INTERIOR
UNITED STATES GEOLOGICAL SURVEY

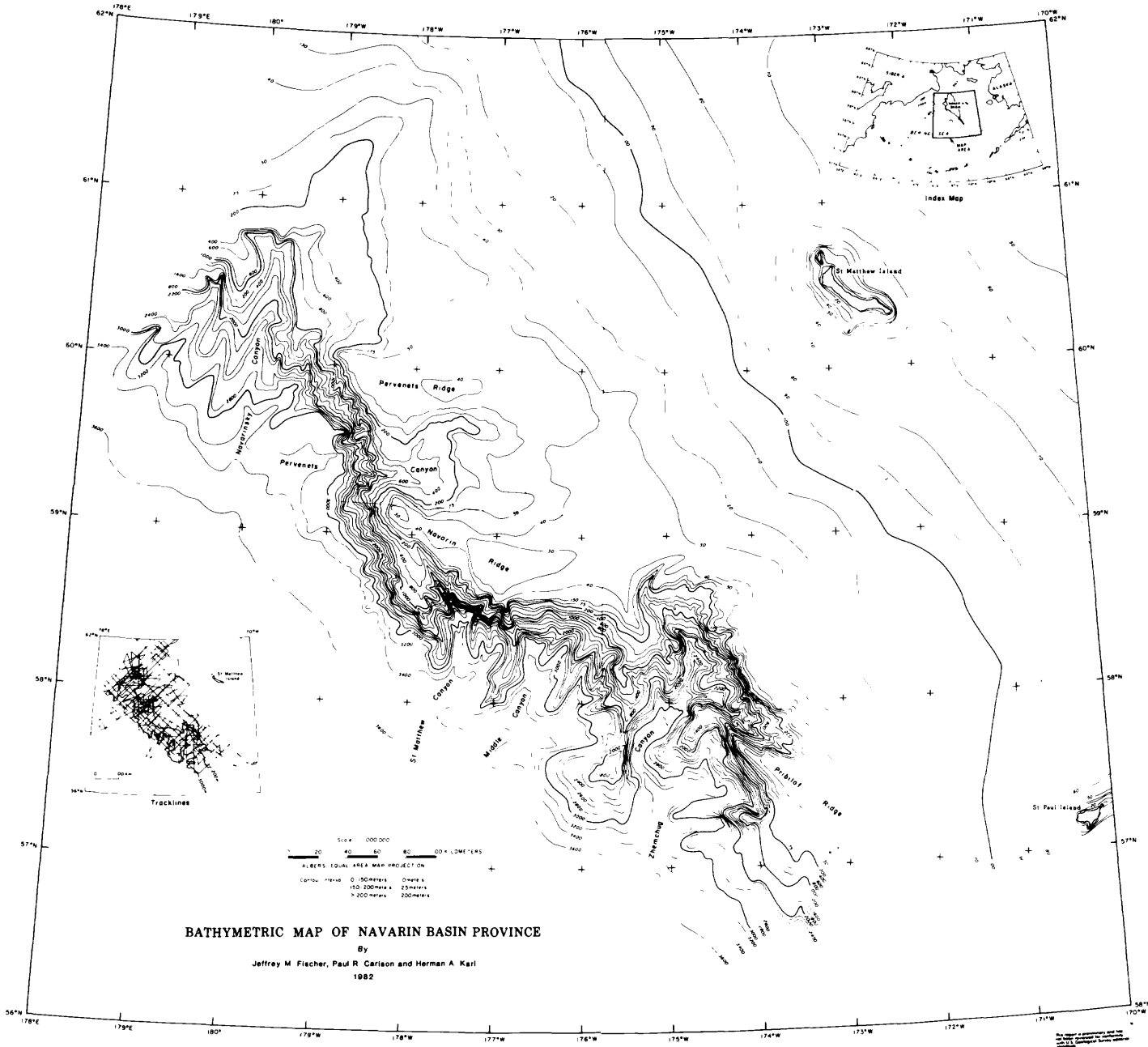


Figure 2. Bathymetric map of Navarin Basin province. Large scale map is available as Open-File Report 82-1038 (Fischer and others, 1982).

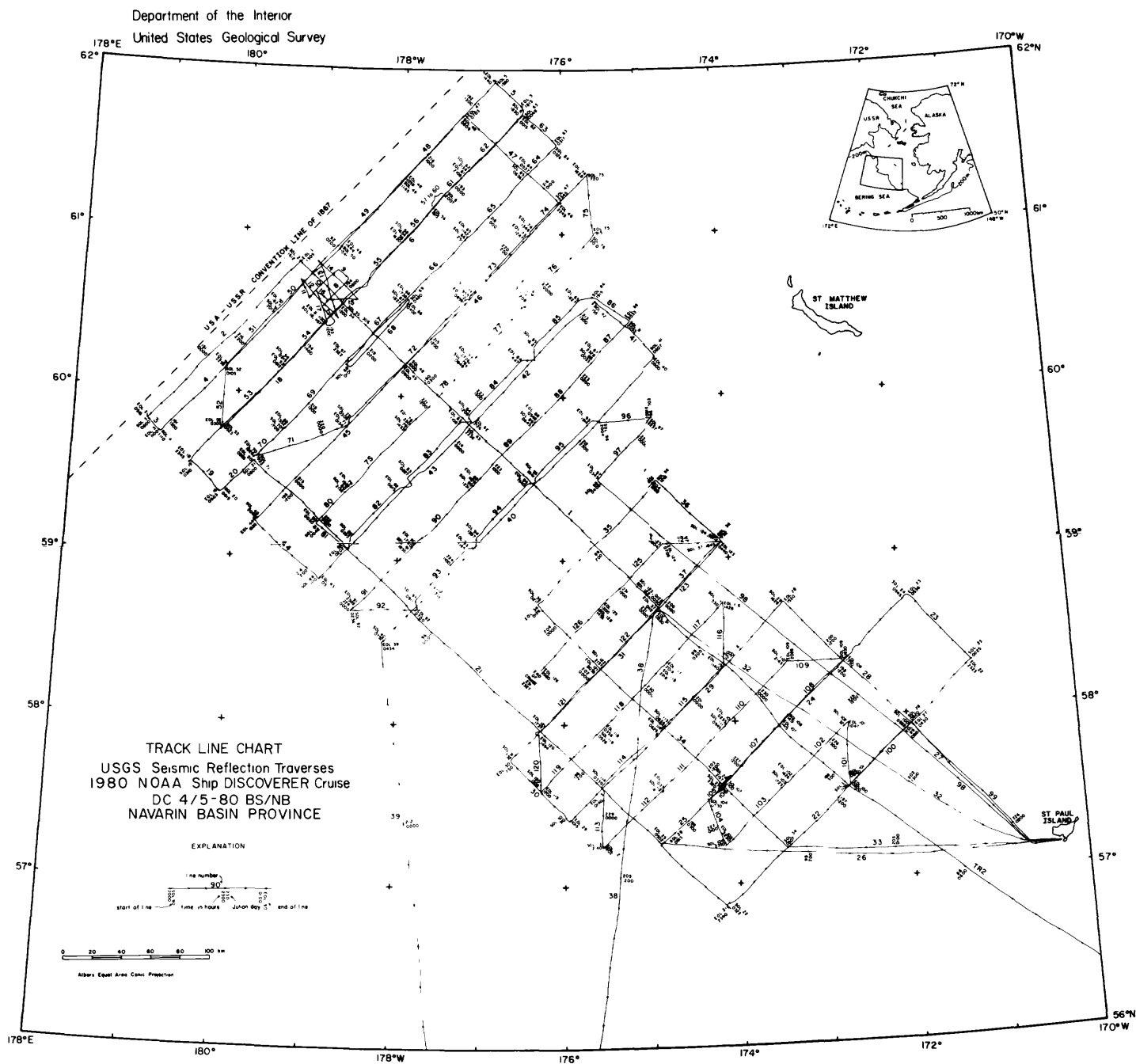


Figure 3. Track lines of high-resolution seismic reflection profiles collected during cruise DC4/5-80-BS/NB, summer 1980. Large scale map is available as Open-File Report 81-1221 (Carlson and Karl, 1981).

United States Geological Survey
Department of the Interior

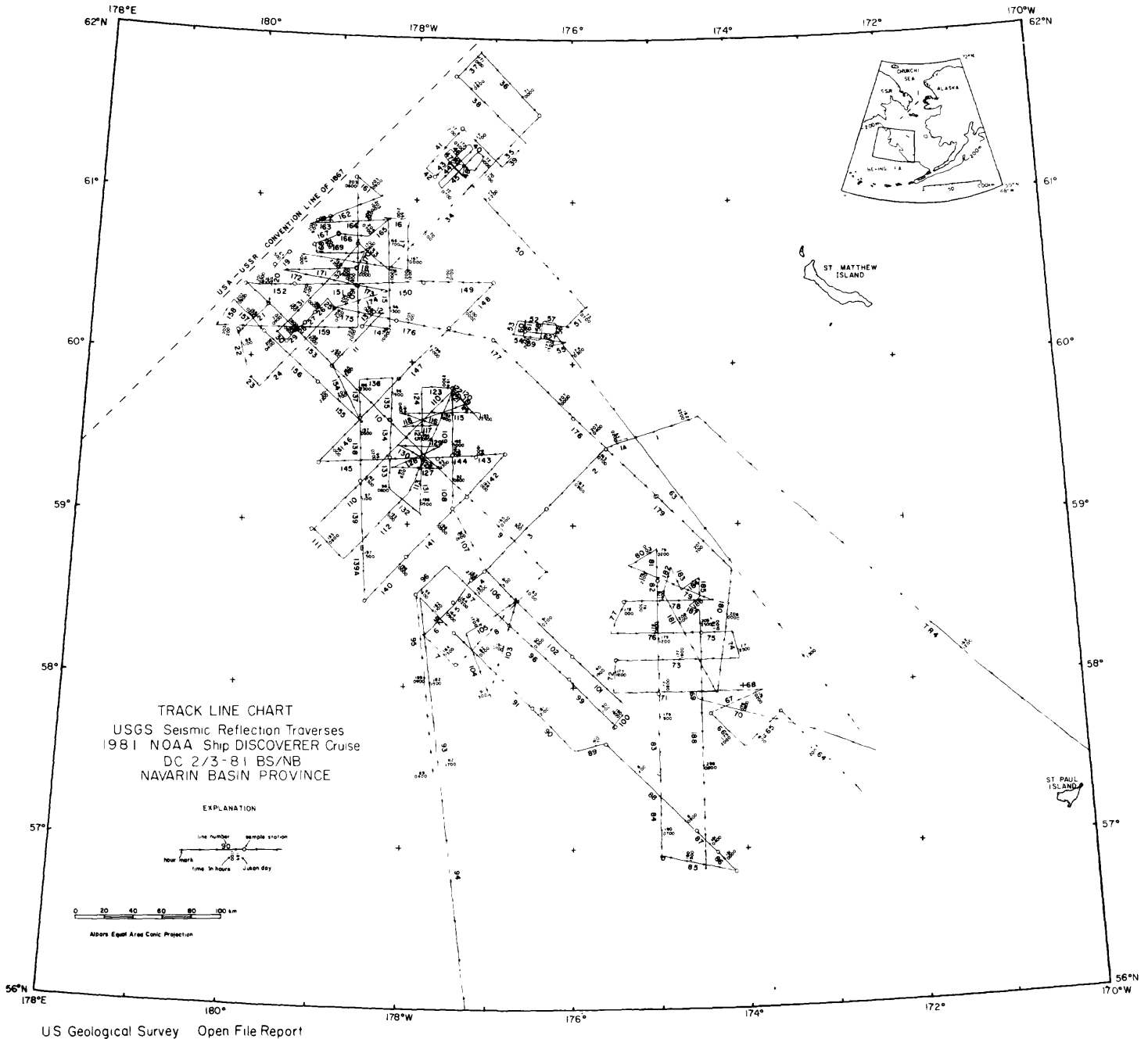


Figure 4. Track lines of high-resolution seismic reflection profiles collected during cruise DC2/3-81-BS/NB, summer 1981. Large scale map is available as Open-File Report 82-786 (Carlson and Karl, 1982).

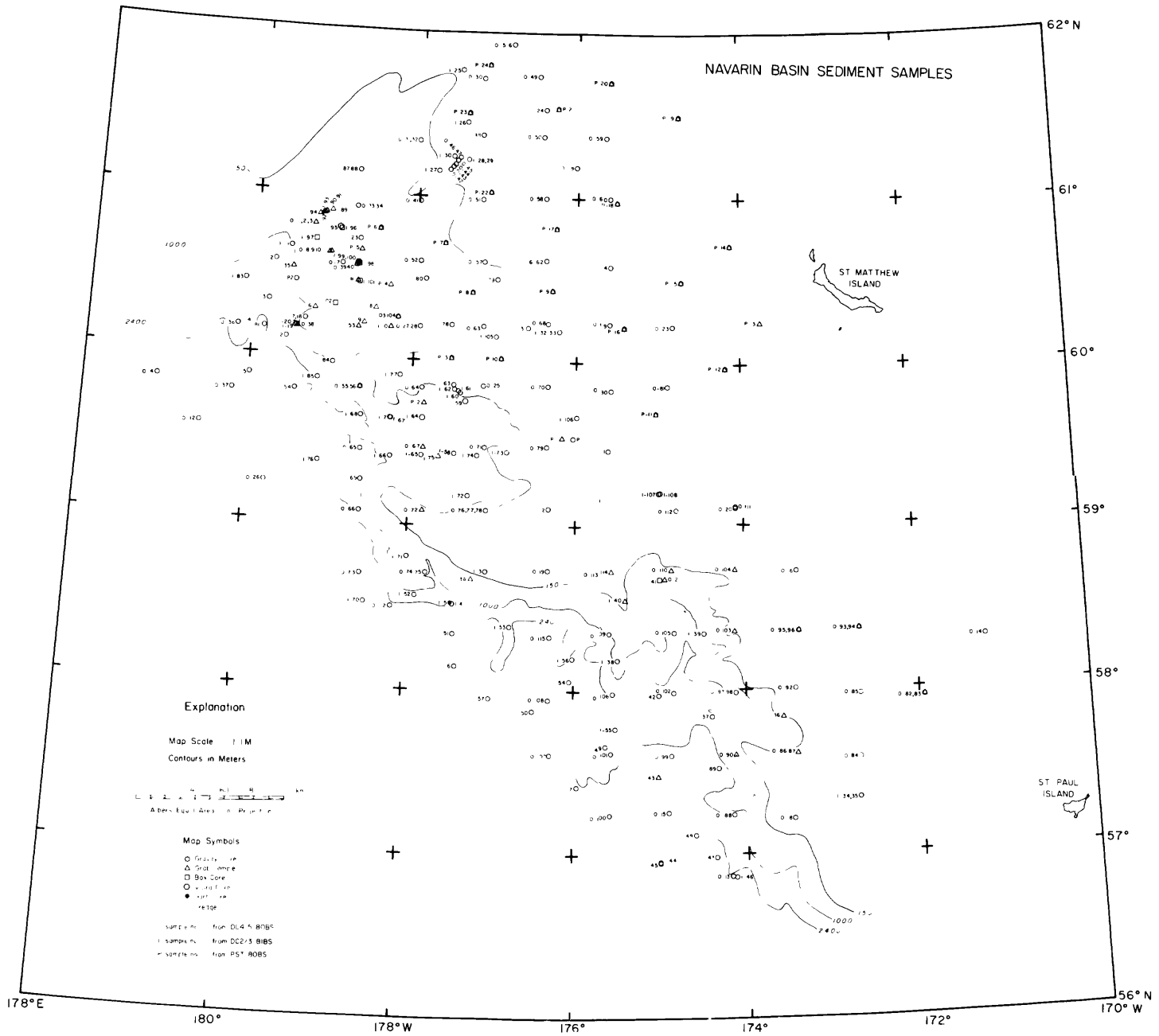


Figure 5. Locations of sediment samples. Large scale map is available as Open-File Report 82-958 (Karl and Carlson, 1982).

CHAPTER 1: REPORTS PERTAINING TO NAVARIN BASIN PROVINCE
PUBLISHED AS OF JANUARY 1983

- Baldauf, J. G., 1982, Identification of the Holocene-Pleistocene boundary in the Bering Sea by diatoms: *Boreas*, v. 11, p. 113-118.
- Carlson, P. R. and Karl, H. A., 1981, Geologic hazards in Navarin Basin province, northwestern Bering Sea: U.S. Geological Survey Open-File Report 81-1217, 149 p.
- Carlson, P. R., and Karl, H. A., 1981, High-resolution seismic reflection profiles: Navarin Basin province, northern Bering Sea, 1980: U.S. Geological Survey Open-File Report 81-1221, 4 p., 1 map, scale 1:1,000,000.
- Carlson, P. R., and Karl, H. A., 1982, High-resolution seismic reflection profiles: Navarin Basin province, northern Bering Sea, 1981: U.S. Geological Survey Open-File Report 82-786, 5 p., 1 map, scale 1:1,000,000.
- Carlson, P. R., Fischer, J. M., and Karl, H. A., 1983, Two newly discovered submarine canyons on Alaskan continental margin of Bering Sea: U.S. Geological Survey Open-File Report 83-24, 36 p., 1 map, scale 1:250,000.
- Carlson, P. R., Karl, H. A., Fischer, J. M., and Edwards, B. D., 1982, Geologic hazards in Navarin Basin province, northern Bering Sea: 14th Offshore Technology Conference, Houston, Tex., Proceedings, v. 1, p. 73-87.
- Carlson, P. R., Karl, H. A., Johnson, K. A., and Fischer, J. M., 1981, Morphology, sedimentology, and genesis of three large submarine canyons adjacent to Navarin Basin, Bering Sea: *American Assoc. Petroleum Geol. Bull.*, v. 65, p. 909.
- Carlson, P. R., Karl, H. A., Johnson, K. A., and Fischer, J. M., 1982, Submarine canyons flanking Navarin Basin, Bering Sea: U.S. Geological Survey Circular (Accomplishments in Alaska), 844, p. 139-141.
- Carlson, P. R., Karl, H. A., and Quinterno, Paula, 1982, Sedimentologic processes in world's largest submarine canyons, Bering Sea, Alaska: *Geol. Soc. of America, Abstracts with Programs*, v. 14, no. 7, p. 459-460.
- Fischer, J. M., Carlson, P. R., and Karl, H. A., 1982, Bathymetric map of Navarin Basin province, northern Bering Sea: U.S. Geological Survey Open-File Report 82-1038, 11 p., 1 map, scale 1:1,000,000.
- Karl, H. A., Cacchione, D. A., and Carlson, P. R., 1982, Large sand waves in canyon heads, Bering Sea: products of internal waves or density currents: 11th International Sedimentologic Congress, Hamilton, Ontario, Canada, p. 73.

- Karl, H. A., and Carlson, P. R., 1981, Large sediment waves at the shelf edge, northern Bering Sea: Geological Society of America, Abstracts with Programs, v. 13, p. 483.
- Karl, H. A., and Carlson, P. R., 1982, Location and description of sediment samples: Navarin Basin province, Bering Sea, 1980-81: U.S. Geological Survey Open-File Report 82-958, 5 p., 2 maps, scale 1:1,000,000.
- Karl, H. A., and Carlson, P. R., in press, Large sand waves in submarine canyon heads, Bering Sea: preliminary hypothesis of their depositional history: Geo Marine Letters, 17 ms.p.
- Karl, H. A., Carlson, P. R., and Cacchione, D. A., 1981, Factors influencing sediment transport at the shelf break: Am. Assoc. Petroleum Geol. Bull., v. 65, p. 943.
- Karl, H. A., Carlson, P. R., and Cacchione, D. A., 1983, Factors that influence sediment transport at the shelf break: In: Stanley, D. J., and Moore, G., (editors). Shelf-slope boundary: Critical interface on continental margins: Society Economic Paleontologists and Mineralogists Special Publication No. 33, p. 219-231.
- Karl, H. A., Carlson, P. R., and Lamb, B., 1982, Sediment waves in the head of Navarinsky, Pervenets, and Zhemchug submarine canyons, northwestern Bering Sea: U.S. Geological Survey Circular (Accomplishments in Alaska) 844, p. 141-143.
- Marlow, M. S., Carlson, P., Cooper, A. K., Karl, H., McLean, H., McMullin, R., and Lynch, M. B., 1981, Hydrocarbon resource report for proposed OCS lease sale 83, Navarin Basin, Alaska: U.S. Geological Survey Open-File Report 81-252, 75 p.
- Quinterno, Paula, Blueford, J. R., and Baldauf, J. G., 1981, Micropaleontologic analysis of Navarin Basin, Bering Sea, Alaska: American Assoc. Petroleum Geol. Bull., v. 65, p. 975.
- Vogel, T. M., Kvenvolden, K. A., Carlson, P. R., and Karl, H. A., 1981, Geochemical prospecting for hydrocarbons in the Navarin Basin province: American Assoc. Petroleum Geol. Bull., v. 65, p. 1004.

CHAPTER 2: GEOLOGIC HAZARDS

by

H. A. Karl and P. R. Carlson

Based on data collected during the 1980 and 1981 DISCOVERER cruises (Carlson and Karl, 1980; 1982; Karl and Carlson, 1982) and the results of an Environmental Hazards Workshop that was part of the Navarin Synthesis meeting convened by NOAA/OCSEAP and held in Anchorage on 25-27 October, 1982, we have identified 10 elements and processes that are potential hazards to commercial development of the Navarin basin province. These are:

- Sea ice
- Superstructure icing
- Waves
- Fog
- Sediment mass movement
- Seismicity
- Faulting
- Gas-charged sediment
- Large bedforms
- Unstable sediment

Sea ice, superstructure icing, waves, and fog obviously are not seafloor geologic hazards, and, therefore, we do not discuss these at length. These environmental hazards are considered by other OCSEAP investigators-oceanographers and meteorologists- and specific treatments of these hazards are found in their reports. In this report we only mention briefly the effects of these four hazards on commercial development. Superstructure icing and fog are operational hazards and must be dealt with on a day-to-day basis. The wave climate in the Navarin area can be severe; however, industry is currently operating in areas that have a more severe wave climate, for example, the North Sea. Sea ice is a problem for part of the year in Navarin, however, it is less of a problem than in the Beaufort Sea which is presently being developed for oil and gas. Water depth and distance from land, however, are factors which may complicate development of Navarin basin. Consequently, structures that are now successful in the North Sea and the Beaufort Sea may require additional engineering before use in Navarin basin.

The six elements and processes that are seafloor geologic hazards have been described in depth in several reports and papers written and published since the 1980 annual report, Geologic Hazards in Navarin basin, was issued; (see Chap. 1 for list of reports). Figure 6 shows the distribution of geohazards mapped during the 1980 and 1981 field seasons; maps of geotechnical indices are presented in Chapter 7 of this report.

Mass movement of sediment is ubiquitous on the slope in water depths greater than about 200 m and in the heads of the submarine canyons (Fig. 6; Carlson and others, 1982; in press). Sediment mass movement is the process most likely to pose a hazard to the siting of drilling structures, production platforms, and pipelines. We are not able to assess the recency or the

frequency of mass failures in Navarin basin province. Industry has built structures in areas prone to the mass failure of sediment deposits, the Mississippi delta, for example; however, the scale of the slump and slide blocks and the water depth in Navarin basin province may pose additional engineering problems.

Only six earthquakes, each less than magnitude 6, have been reported from Navarin basin province (Meyer, 1976). This data base spans less than the last 100 years. Even though earthquakes have occurred infrequently during the historic past in Navarin basin province, the numerous examples of sediment mass movement suggest that frequent earthquakes of significant magnitude to initiate mass sediment movement have occurred in the geologic past (see Carlson and others; in press).

None of the faults mapped to date show offset of the Holocene seafloor sediment. Although the ages of these faults are unknown, radiocarbon dates of sediment in the Navarin basin province indicate accumulation rates of the upper 6 m of sediment to range from about 10 to 25 cm/10³ yr (Askren, 1972; Knebel, 1972; Carlson and Karl, Chap. 4, this report). Therefore, faults that reach within 2-3 m of the seafloor may cut sediment as young as Holocene and are considered to be active.

Gas-charged sediment can have a lower shear strength and bearing capacity than does equivalent gas-free sediment (Nelson and others, 1978; Whelan and others, 1976). An increase in the concentration of free or bubble-phase gas results in an increase of pore pressure and a concomitant decrease in shear strength until failure can occur. Such increases in bubble-phase gas can result from drilling into gas-charged sediment or disruption of the sediment by cyclic loading, and this may lead to failure of pipelines or platforms (U.S. Geological Survey, 1977). Examples of gas-charged sediment identified on high-resolution seismic-reflection profiles are shown in Carlson and others (1982). The potential hazard of gas-charged sediment will have to be assessed by the surveying of specific sites chosen for development.

Large bedforms are found in the heads of the submarine canyons incising the Navarin continental margin (Fig. 6; Karl and Carlson, in press). The bedforms occur on a substrate of silty, very fine sand and have wavelengths of about 600 m and heights that vary between 5-15 m. We do not know if the sand waves are active. If the sand waves are active, they, as well as the processes responsible for them, could represent potential hazards.

A regional study of geotechnical properties of Navarin basin sediments are discussed in Chapter 7. It will be necessary to conduct geotechnical analyses on cores collected at specific sites chosen for development in order to determine design criteria for structures with foundations on the seafloor.

References

- Askren, D. R., 1972, Holocene stratigraphic framework southern Bering Sea continental shelf: MS thesis, Univ. of Washington, 104 p.
- Carlson, P. R. and Karl, H. A., 1981, High-resolution seismic reflection profiles: Navarin basin province, northern Bering Sea, 1980: U.S. Geological Survey Open-File Report 81-1221, 4 p., 1 map, scale 1:1,000,000.
- Carlson, P. R. and Karl, H. A., 1982, High-resolution seismic reflection profiles: Navarin basin province, northern Bering Sea, 1981: U.S. Geological Survey Open-File Report 82-786, 5 p., 1 map, scale 1:1,000,000.
- Carlson, P. R., Karl, H. A., and Edwards, B. D., in press, Puzzling features in the head of Navarinsky Canyon, Bering Sea: *Geo-Marine Letters*, v. 2.
- Carlson, P. R., Karl, H. A., Fischer, J. M., and Edwards, B. D., 1982, Geologic hazards in Navarin basin province, northern Bering Sea: *Proceedings Offshore Tech. Conf.*, v. 1, p. 73-87.
- Karl, H. A. and Carlson, P. R., in press, Large sand waves in Navarinsky Canyon head, Bering Sea: *Geo-Marine Letters*, v. 2.
- Karl, H. A. and Carlson, P. R., 1982, Location and description of sediment samples: Navarin basin province, Bering Sea, 1980-81: U.S. Geological Survey Open-File Report 82-958, 5 p., 2 maps, scale 1:1,000,000.
- Knebel, H. J., 1972, Holocene sedimentary framework of the east-central Bering Sea continental shelf: Ph.D. Thesis, Univ. Washington, Seattle, 186 p.
- Meyers, H., 1979, A historical summary of earthquake epicenters in and near Alaska: NOAA Tech. Memorandum EDS NGSDC-1, 80 P.
- Nelson, H., Kvenvolden, K. A., and Clukey, E. C., 1978, Thermogenic gases in near-surface sediments of Norton Sound, Alaska: In, *Proceedings of the 1978 Offshore Technology Society*, p. 2623-2633.
- U.S. Geological Survey, 1977, An investigation of Pennzoil's blow-out and loss of platform: U.S. Geological Survey unpublished administrative report, 22 p.
- Whelan, T., Coleman, J. M., Robert, H. H., and Sukayda, J. N., 1976. The occurrence of methane in recent deltaic sediments and its effect on soil stability: *Bull. of the International Association of Engineering Geology*, no. 14, p. 55-64.

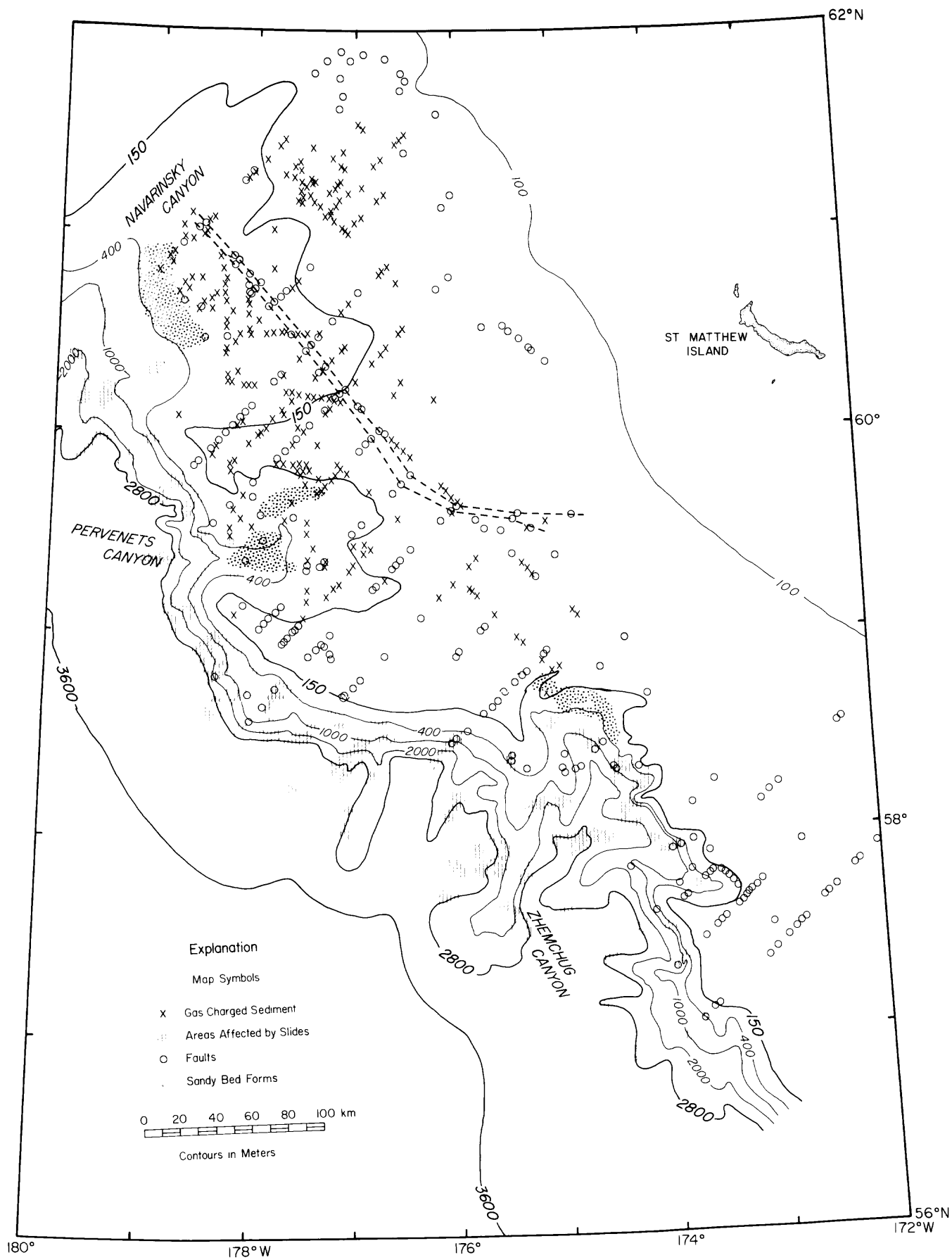


Figure 6. Map of seafloor geologic hazards in Navarin Basin province.

CHAPTER 3: TEXTURAL VARIATION OF SURFICIAL BOTTOM SEDIMENT

by

H. A. Karl and P. R. Carlson

INTRODUCTION

A total of 278 sediment sampling stations were occupied during the 1980 POLAR STAR cruise and the 1980 and 1981 DISCOVERER cruises (Karl and Carlson, 1982, Fig. 5). The distribution of sediment types derived from visual descriptions of surface samples reveals that (1) silts and sandy silts generally characterize the shelf and slope, (2) zones of coarser sediment (coarse silt and sand) occur at the shelf edge, on the upper slope and in the heads of submarine canyons, (3) surficial sediment on the shelf tends to be coarser in the southeastern part of the area than elsewhere on the shelf, and (4) muds typify the lower slope and rise (see Karl and Carlson, 1982).

METHODS

Subsamples taken from the gravity cores and grab samples were soaked in H₂O₂ solution or acetone solution to remove oxidizable organic matter. The samples were then wet sieved on a 63 micron screen to separate the mud fraction (<63 microns) and the sand fraction (>63 microns). If gravel (>2 mm) was present, it was separated from sand by dry sieving. The fine-sediment fraction (<63 microns) was analyzed by standard pipette method and the sand-size material analyzed by standard rapid settling tube (RSA) method. Statistical parameters were calculated as moment measures.

RESULTS

Table 1 contains the results of detailed sediment analyses of eight cores and grab samples selected as typical examples of each textural environment listed above (Fig. 7). All the samples are poorly sorted (Table 1, Fig. 8). Mean grain-size of the rise and slope samples is in the very fine silt class. The distribution of sediment sizes in the rise and slope samples is very similar; the samples that happen to have been chosen are both weakly bimodal and differ only in that the dominant mode shifts from clay (10.5 phi) on the rise to fine silt (6.5 phi) on the lower slope (Fig. 9). Samples from the shelf edge are considerably coarser than samples from the slope and rise with mean grain-sizes of 0.02 mm and 0.07 mm. The finer of the shelf-edge samples overlaps mean grain diameters typical of the shelf (Fig. 8). Sediment in both shelf-edge samples is concentrated in the coarser silt and finer sand classes with modes in the coarse silt (4.5 phi) and fine sand (3.5 phi) classes (Fig. 9). Grain-size distribution of the sample (80-G85) from the southeastern part of the shelf resembles shelf-edge distributions in that sediment tends to be concentrated in the finer sand and coarser silt classes with a strong mode in the coarse silt (4.5 phi) class (Fig. 9). Sample 80-G23 from the northwestern part of the shelf differs from sample 80-G85 in that sediment particles are more uniformly distributed over the very fine sand through clay classes with a weak mode in the coarse silt class (Fig. 9). The

coarsest mean grain-sizes occur in the heads of the submarine canyons. In the samples considered here, sediment particles are concentrated in the sand classes with a very strong mode in the fine sand (2.5 phi) class (Fig. 9).

DISCUSSION

Except for the samples from the rise and slope, the factors responsible for these grain-size distributions and regional textural variations are not obvious. The predominance of fine silt and clay size material in the rise and slope samples is typical of deep water environments. Depositional conditions in these environments during the low stands of sea level in the Pleistocene probably would not have been appreciably different than present-day conditions. This, however, is not true of the shelf and canyon heads. The zones of coarser sediment at the shelf edge and in the canyon heads could be due in part to lower sea levels when shorelines were at or near these areas. In which case coarser sediment was either supplied to the shelf edge and canyon heads by streams, for example, or energy levels were sufficiently high to winnow out the fines from sediment being deposited. Alternatively, the coarser sediment in these environments relative to the shelf and slope might reflect modern processes that supply sufficient energy to winnow sediment at the shelf edge and in the canyon heads. The Bering Slope Current, which flows northward parallel to the slope, and internal waves, which may be focused in and adjacent to the heads of the submarine canyons, are potential mechanisms to supply energy to winnow sediments. The finer shelf sediments in the northwestern section of the shelf relative to the southeastern part may indicate that relict sediment from lower sea levels is being diluted with finer material following flooding of the shelf; present sediment sources are over 300 km distant. These hypothesis are conjectures, however, as not enough textural data is available at present to allow us to chose between these interpretations.

REFERENCES

- Karl, H. A., and Carlson, P. R., 1982, Location and description of sediment samples: Navarin basin province, Bering Sea, 1980-81: U.S. Geological Survey Open-File Report 82-958, 5 p.

Table 1. Results of grain-size analysis on selected samples

Environment	Shelf		Shelf Edge		Slope 81-G13 gravity	Rise 81-G70 gravity	Canyon Head	
	80-G23 gravity core	80-G85 gravity core	81-VV40 Van Veen	81-G63 gravity			81-VV75 Van Veen	81-VV89 Van Veen
Depth of subsample (cm)	10-12	10-12	0-10	23-33	10-15	40-50	0-10	0-10
% Gravel	0.00	0.00	0.00	0.00	0.00	0.00	0.00	19.05
% Sand	10.38	20.82	74.20	21.34	5.11	3.68	94.12	76.43
% Silt	59.99	67.23	22.11	61.66	57.57	51.97	4.68	3.84
% Clay	29.62	11.94	3.68	16.99	37.30	44.33	1.19	0.66
Mean grain size (0)	6.65	5.34	3.77	5.59	7.31	7.65	2.93	2.05
Mean grain size (mm)	0.010	0.025	0.07	0.02	0.006	0.005	0.13	0.24
Std. deviation (0)	2.26	1.90	1.46	2.17	2.07	2.11	0.96	1.92
Skewness (0)	0.27	1.12	2.23	0.94	0.03	-0.18	2.15	-0.50
Kartosis (0)	-1.01	0.70	5.63	-0.19	-0.98	-1.07	15.73	1.10

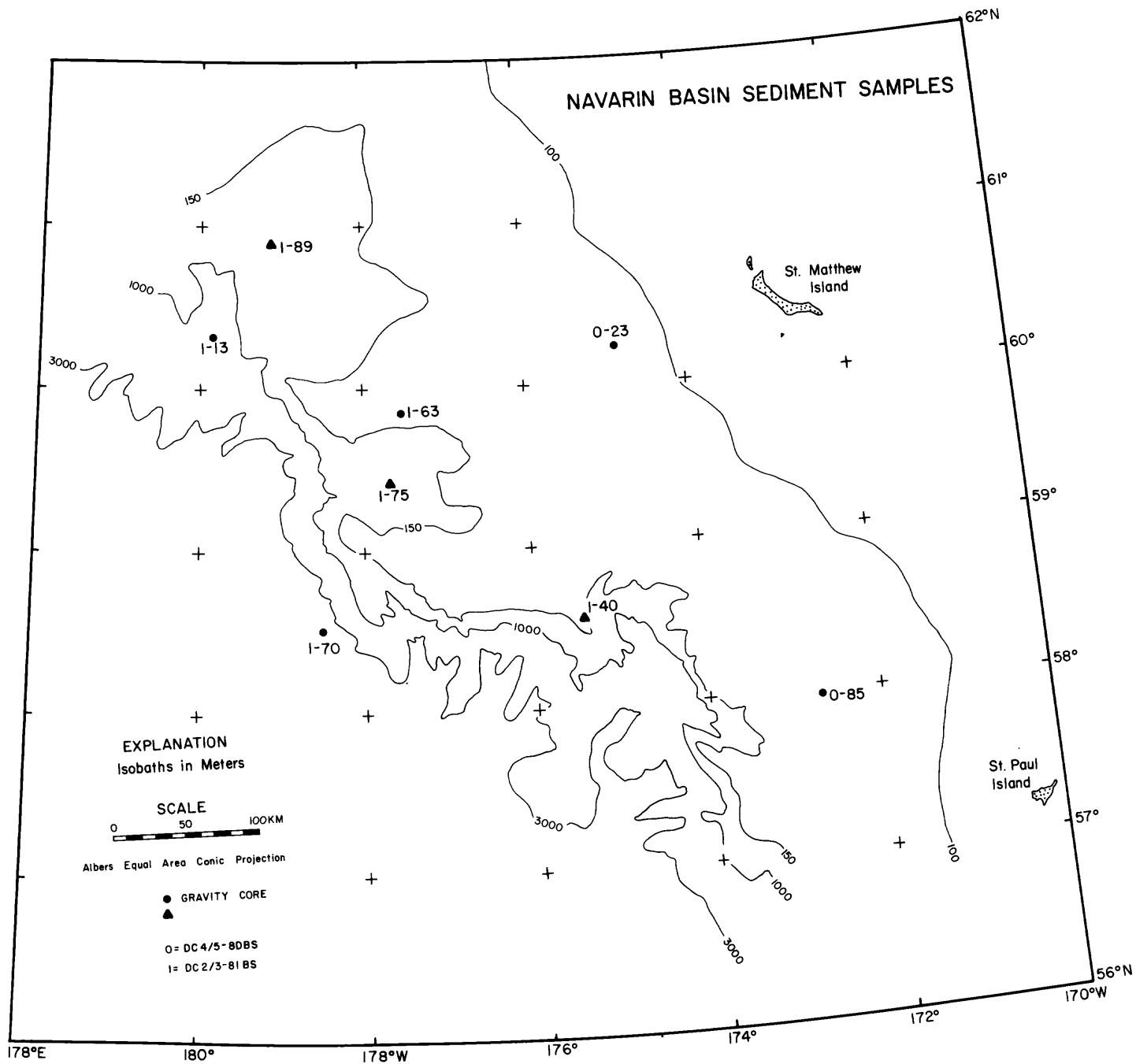


Figure 7. Location of sediment samples selected as typical examples of textural environments characterizing Navarin Basin province. (The solid triangle identifies Van Veen samples).

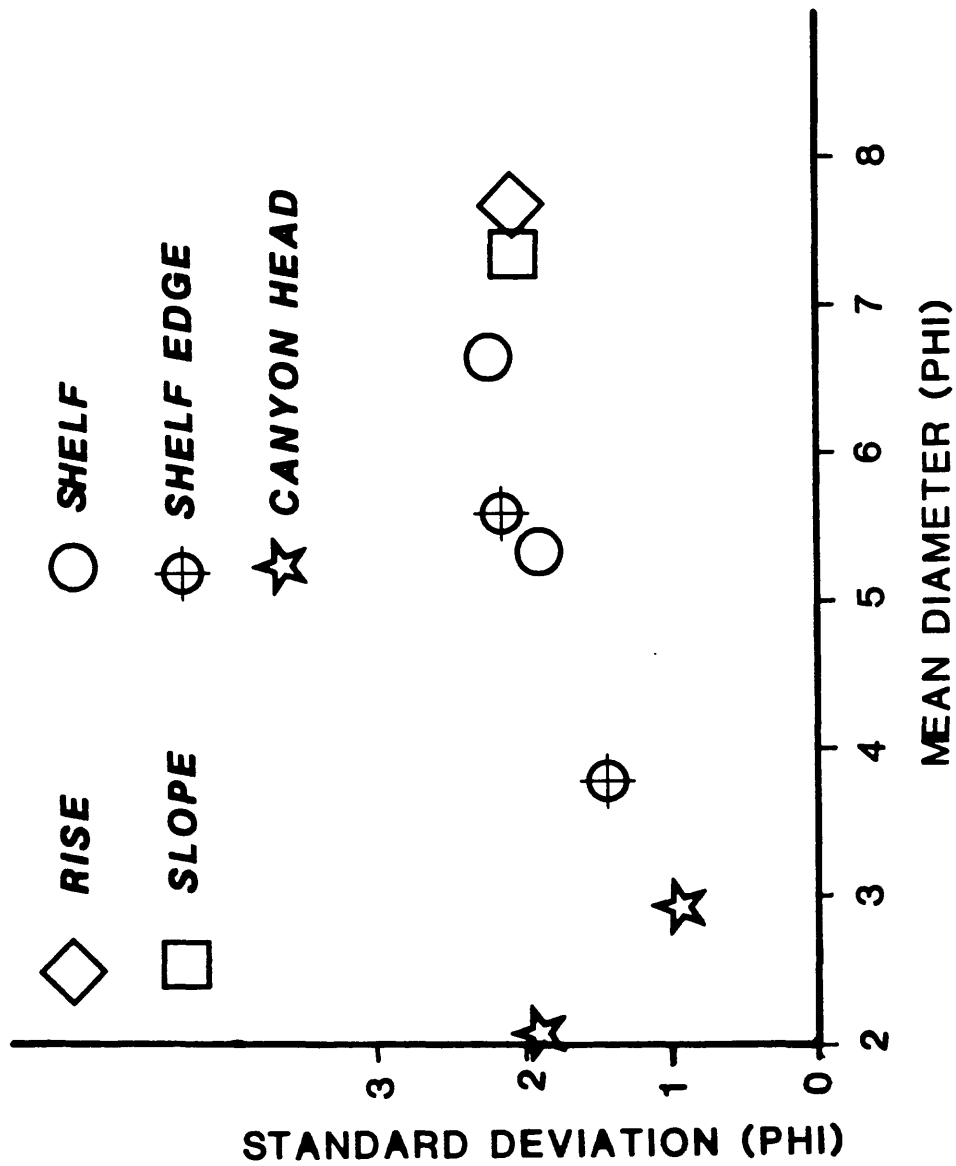


Figure 8. Plot of mean diameter vs. standard deviation.

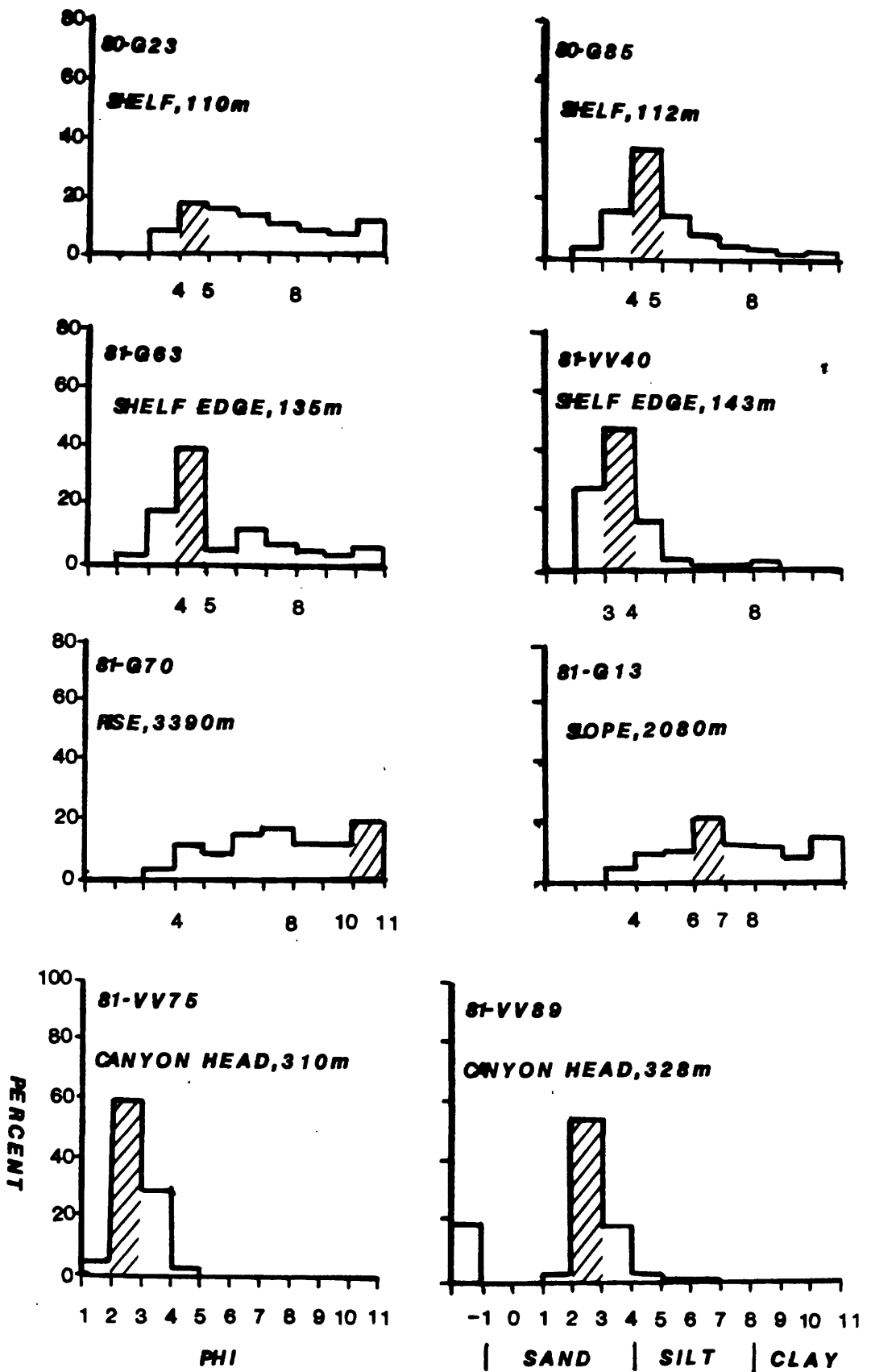


Figure 9. Histograms of selected samples. Modes identified by hachuring; dominant mode is hatchured in biomodal samples.

CHAPTER 4: RATES OF SEDIMENT ACCUMULATION

by

Paul R. Carlson and Herman A. Karl

INTRODUCTION

The Navarin basin province is located on the outer part of the flat, wide Bering continental shelf, a great distance (>300 km) from modern sources of detrital sediment. However, during low stands of sea level the ancestral Anadyr and Yukon Rivers must have transported vast quantities of sediment across the shelf where the suspended and bottom sediments were entrained in the coastal currents that were sweeping through what is the present site of the Navarin basin. In order to understand the development of the Navarin continental margin, rates of sediment accumulation on the margin must be determined. This chapter presents some preliminary estimates of sediment accumulation rates based upon C-14 measurements of gravity core sub-samples from the Navarin shelf, slope, and rise.

DATA COLLECTION AND ANALYSIS

Gravity cores (8 cm diameter) subsampled for radiocarbon dating were collected on two cruises of the NOAA ship DISCOVERER in 1980 and 1981 (Karl and Carlson, 1982). A total of 22 cores were selected for dating (Table 2; Fig. 10). The cores collected were split longitudinally. After each cruise, preliminary studies of core descriptions (including X-radiographs), microfaunal contents, organic carbon measurements, and interpretations of high-resolution seismic reflection records were utilized to select the cores for radiocarbon dating. The working half of each selected core was carefully sub-sampled to avoid the "smear-affect" along the core-liner. Sufficient sediment was collected to provide the analyst with about one gram of carbon from the "whole-core" samples. The intervals sampled from each core are listed in Table 2. Analyses were performed by the USGS radiocarbon dating lab in Menlo Park, California, for the 1980 cores and by Geochron Labs in Cambridge, Massachusetts for the 1981 cores.

Calculations of preliminary rates of sediment accumulation (Table 3) are based on the assumption of a constant rate of sediment deposition to a depth in the core of the mid-point of the sampled interval.

DISCUSSION

If we compare the rate of sediment accumulation with water depth (Table 3), some trends emerge for the various physiographic subdivisions of the Navarin continental margin. The average rate for all the shelf sub-samples (<150 m water depth) analysed is $14.1 \text{ cm}/10^3 \text{ yrs}$. However, a plot of these values (Fig. 11) shows that the samples make up two groups. A cluster of four cores located between the heads of Navarinsky and Pervenets Canyons have an average rate of sediment accumulation of $21 \text{ cm}/10^3 \text{ yrs}$, whereas shelf sediment north and south of the cluster averages $8.5 \text{ cm}/10^3 \text{ yrs}$, including a low value of $2 \text{ cm}/10^3 \text{ yrs}$ from a core taken less than 10 kilometers from the

shelf-slope break. The four cores that have an average rate of 21 cm/10³ yrs plot near the center of greatest sediment thickness in Navarin basin (Chapter 6, this volume). Previous sedimentologic studies in the region illustrate the variable nature of the rates of sediment accumulation on the Bering shelf. Knebel (1972) reported rates ranging from 2.5 to 40 cm/10³ yrs for cores collected northeast of Navarin basin. Askren (1972) reported rates ranging from 11 to 67 cm/10³ yrs for cores collected along the southeastern edge of Navarin basin.

Accumulation rates of sediment cored on the upper slope range from 2 to nearly 10 cm/10³ yrs, with an average value of 5 cm/10³ yrs (Table 3). Eight of eleven of these subsamples yielded dates greater than 25,000 yrs BP, half of which came from sediment less than one meter deep in the core, suggesting either a very slow rate of deposition or erosion of some of the surficial sediment.

Cores from the lower slope range in accumulation rates from about 4 to 37 cm/10³ yrs with an average of 15 cm/10³ yrs (Table 3). Age dates from the upper meter of these cores, except 0-66 which was obtained from mid-slope depths, are less than 10,000 yrs B.P. indicating a much more rapid rate of deposition than on the upper slope. An explanation for the large difference in rates between upper and lower slope may be the widespread mass movement that has been noted on the Navarin continental slope (Carlson and others, 1982a), resulting in removal of sediment from the upper slope and deposition on the lower slope and rise.

Continental rise sediment apparently has accumulated at rates ranging from about 7 to 21 cm/10³ yrs, with an average rate of nearly 15 cm/10³ yrs (Table 3). Some of the cores from the lower slope and rise that are associated with the large submarine canyon systems contain coarse, graded layers attributed to turbidity current deposition (Carlson and others, 1982b). Deposition recorded by these cores that contain coarse layers interbedded with hemiplagic muds must be episodic, which very likely accounts for the variability of ages in core 0-26 for example (Table 3).

REFERENCES

- Askren, D. R., 1972, Holocene stratigraphic framework - southern Bering Sea continental shelf: M.S. Thesis, Washington, Univ., Seattle, 104 p.
- Carlson, P. R., Fischer, J. M., Karl, H. A., and Larkin, C., 1983, Isopach map of unit A, youngest sedimentary sequence in Navarin basin, Bering Sea, in Karl, H. A. and Carlson, P. R. eds., Surface and Near-surface Geology, Navarin Basin Province: Results of the 1980-81 Field Seasons: U.S. Geological Survey Open-File Report 83- , in press.
- Carlson, P. R., Karl, H. A., Fischer, J. M., and Edwards, B. D., 1982a, Geologic hazards in Navarin basin province, northern Bering Sea: 14th Offshore Technology Conference, Houston, Texas, Proceedings v. 1, p. 73-87.
- Carlson, P. R., Karl, H. A., and Quintero, Paula, 1982b, Sedimentologic processes in world's largest submarine canyons, Bering Sea, Alaska: Geological Society of America, Abstracts with Programs, v. 14, no. 7, p. 459-460.
- Karl, H. A. and Carlson, P. R., 1982, Location and description of sediment samples: Navarin basin province, Bering Sea, 1980-81: U.S. Geological Survey Open-File Report 82-958, 5 p., 2 map sheets, scale 1:1,000,000.
- Knebel, H. J., 1972, Holocene sedimentary framework of the east-central Bering Sea continental shelf: Ph.D. Thesis, Washington, Univ., Seattle, 186 p.

Table 2. C-14 dates of Navarin samples

<u>Core No.*</u>	<u>Depth in core (cm)</u>	<u>C-14 date (yrs BP)</u>	<u>Water depth (m)</u>
0- 12	211-230	16,670 ± 100	3164
0- 13	188-228	5,580 ± 45	2692
0- 13	245-270	34,520 ± 490	"
0- 26	188-222	10,880 ± 80	3373
0- 26	235-260	33,990 ± 610	"
0- 26	322-333	33,300 ± 1800	"
0- 33	65- 90	28,980 ± 2200	210
0- 33	210-240	28,200 ± 3000	"
0- 42	170-183	13,650 ± 100	141
0- 44	125-145	14,900 ± 110	138
0- 66	65- 84	19,370 ± 160	1336
0- 66	325-335	37,500 ± 1200	"
0- 66	380-385	>32,000	"
0-115	170-200	9,505 ± 300	2870
0-115	237-262	19,990 ± 1400	"
1- 02	100-130	11,755 ± 395	143
1- 03	0- 30	7,375 ± 270	133
1- 15	65- 90	5,330 ± 180	2750
1- 15	250-275	15,975 ± 850	"
1- 31	160-190	8,815 ± 355	137
1- 32	160-190	7,500 ± 305	130
1- 44	65- 90	4,460 ± 190	3400
1- 44	220-245	10,925 ± 365	"
1- 58	25- 50	9,215 ± 310	179
1- 58	60- 88	>37,000	"
1- 58	240-265	>27,000	"
1- 65	25- 50	10,485 ± 355	436
1- 65	160-185	>32,000	"
1- 66	65- 90	>37,000	580
1- 67	65- 90	17,725 ± 680	167
1- 88	65- 90	>29,000	205
1- 88	350-375	>37,000	"
1-105	160-190	8,385 ± 310	144
1-106	160-190	8,700 ± 355	135
1-107	65- 90	8,900 ± 290	116

* 0 = DC 4/5-80 1 = DC 2/3-81

Table 3. C-14 dates and rates of sediment accumulation listed by water depth.

	<u>Core No.*</u>	<u>Water Depth (m)</u>	<u>C-14 Date (yrs BP)</u>	<u>Depth in core (cm)</u>	<u>Rate of Accumulation (cm/1000 yrs)</u>
Shelf	1-107	116	8,900	77	8.8
	1- 32	130	7,500	175	23.3
	1- 03	133	7,375	15	2.0
	1-106	135	8,700	175	20.1
	0- 44	138	14,900	135	9.1
	1- 31	137	8,815	175	19.9
	0- 42	141	13,650	176	12.8
	1- 02	143	11,755	115	9.8
	1-105	144	8,385	175	20.9
<hr/>					
Slope (upper)	1- 67	167	17,725	77	4.4
	1- 58	179	9,215	37	4.1
	"	"	>37,000	74	<2.0
	"	"	>27,000	252	<9.4
	1- 88	205	>29,000	77	<2.7
	"	"	>37,000	363	<9.8
	0- 33	210	28,980	77	2.7
	"	"	28,200	225	8.0
	1- 65	436	10,485	37	3.6
	"	"	>32,000	172	5.4
	1- 66	580	>37,000	77	<2.1
	<hr/>				
	0- 66	1,336	19,370	74	3.9
	"	"	>37,500	330	8.8
	"	"	>32,000	382	11.9
Slope (lower)	0- 13	2,692	5,580	208	37.1
	"	"	34,520	257	7.5
	1- 15	2,750	5,330	77	14.6
	"	"	15,975	262	16.5
	0-115	2,870	9,505	185	19.5
	"	"	19,990	249	12.5
<hr/>					
Rise	0- 12	3,164	16,670	220	13.3
	0- 26	3,373	10,880	215	19.8
	"	"	33,990	247	7.3
	"	"	33,300	327	9.9
	1- 44	3,400	4,460	77	17.5
	"	"	10,925	232	21.3

*0 = DC 4/5-80; 1 = DC 2/3-81

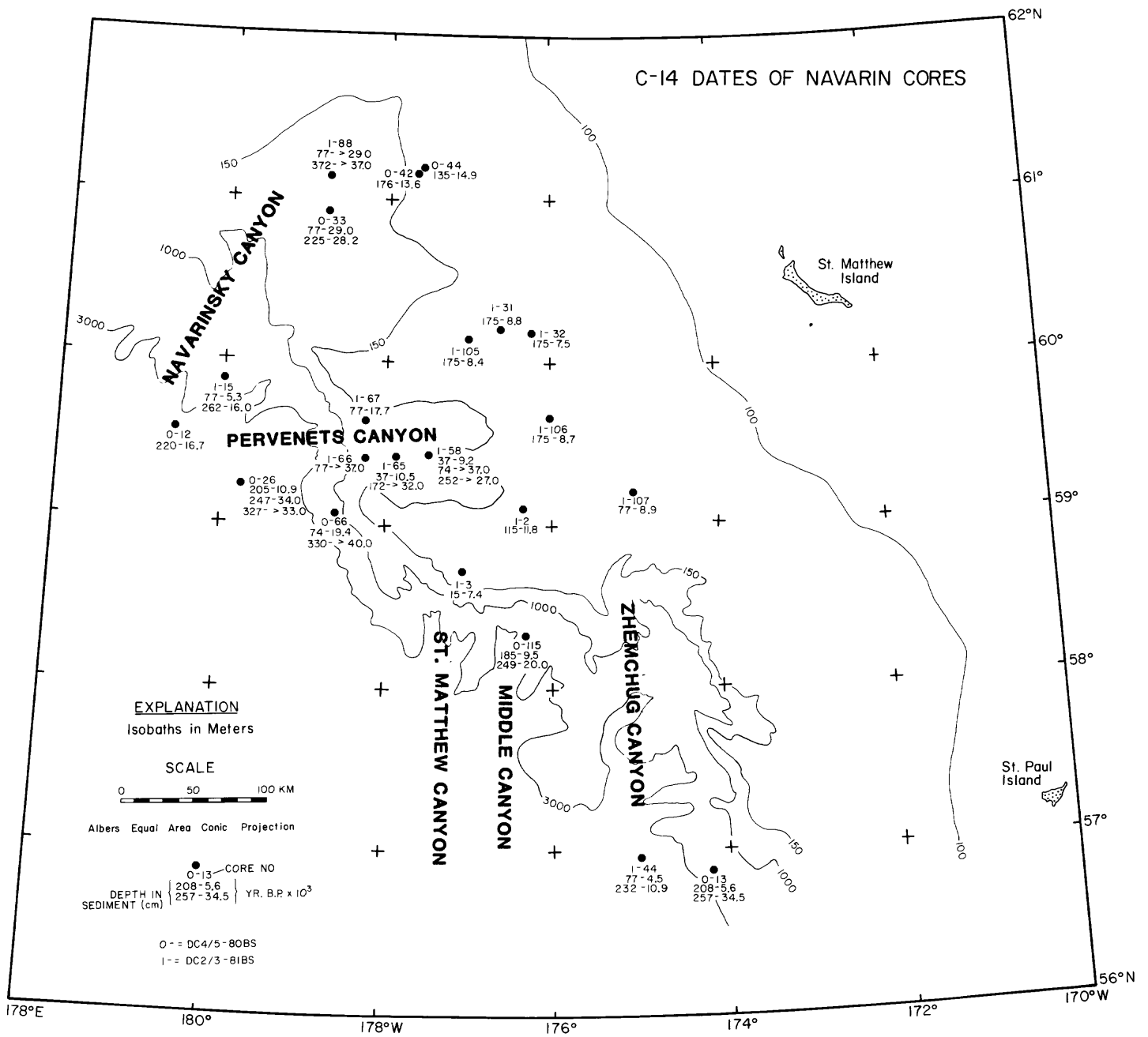


Figure 10. Location map of cores subsampled for C-14 dating.

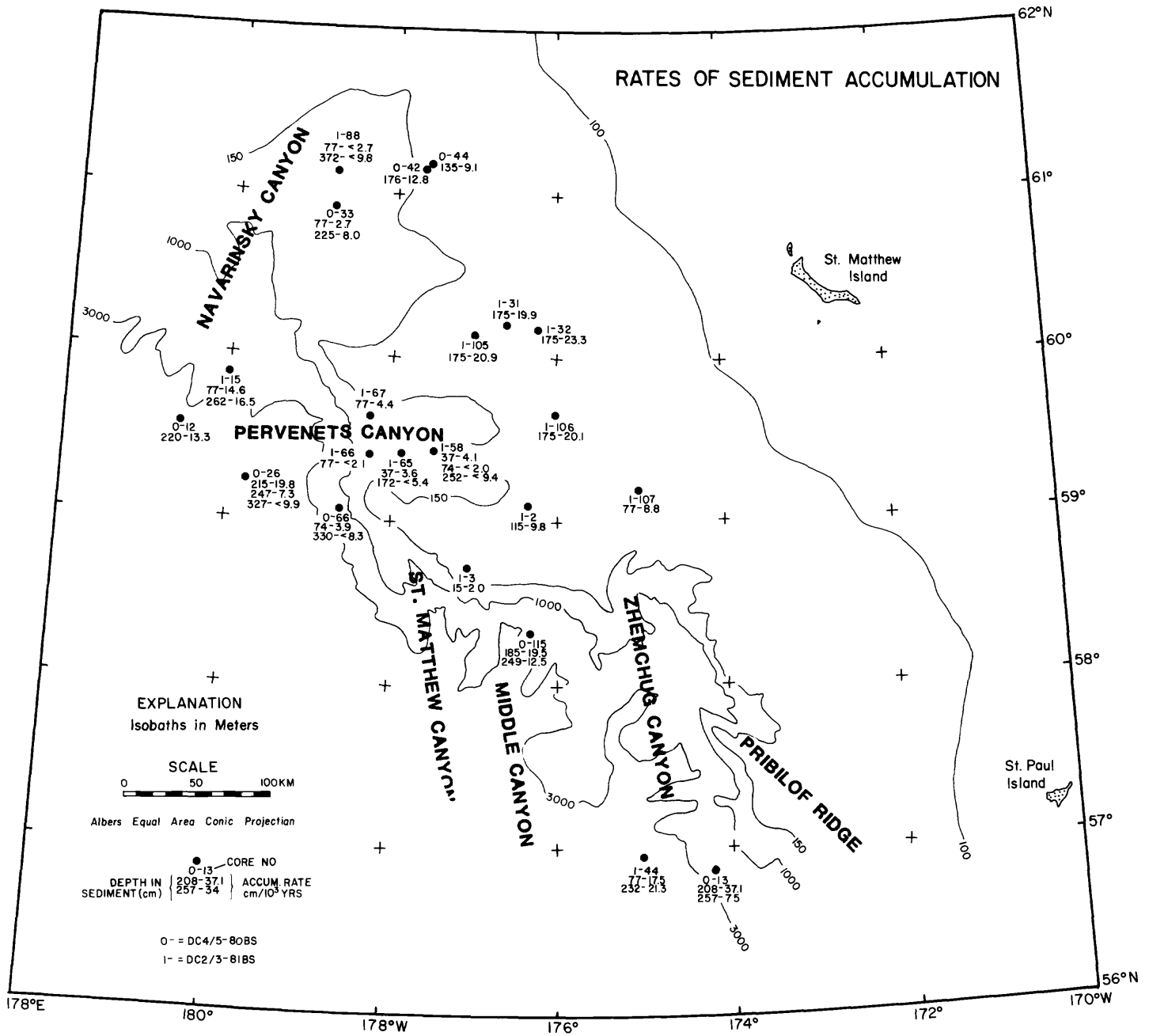


Figure 11. Map of dated cores showing calculated preliminary accumulation rates of sediment.

CHAPTER 5: PRE-QUATERNARY ROCKS AND SEMI-CONSOLIDATED SEDIMENT
FROM THE NAVARIN CONTINENTAL MARGIN

by

Paul R. Carlson, Jack G. Baldauf, and Christopher Larkin

INTRODUCTION

The purpose of this chapter is to describe pre-Quaternary rocks and semi-consolidated sediment that have been collected from the outer shelf and slope of the Navarin basin province. This chapter also compares these samples to rocks dredged from other parts of the Bering continental margin.

Although many of the samples we collected in 1980 and 1981 (Karl and Carlson, 1982) are limited to the unconsolidated Holocene sediment blanket that covers most of the Navarin province, a few of the gravity cores penetrated through thin spots in the Holocene sediment cover into the underlying Pleistocene unit (Baldauf, 1982; Quinterno, 1981). Also, two gravity cores recovered semi-consolidated Tertiary-age strata that was cropping out on the continental slope. In addition to these cores, we also collected one chain-bag dredge of pre-Quaternary rocks from a steep scarp on the south side of Zhemchug Canyon. The locations of these three samples (1 dredge and 2 cores) are shown in figure 12.

Pre-Quaternary rocks also have been dredged from the Navarin margin from the USGS RV S.P. LEE (Marlow and others, 1979; Jones and others, 1981; see Fig. 12). Additional dredge samples were collected along the Bering margin south of Navarin basin from the RV THOMAS G. THOMPSON (Hopkins and others, 1969) and from the USGS RV SEA SOUNDER (Vallier and others, 1980).

RESULTS

Preliminary analyses of samples we collected in the Navarin province show that two cores and a single dredge haul recovered pre-Quaternary age material.

Core 80-106 (DC 4/5-80-106). Core 106 was taken from the lower continental slope at a water depth of 1785 m on the north side of a ridge separating Middle and Zhemchug Canyons (Fig. 12). This gravity core recovered 55 cm of very stiff olive gray (5Y 3/2) clayey silt with shale chips scattered throughout the lower 15 cm of the recovered interval. Diatoms from this semi-lithified core were assigned to the Denticulopsis seminae var. fossilis - D. kamtschatica zone of Barron (1980) which is the age equivalent of early late Pliocene. An organic carbon analysis of a subsample (10-12 cm depth) from this core produced a value of 0.36 percent.

Core 81-46 (DC 2/3-81-46). Gravity core 46 was collected from the base of the continental slope south of Zhemchug Canyon in water 2530 m deep (Fig. 12). The 70 cm long core contained the most distinctive color change of any of the cores we collected. The upper 28 cm consisted of light olive brown (5Y 5/6) mud. At about 27-30 cm, there was an abrupt color change to a dark olive green gray (5GY 4/1) mud. There was no apparent textural change.

Organic carbon contents of these two different colored muds was very similar, 0.41% at 11-15 cm and 0.48% at 45-49 cm. Clay mineral content in the two muds was quite different, however, with the upper unit containing 61% smectite, 18% illite, and 21% kaolinite plus chlorite compared to 46% smectite, 24% illite, and 30% kaolinite plus chlorite in the lower unit. Diatoms from both color units in this core are late Pliocene in age.

Dredge-1 (DC 4/5-80-91). A steep scarp on the wall of Pribilof Ridge, south of the main axis of Zhemchug Canyon (Fig. 12), was sampled by chain bag dredge in water depths between 2200 and 268 m. The dredge recovered a rather wide variety of rocks including one piece of ultra-basic rock (Pyroxenite), several small pieces of basalt, a large (40X28 cm) angular boulder of greenstone (probably metamorphosed basalt), several pieces of highly indurated conglomerate, an angular piece of black argillite, a small fragment of limestone, a small piece of calcareous siltstone, a small piece of calcareous sandstone, and many pieces of diatomaceous mudstone.

The cobble-size piece of limestone was found to be barren of calcareous nannofossils and of pollen and spores, thus not datable. The diatoms in the numerous pieces of mudstone provided age information ranging from early to late Miocene and the calcareous sandstone contained reworked mid-late Miocene diatoms.

Organic carbon contents of the mudstones range from 0.24% to 0.77% and average 0.56%. Carbonate carbon contents of the mudstones were all 0.01% or less. The calcareous siltstone has an organic carbon content of 0.79% and an inorganic carbon value of 3.63%. The limestone fragment consists of 0.72% organic and 7.28% inorganic carbon. The sandstone had the lowest organic carbon content of all samples measured (0.12%), but yielded a inorganic carbon value of 2.74%. Our carbon values agree quite closely with those reported by Vallier and others (1980), for rocks south of Navarin that yielded average organic carbon values of 0.52% and with Jones and others (1981) for mudstones from the northern half of the Bering margin, especially the Navarin margin, that have average organic carbon values of 0.55%. The inorganic carbon content of those mudstones averaged 0.08%. Jones and others (1981) also reported values from volcanic sandstones and tuffs that averaged 0.28% organic and 0.70% carbonate carbon, and from muddy and tuffaceous limestones that averaged 0.64% organic and 7.36% carbonate carbon. By way of comparison with the Tertiary mudstone samples dredged from the Bering margin, average organic carbon values of 93 Quaternary-age muds and sandy muds from cores we collected throughout the Navarin basin province was 0.83%, with the values ranging from 0.26% to 1.56%; inorganic carbon values also were higher than those of the Tertiary mudstones, averaging 0.13%, and ranging from 0.03% to 0.57% (Fischer, 1981).

A point count of 400 grains in a thin section of the mid-late Miocene sandstone (DC4/5-80-91) yielded a composition of quartz 37%, feldspar 17%, rock fragments 40% (61% of r.f. are volcanic), glauconite 3%, heavy minerals 2%, and others 1% including diatoms, and forams. The grains are sub-angular to sub-rounded, poorly-sorted, and range in size from fine sand to granules;

the intergranular cement consists of microcrystalline calcite and makes up about 30% of the sample. According to Folk (1974), this sandstone would be classified as a submature calcareous volcanic arenite.

REFERENCES

- Baldauf, J. G., 1982, Identification of the Holocene-Pleistocene boundary in the Bering Sea by diatoms: *Boreas*, v. 11, p. 113-118.
- Barron, J. A., 1980, Lower Miocene to Quaternary diatom biostratigraphy of Leg 57, off northeastern Japan, Deep Sea Drilling Project, In, Honza, E. and others, Initial Reports of the Deep Sea Drilling Project, p. 641-685: Washington, D. C. (U.S. Government Printing Office).
- Fischer, J. M., 1981, Carbon contents of Navarin basin sediments, In, Carlson, P. R. and Karl, H. A. (eds.), Seafloor Geologic Hazards, Sedimentology, and Bathymetry: Navarin Basin Province, Northwestern Bering Sea: U.S. Geological Survey Open-File Report 81-1217, p. 44-57.
- Fischer, J. M., Carlson, P. R., and Karl, H. A., 1982, Bathymetric map of Navarin continental margin, Bering Sea: U.S. Geological Survey Open-File Report 82-1038, 11 p., 1 map sheet 1:1,000,000.
- Folk, R. L., 1974, Petrology of sedimentary rocks: Hemphill Publishing Co., Austin, Tex. 182 p.
- Hopkins, D., Scholl, D. W., Addicott, W. O., Pierce, R. L., Smith, P. B., Wolfe, J., Gershenovich, D., Kotenev, B., Lohrman, J. E., Lipps, J. H., and Obradovich, J., 1969, Cretaceous, Tertiary, and early Pleistocene rocks from the continental margin in the Bering Sea: Geological Society of America, Bull. 80, p. 1471-1486.
- Jones, D. M., Kingston, M. J., Marlow, M. S., Cooper, A. K., Barron, J. A., Wingate, F. H., and Arnal, R. E., 1981, Age, mineralogy, physical properties, and geochemistry of dredge samples from the Bering Sea continental margin: U.S. Geological Survey Open-File Report 81-1297, 68 p.
- Karl, H. A. and Carlson, P. R., 1982, Location and description of sediment samples: Navarin Basin province, Bering Sea, 1980-81: U.S. Geological Survey Open-File Report 82-958, 5 p., 2 maps, scale 1:1,000,000.
- Marlow, M. S., Cooper, A. K., Scholl, D. W., Vallier, T. L., and McLean, H., 1979, Description of dredge samples from the Bering Sea continental margin: U.S. Geological Survey Open-File Report 79-1139.
- Quinterno, P. J., 1981, Preliminary report on benthic foraminifers from Navarin basin province, Bering Sea, Alaska, In, Carlson, P. R. and Karl, H. A., (eds.), Seafloor Geologic Hazards, Sedimentology, and Bathymetry: Navarin Basin Province, Northwestern Bering Sea: U.S. Geological Survey Open-File Report 81-1217, p. 114-129.
- Vallier, T. L., Underwood, M. B., Gardner, J. V., and Barron, J. A., 1980, Neogene sedimentation on the outer continental shelf margin, southern Bering Sea: *Marine Geology*, v. 36, p. 269-287.

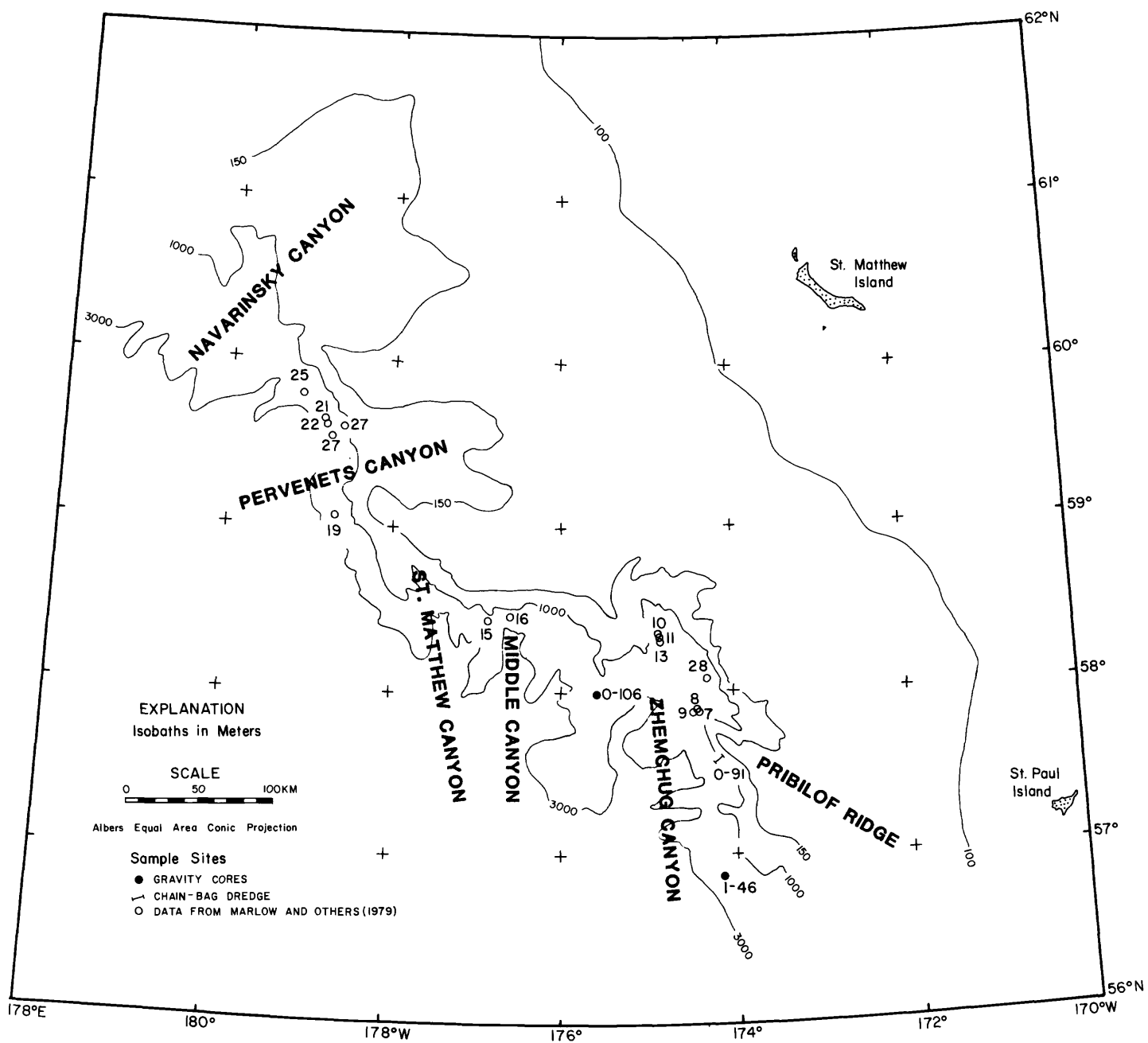


Figure 12. Locations of dredge hauls and gravity cores, Navarin margin.

CHAPTER 6: ISOPACH MAP OF SEISMIC UNIT A, YOUNGEST SEDIMENTARY SEQUENCE IN NAVARIN BASIN

by

Paul R. Carlson, Jeffrey M. Fischer,
Herman A. Karl, and Christopher Larkin

INTRODUCTION

Navarin Basin as defined by Marlow and others (1976) consists of a thick (>12 km) section of Mesozoic and Cenozoic sedimentary material that covers an area of 49,700 km² on the northwestern portion of the Bering continental shelf (Fig. 13). The main part of the basin, as delineated by the 2 km isopleth, is oriented northwest-southeast, parallel to the shelf-slope break.

The principal map in this chapter shows the thickness of only the uppermost unit, herein referred to as unit A, of the Navarin basin sedimentary sequence (Fig. 14). Figure 13 provides a comparison of the area covered by the isopached Unit A and the entirety of Navarin basin as mapped by Marlow and others (1979).

DATA COLLECTION AND REDUCTION

The high-resolution seismic-reflection data used in the development of the unit A isopach map were collected on cruises of the NOAA ship DISCOVERER in 1980 (DC 4/5-80) and 1981 (DC 2/3-81) (Carlson and Karl, 1981; 1982). Navigational control was by Loran C updated by satellite "fixes." Thicknesses of sediment seen on 3.5 kHz and minisparker records were measured on a digitizing table at five minute intervals. The Unit A was defined by a relatively flat-lying strong, persistent reflector that marked the base of the uppermost sedimentary unit (Fig. 15). This reflector could be traced with confidence throughout the mapped portion of the basin. The edges of the isopached area mark either an area where the reflector crops out at the seafloor (at least appears to do so within the limits of resolution of the high-resolution profiles) or the reflector can not be traced further due to one of three factors (1) poor quality records, (2) disappearance or loss of strength of the reflector, or (3) insufficient track line coverage.

DISCUSSION

Unit A, the uppermost seismic-stratigraphic unit in the Navarin basin sequence, has been mapped over an area of 100,000 km² on the outer shelf in the northern Bering Sea (Fig. 14). This unit consists of unconsolidated sediment that ranges in type from clayey silt to muddy sand (Karl and Carlson, 1982) of Quaternary age (Baldauf, 1981). The average thickness of this unconsolidated unit is about 20 m. Unit A attains a maximum thickness of 45 m within a narrow (5-10 km wide) elongate trough located near the southeastern edge of Navarinsky Canyon, and just east of the deepest part of Navarin Basin (Fig. 13 and 14). This trough is part of a broader (40 km wide), shallower (30 m thick) depression filled with unit A sediment, that

parallels the shelf break in present water depths of 130-150 m. The isopached unit pinches out to the northwest near the head of Navarinsky Canyon and also near the head of Pervenets Canyon (Fig. 14). We have collected gravity cores near both canyons across the area of the outcropping reflector and are attempting to date this unit. At this time, we can only estimate that Unit A is less than 30,000 yrs B.P. based on C-14 dates and faunal data obtained from cores collected near the "pinchouts" (see Chapter 4).

REFERENCES

- Baldauf, J. G., 1981, Diatom analysis of late Quaternary sediments from Navarin Basin province, Bering Sea, Alaska, in Carlson, P. R. and Karl, H. A., eds., Seafloor geologic hazards, sedimentology, and bathymetry: Navarin Basin province, northwestern Bering Sea: U. S. Geological Survey Open-File Report 81-1217, p. 100-113.
- Carlson, P. R. and Karl, H. A., 1981, High-resolution seismic reflection profiles: Navarin Basin province, northern Bering Sea, 1980: U.S. Geological Survey Open-File Report 81-1221, 4 p., 1 map, scale 1:1,000,000.
- Carlson, P. R. and Karl, H. A., 1982, High-resolution seismic reflection profiles collected in 1981 in Navarin Basin province, Bering Sea: U.S. Geological Survey Open-File Report 82-786, 5 p., 1 map, scale 1:1,000,000.
- Karl, H. A. and Carlson, P. R., 1982, Location and description of sediment samples: Navarin Basin province, Bering Sea, 1980-81: U.S. Geological Survey Open-File Report 82-958, 5 p., 2 map sheets, scale 1:1,000,000.
- Marlow, M. S., Scholl, D. W., Cooper, A. K., and Buffington, E. C., 1976, Structure and evolution of Bering Sea shelf south of St. Lawrence Island: American Association of Petroleum Geologists Bulletin, v. 60, p. 161-183.
- Marlow, M. S., Cooper, A. K., Parker, A. W., and Childs, J. R., 1979, Isopach map of strata above acoustic basement in the Bering Sea: U.S. Geological Survey Miscellaneous Field Studies Map MF-1164. 1 map sheet, scale 1:2,500,000.

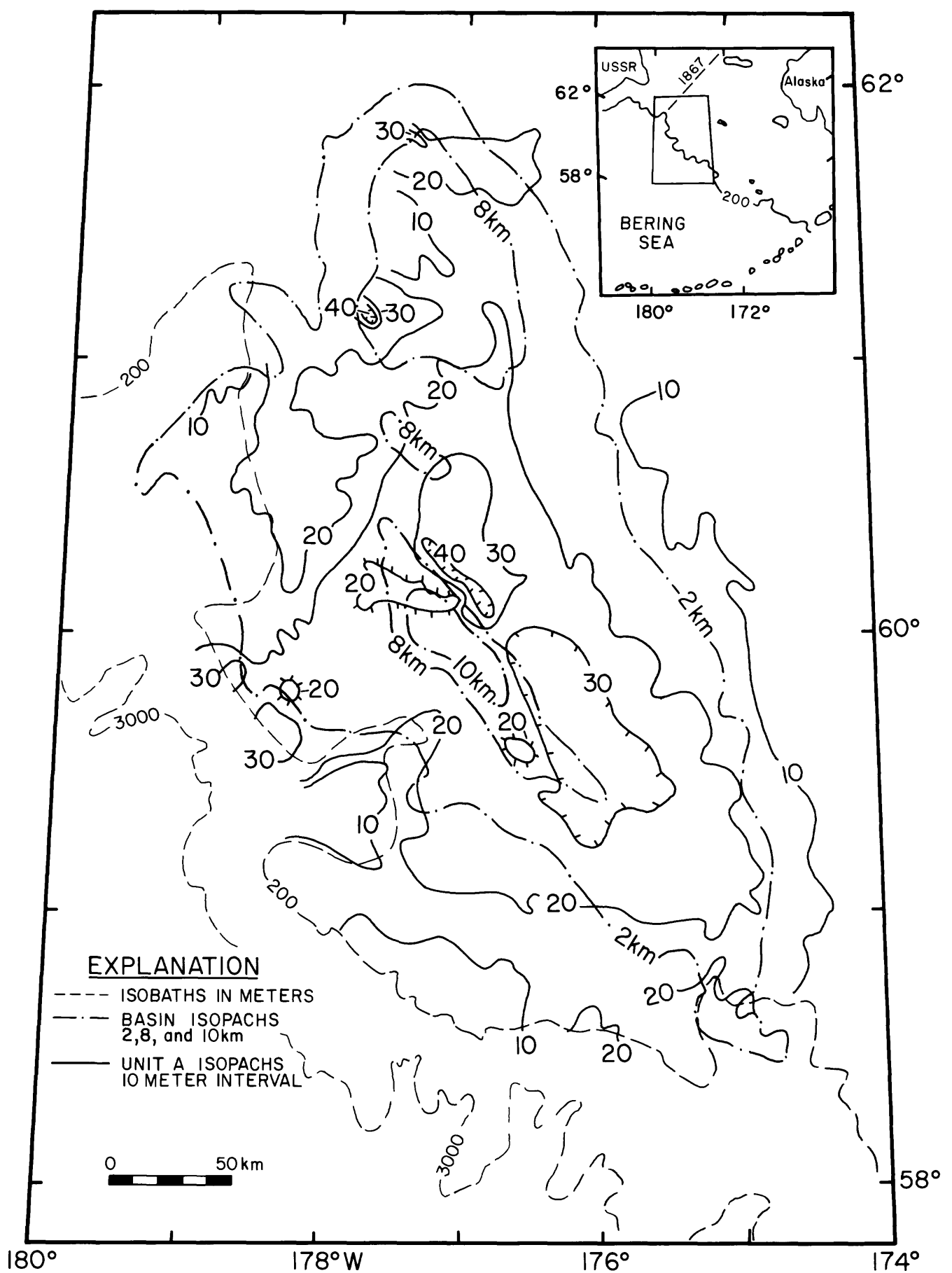
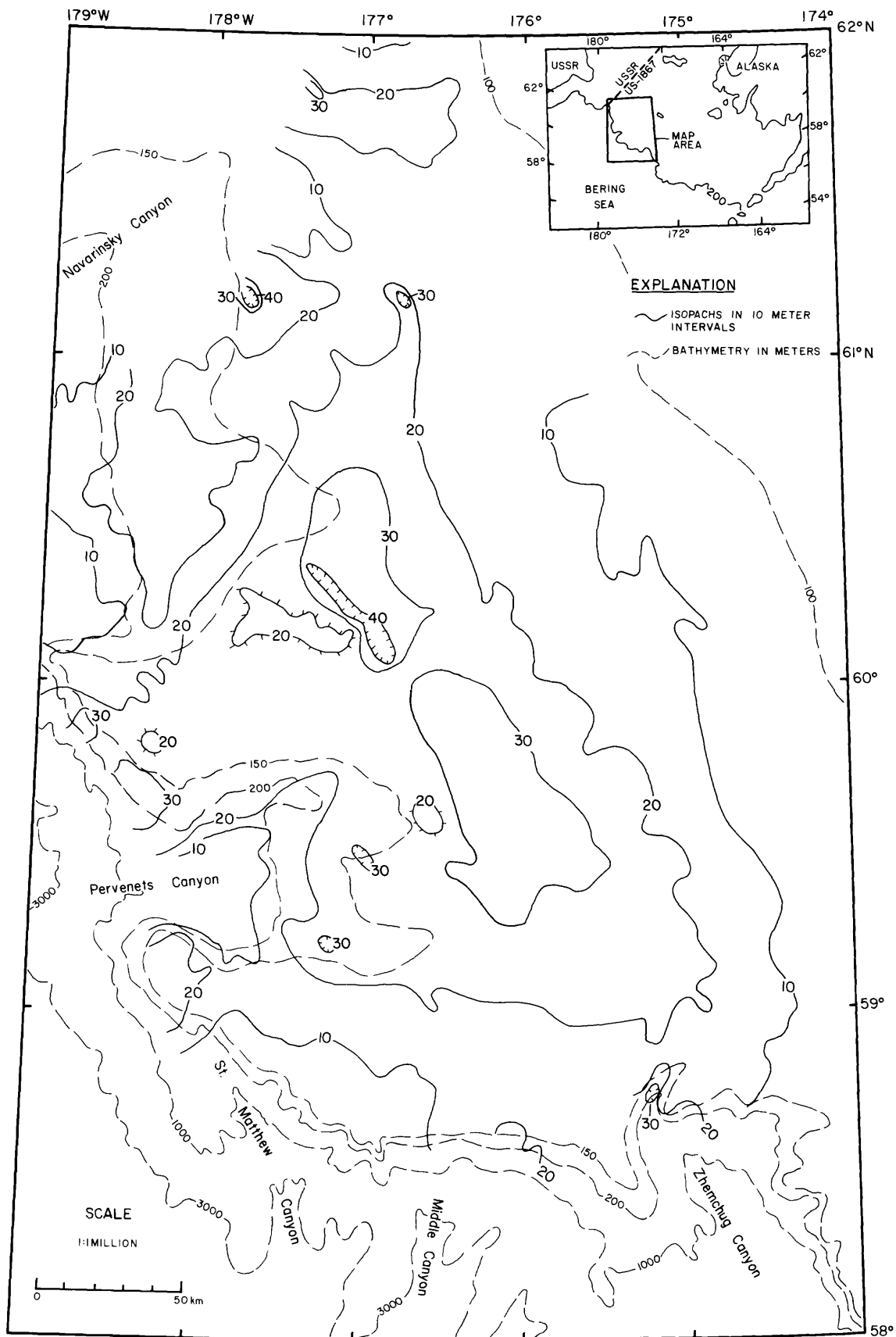


Figure 13. Isopach map of unit A superimposed on selected isopachs of strata above acoustic basement. Navarin Basin isopach above basement after Marlow and others (1979).



ISOPACH MAP OF UNIT A, YOUNGEST STRATIGRAPHIC SEQUENCE IN NAVARIN BASIN

Figure 14. Isopach map of unit A, youngest stratigraphic sequence in Navarin Basin.

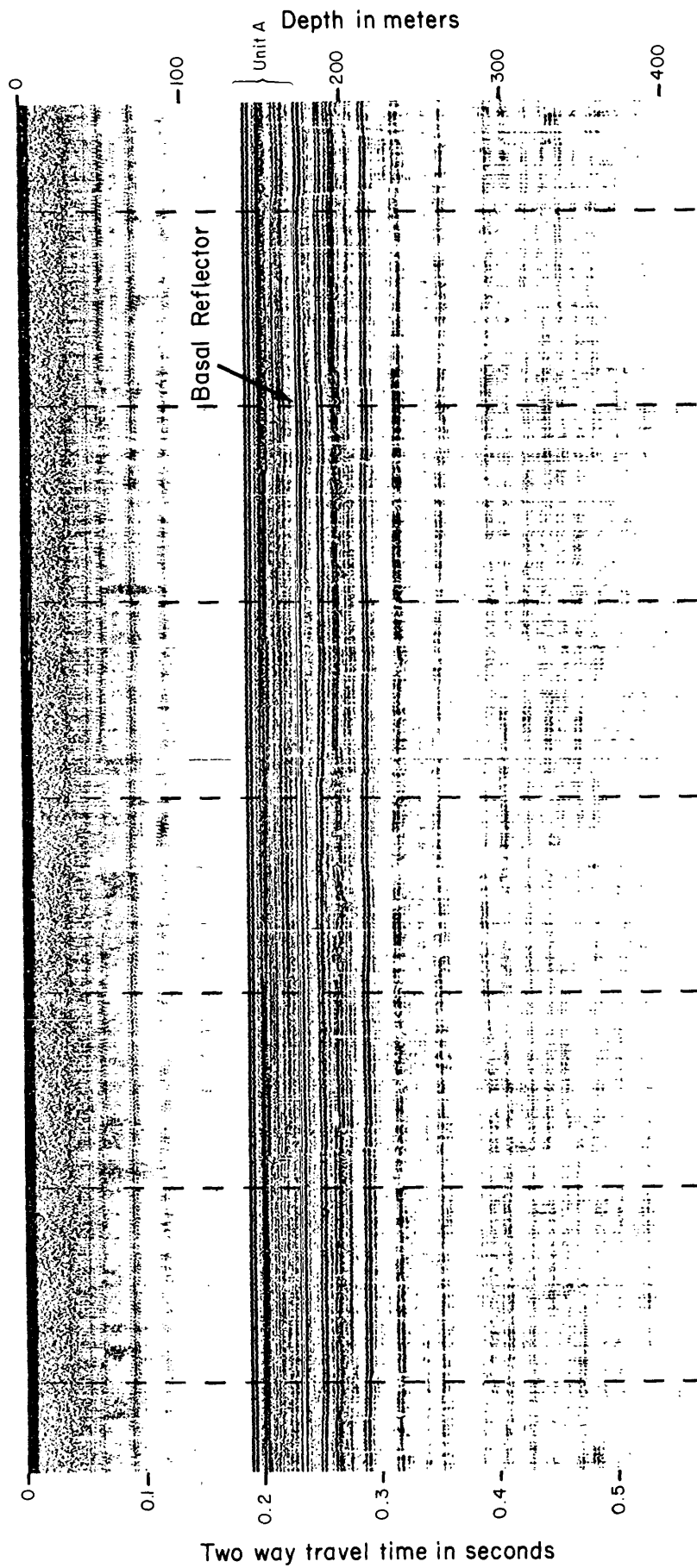


Figure 15. Minisparker profile (1000 J) showing seismic reflector (marked by arrow) that marks the base of isopached unit A. Vertical exaggeration ~8.5x.

CHAPTER 7: SUMMARY OF NAVARIN BASIN GEOTECHNICAL CHARACTERISTICS

by

Brian D. Edwards and Homa J. Lee

INTRODUCTION

Geotechnical properties were determined on recovered cores as a means of assessing sedimentary processes of engineering importance. One such property, the estimated in place shearing strength, is a critical sediment geotechnical property used in the evaluation of geologic hazards. Also determined were index properties and consolidation (i.e., relative degree of compaction) characteristics of the sediment. Index properties (e.g., undrained vane shear strength, water content, and grain-size distribution) were measured to classify the sediment and to correlate with advanced strength test results. Consolidation properties were measured to determine the effects of past geologic events (e.g., erosion of overburden).

Figure 16 shows major physiographic features in the Navarin Basin province. Of the 212 gravity cores and grab samples collected from the R/V Discoverer in 1980 and 1981 (Fig. 16), 149 were analyzed for geotechnical information. The majority of these cores were analyzed only for simple index properties (vane shear strength and water content). Seven cores from the 1980 R/V Discoverer cruise were taken as replicate cores at selected coring sites (Fig. 16). Each replicate core was analyzed for the index properties listed above in addition to grain specific gravity, Atterberg limits, one-dimensional consolidation characteristics, and static and cyclic triaxial shear strength.

After collection, each core was cut into multiple sections onboard ship using a rotary knife blade cutter. Core sections, excluding those of replicate cores, were split longitudinally using a specially designed, knife blade cutting system and a wire saw. Although sample disturbance is aggravated by such longitudinal splitting, this procedure allows more frequent downcore testing while maintaining sample integrity for other analyses (e.g., X-ray radiography, photography, and textural analysis). Testing for undrained vane shear strength and water content subsampling was conducted onboard ship.

The replicate cores collected for more advanced geotechnical testing were sectioned as described above, but were not split longitudinally. Vane shear tests were conducted and water content subsamples were taken at the top of each unsplit core section. End caps were sealed on both ends of each core section. The core sections were then wrapped in cheesecloth, sealed with a non-shrinking, microcrystalline wax, labelled, and stored vertically in refrigeration. The replicate cores were shipped by refrigerated air transport from Kodiak, Alaska, to refrigerated storage facilities at the U.S. Geological Survey laboratory in Palo Alto, California. These cores were subsequently shipped by refrigerated freight to Ertec Western, Inc., a commercial geotechnical testing laboratory in Long Beach, California, for advanced geotechnical analyses.

TESTING PROGRAM

Index Property Tests

Undrained Vane Shear Strength

Methods. Strength measurements were made using a motorized miniature vane shear device. Tests were made with a four-bladed 1/2 inch diameter and 1/2 inch tall vane which was inserted into the cores so the top of the vane was buried by an amount equivalent to blade height. Torque was applied to the vane through either a torque cell or a calibrated spring. Rotation rate of the torque cell and the top of the calibrated spring was a constant 90° per minute. When the spring system was used, torsion was measured and correlated directly with torque applied at the vane. Because of the spring's flexibility, rotation rate at the vane changed throughout the test. Tests were made on the ends of each core section and at 20 cm intervals on longitudinally split core sections.

Undrained vane shearing strength (S_v), as determined with the Wykeham-Ferrance device, was calculated from peak torque by assuming that the sediment builds a peak shearing resistance everywhere, and at the same time, along a right-circular cylinder inscribed around the vane. This term (S_v) is commonly equated with the undrained shear strength of the sediment (S_u).

Findings. The Navarin Basin province can be divided into 3 morphologic zones: (1) the shelf, typically shallower than the 150 m isobath; (2) the shelf edge and uppermost slope (about 150 to 200 m); and (3) the continental slope and uppermost continental rise (about 200 m to 3600 m). The shelf edge and uppermost slope is typically a zone of sand and muddy sand (Karl and others, 1981). Because vane shear strengths of cohesionless sediments, such as those at the shelf edge, have little value due to pore water drainage during sampling and testing, the zone of cohesionless sediment has been identified and excluded from the data base for undrained vane shear strength.

The areal distribution of vane shear strength at a subbottom depth of 1 m is shown in Figure 18. On the shelf, undrained vane shear strengths range from 2 kPa to 22 kPa. A zone of relatively weak sediment (<10 kPa) occupies the shelf about 150 km west of St. Matthew Island. West of this zone, adjacent to Pervenets Ridge, is a zone of relatively high (>15 kPa) shear strength. To the southeast, near the head of Zhemchug Canyon, is another zone of relatively high (>10 kPa) shear strength. For slope cores, shear strengths at a 1 m subbottom depth ranged from 2 kPa to 51 kPa. Shear strengths were relatively high (>10 kPa) at the heads of canyons (e.g., Navarinsky Canyon). Most of the lower slope sediment, below 1500 m, had shear strengths less than 5 kPa. Three sites, one in Pervenets Canyon, one below Navarin Ridge, and a third at the headwall of Zhemchug Canyon, had high shear strengths (ranging from 38 to 51 kPa). Data from consolidation tests show that these high strengths likely represent older sediments exposed due to slumping or erosion.

All the cores recovered on the shelf were less than 3 m long and were concentrated in the northern part of the area. Some slope and rise cores, however, achieved penetrations of up to 5 m. At these greater subbottom

depths the isolated sites of high shear strength identified at the 1 m horizon become zones of anomalously strong sediment (see Fig. 19) and likely represent older (possibly Pleistocene?) sediment exposed by slumping or erosion. Shear strengths at 5 m subbottom depth ranged from 5 kPa to 27 kPa.

Water Content

Methods. Water content (computed as percent dry weight of sediment) and bulk density subsamples were obtained from the location of the vane test immediately following strength testing. These samples were taken with a small tube sampler and stored in sealed sample bottles for subsequent analyses at the shorebased laboratory.

Water contents were determined following ASTM Standard D2216-80. The data were salt corrected using an assumed salinity of 32.5 parts per thousand.

Findings. The areal distribution of water content at a subbottom depth of 1 m is shown in Figure 20. Shelf sediments at 1 m have water contents ranging from 20% to 137% with the highest values being associated with the zone of weak sediment 150 km west of St. Matthew Island. The lowest measured water contents are associated with the Navarin Ridge. At a 1 m subbottom depth on the slope and rise, water contents increase to the south and with increasing water depth (Fig. 20). With increasing subbottom depth on the slope and rise, water contents decrease across the entire area; values increase to the south and with increasing water depth (e.g., Fig. 21).

Bulk densities were computed directly from the water content data following standard formulas and assuming 100% saturation (e.g., Lambe and Whitman, 1969). In place effective overburden stress (σ'_v) was computed as:

$$\sigma'_v = \sum_0^z \gamma'_c \Delta z \dots \dots \dots (2)$$

where γ'_c = sediment submerged bulk density; $\gamma'_c = \gamma_c - \gamma_{sw}$
 γ_c = sediment bulk density
 γ_{sw} = density of seawater
 z = subbottom depth in cm

Values of σ'_v are summarized in Table 4a.

Grain Specific Gravity

Twenty-one grain specific gravity tests were performed in accordance with ASTM Standard D854-58. Most of the sample specimens were taken from trimmings of the triaxial test samples. Salt corrections were not applied in the computations. Values of grain specific gravity ranged from 2.55 to 2.77, with an average value of 2.64. The smaller values are lower than most continental shelf sediment grain specific gravity values and likely indicate the presence of diatoms.

Atterberg Limits

Methods. Atterberg Limits tests were performed on 50 samples following the procedures of ASTM Standards D423-66, D424-59, and D2217-66. A salt correction assuming a salinity of 32.5 parts per thousand was applied in the computation.

Findings. The plasticity index (PI) ranged from 3 to 38 and the liquid limit (LL) ranged from 27 to 83. On a plot of liquid limit versus plasticity index (plasticity chart, Fig. 22), Navarin Basin province sediment varies dramatically. Within the Unified Soil Classification System (e.g., Mitchell, 1976), descriptive names are assigned to different parts of the plasticity chart based on empirical observations. According to the terminology of this system, Navarin Basin shelf sediments (cores G61, G111) are inorganic silts of medium to high compressibility and are more highly compressible (core G61) in the northern part of the province near Navarinsky Canyon. Sediment from Navarinsky Canyon, (cores G31 and G34) however, is typically inorganic clay of low to medium plasticity combined with some inorganic silts of medium compressibility. Farther south, near the head of St. Matthew Canyon (core G74), the sediment behaves as a highly compressible inorganic silt or organic clay exhibiting a wide range of liquid limit and plasticity index values. This behavior likely reflects significant variations in diatom content. Slope sediment near the head of Zhemchug Canyon (core G97) behaves as a highly compressible inorganic silt.

Grain-Size Distribution

Procedures and results from grain-size analyses of surficial sediments are summarized in Chapter 3, this report.

Advanced Geotechnical Tests

Consolidation Tests

Methods. One dimensional consolidation tests were performed on 15 specimens in general accordance with ASTM D2435-70. Maximum past overburden stress (σ'_{vm}) was determined by the Casagrande procedure (Casagrande, 1936); values are summarized in Table 4a. These maximum past stresses were used to determine consolidation pressures for triaxial tests and to estimate the amount of overburden removal due to slumping or erosion in some areas. Overconsolidation ratios (OCR's, the ratio of σ'_{vm} to σ'_v) are reported in Table 4a. For normally consolidated sediment, $\sigma'_{vm} = \sigma'_v$ and thus OCR=1.

Findings. All of the Navarin Basin sediment tested was overconsolidated as shown in Table 4a. A characteristic of the Navarin replicate cores is very high OCR's at shallow (<30 cm) subbottom depths (e.g., see core G 78, 10-15 cm of Table 4a). Such large OCR's are accentuated by the extreme contrast between σ'_{vm} and σ'_v that characterizes the uppermost part of the cores. Such high levels of overconsolidation are unlikely, however, given the low surface strengths, lack of obvious depositional hiatuses, and uniform increase in vane shear strength with depth which all suggest normal consolidation.

Excluding the uppermost 30 cm, cores G31, G34, G61, and G74 are lightly to moderately overconsolidated (OCR 2-5). Higher levels of overconsolidation were determined for the core recovered from the headwall of Zhemchug canyon (G97) and likely indicates the removal of about 15 m of sediment by slumping. Some shelf cores exhibit high levels of overconsolidation (e.g., OCR 30 for Core G76). The cause of the observed overconsolidation is uncertain. Sediment on the shelf can be subjected to a number of loads capable of inducing this overconsolidation state (e.g., erosion of overlying material, cyclic loading, cementation, ice loading, and subaerial exposure at low sea level stands). At present, we have insufficient data to evaluate these mechanisms.

Strength Evaluation

Methods. A triaxial testing program was designed to evaluate the strength characteristics, including strength degradation due to cyclic loading, of the Navarin Basin sediment. A total of 36 static and 18 cyclic, consolidated, undrained triaxial compression tests were performed in general accordance with procedures described by Bishop and Henkel (1962). Sample specimens were selected using X-ray radiograph interpretations of each core section.

Findings. Preliminary results of the triaxial testing program are presented in Table 4b. Navarin Basin fine-grained sediment is moderately susceptible to strength degradation during cyclic loading. For example, undrained shear strengths typically were reduced to 51% to 80% of static strength (A_D) during 10 cycles of cyclic loading (Table 4b). Core G31 showed an increase in strength during cyclic loading that possibly was erroneous due to procedural difficulties with that test.

SUMMARY OF FINDINGS

- (1) A zone of cohesionless sediment exists at the shelf break.
- (2) Undrained vane shear strengths on the shelf are lowest on the central shelf about 150 km west of St. Matthew Island. Strengths are highly variable across the continental slope, possibly due to slumping, erosion, or changes in the depositional regime. In general, strengths increase downcore, and decrease to the south and with increasing water depth.
- (3) Water contents on the shelf are highest in the zone of weak shelf sediment. Values in the slope province decrease with subbottom depth, and increase to the south and with increasing water depth.
- (4) Grain specific gravities ranged from 2.55 to 2.77 with an average value of 2.64. The variability likely results from changes in diatom content.
- (5) Where plastic behavior is exhibited, Atterberg Limits and the Unified Soil Classification System show the shelf sediment to be mostly inorganic silts of medium to high compressibility. Slope sediments are typically highly compressible inorganic silts or organic clays.

- (6) Navarin Basin sediment is typically overconsolidated, but not heavily except for a few locations. OCR values on the shelf are commonly greater than 10. Elsewhere in the province, values are $OCR \sim 2-5$. About 15 m of sediment has been removed from the headwalls of Zhemchug Canyon (core G97).
- (7) Cyclic loading reduces static strength by 20 to 50%.

NOMENCLATURE

- A_D = cyclic degradation factor applied to S_u as a result of cyclic loading
- LL = liquid limit from Atterberg Limit determinations
- OCR = overconsolidation ratio; defined as $OCR = \sigma'_{vm} / \sigma'_v$
- PI = plasticity index of Atterberg Limits; defined as $PI = LL - PL$
- PL = plastic limit of Atterberg Limit determinations
- S_u = static undrained shear strength
- S_v = undrained peak vane shear strength
- z = subbottom depth in cm
- γ_c = sediment bulk density
- γ'_c = sediment bulk density corrected for the density of seawater;
 $\gamma'_c = \gamma_c - \gamma_{sw}$
- γ_{sw} = density of seawater
- σ'_v = in place effective overburden stress
- σ'_{vm} = maximum past overburden stress

REFERENCES

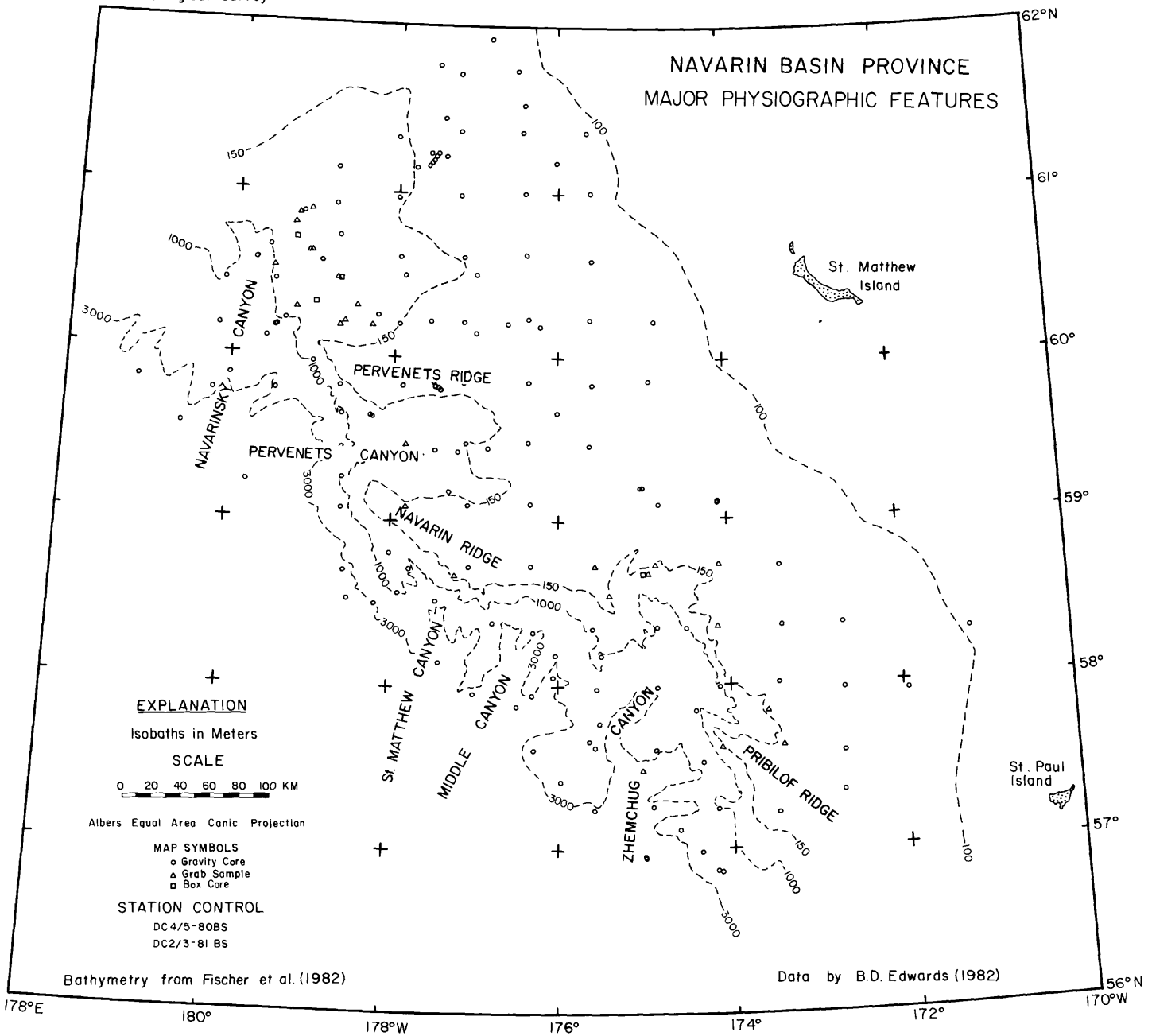
- ASTM, 1982, Annual Book of ASTM Standards, Part 19, Natural Building Stones, Soil and Rock; Philadelphia, 710p.
- Bishop, A.W., and D.J. Henkel, 1962, The Measurement of Soil Properties in Triaxial Test, Second Edition, Edward Arnold, Ltd., London, 228 p.
- Casagrande, Arthur, 1936, The determination of the preconsolidation load and its practical significance: Proc. First Int'l Conf. Soil Mech. Found. Eng., Cambridge, MA, p. 60.
- Fischer, J.M., P.R. Carlson, and H.A. Karl, 1982, Bathymetric map of Navarin Basin province, northern Bering Sea: U.S. Geological Survey Open-File Report 82-1038, 11p.
- Karl, H.A., P.R. Carlson, Jeff Fischer, Ken Johnson, and Beth Lamb, 1981, Textural variations and composition of bottom sediment: in P.R. Carlson and H.A. Karl, Seafloor geologic hazards, sedimentology, and bathymetry: Navarin Basin province, northwestern Bering Sea: U.S. Geological Survey Open-File Report 81-1217, 149p.
- Lamb, T.W., and R.V. Whitman, 1969, Soil Mechanics, John Wiley & Sons, Inc., New York, 553p.
- Mitchell, I.K., 1976, Fundamentals of Soil Behavior, John Wiley and Sons, Inc., New York, 422 p.

Table 4a. Summary of Consolidation test results

Core	Z cm	σ'_{vm} (kPa)	σ'_v (kPa)	OCR
G 31	10-13	30	0.7	43
	119-122	20	8	2.5
	214-217	65	15	4.3
G 34	121-124	35	8	4.4
	220-223	52	15	3.5
G 61	119-121	30	6	5
	223-226	35	11	3.2
G 74	22-25	19	0.7	27
	164-168	30	6	5
G 78	10-15	90	0.8	112
G 76	50-55	100	3.3	30
G 97	35-40	22	2	11
	187-192	116	10	11.6
G 111	15-20	20	1.1	18
	95-100	60	6	10

Table 4b. Summary of triaxial test results -

Core	Depth in Core (cm)	Initial OCR	σ'_v (kPa)	OCR=1 A_D %
G 31	10-13	43	0.7	162
	119-122	2.5	8	
	214-217	4.3	15	
G 34	121-124	4.4	8	80
	220-223	3.5	15	
G 61	119-121	5	6	75
	223-226	3.2	11	
G 74	22-25	27	0.7	63
	164-168	5	6	
G 78	10-15	112	0.8	51
G 76	50-55	30	3.3	
G 97	35-40	11	2	71
	187-192	11.6	10	
G 111	15-20	18	1.1	75
	95-100	10	6	



THIS REPORT IS PRELIMINARY AND HAS NOT BEEN REVIEWED FOR CONFORMITY WITH U.S. GEOLOGICAL SURVEY EDITORIAL STANDARDS

Figure 16. Major physiographic features of Navarin Basin province (after Fischer et al., 1982), and core locations for 1980 and 1981 R/V DISCOVERER cruises.

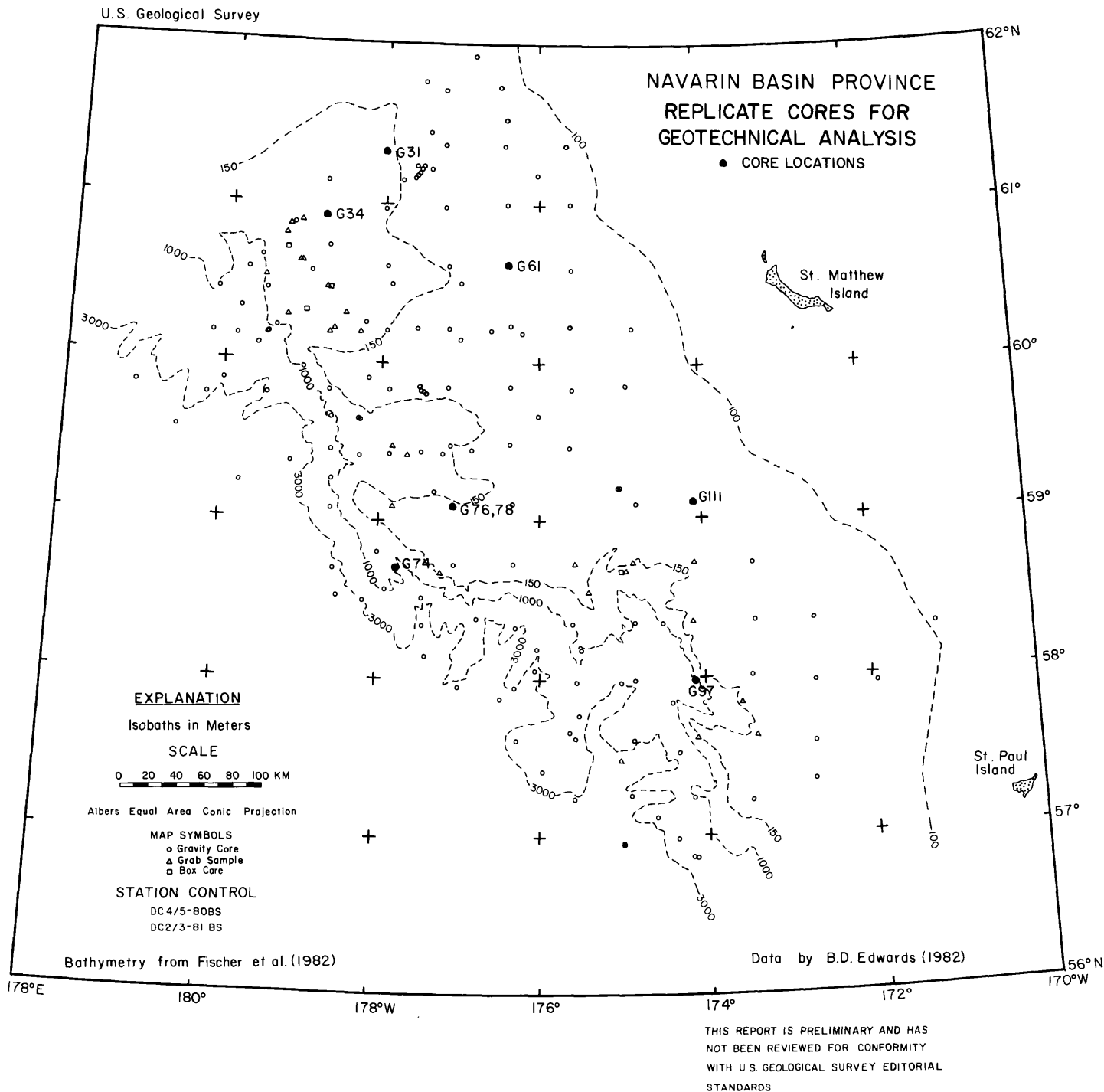
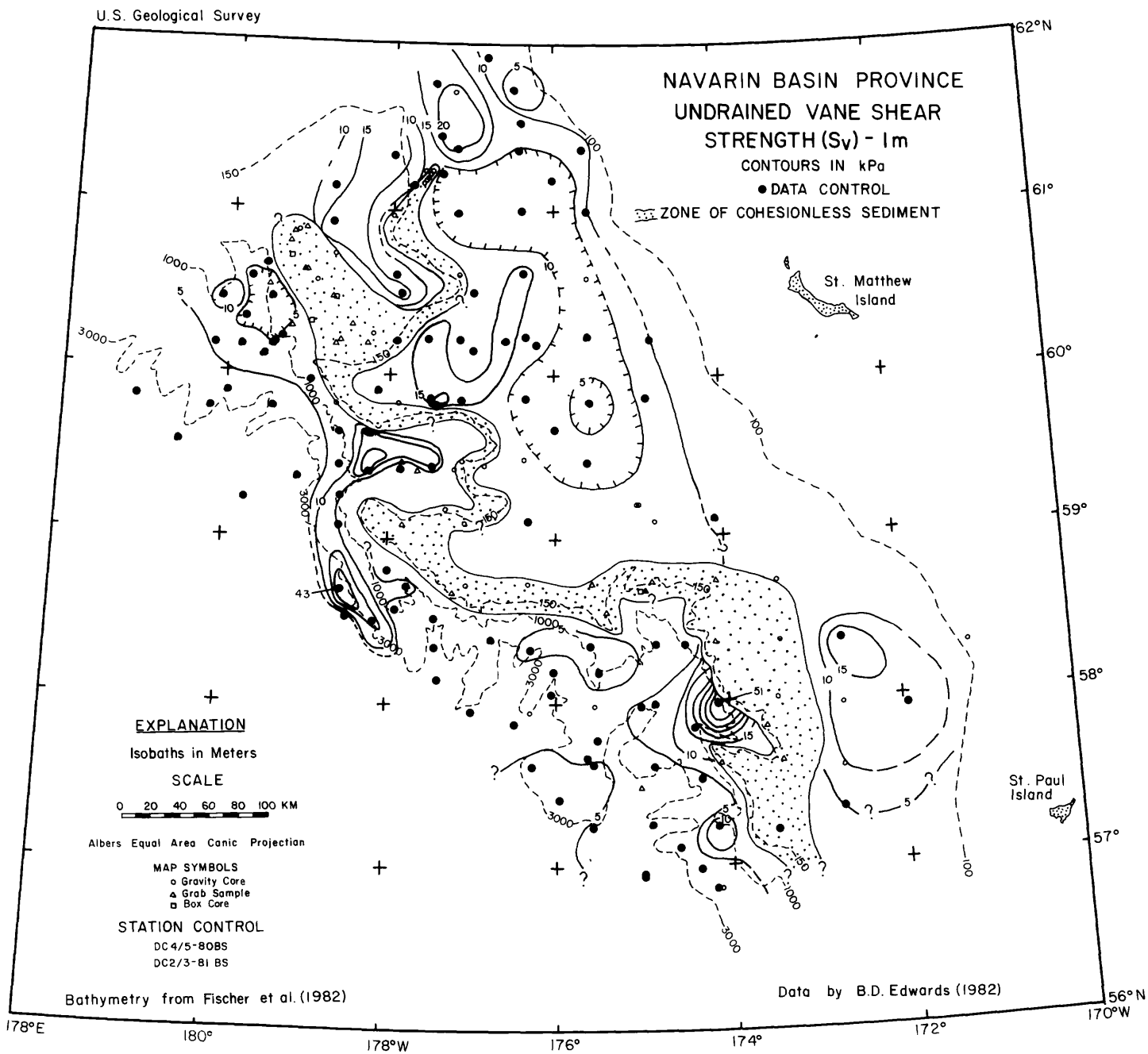
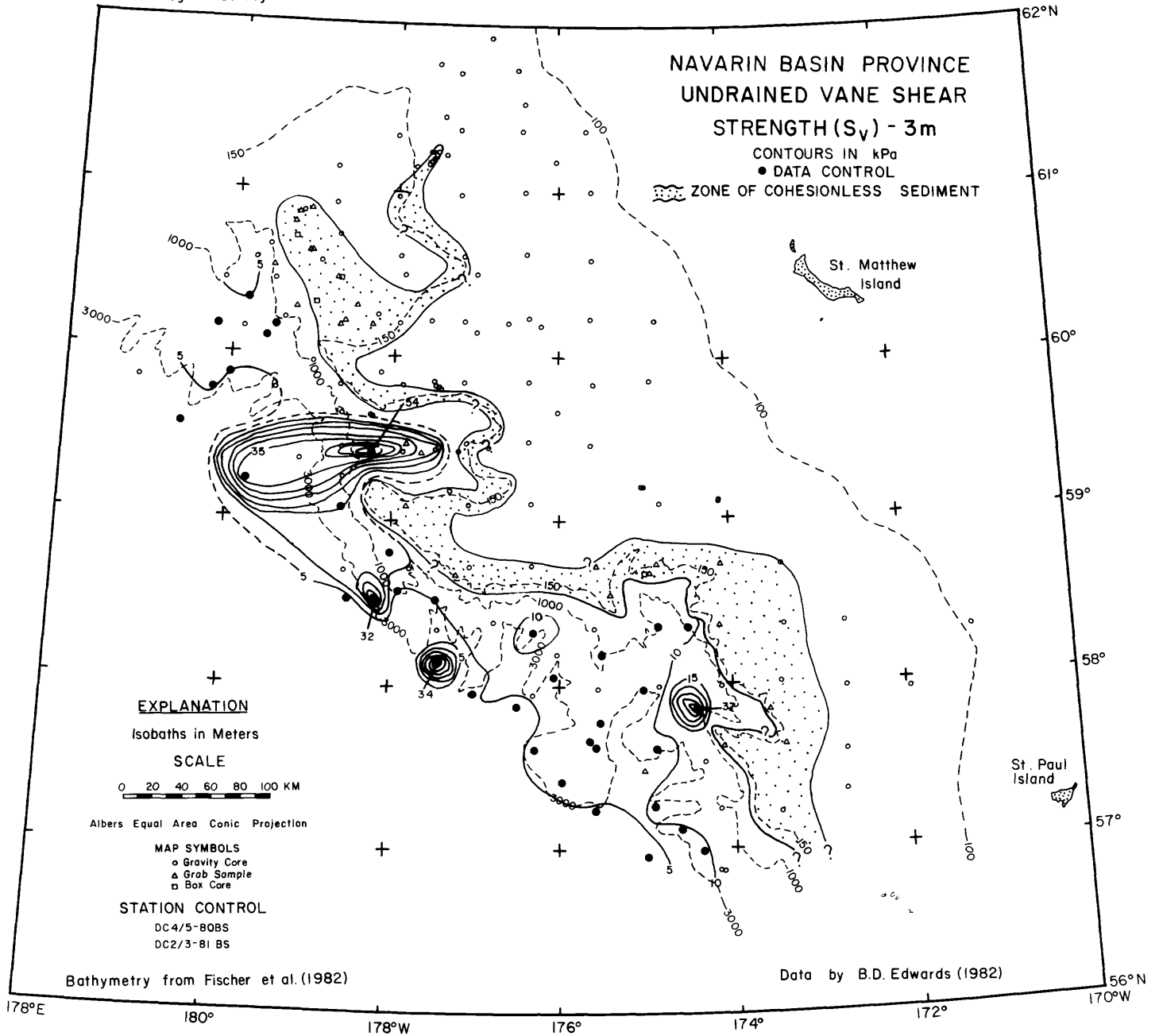


Figure 17. Location map of replicate cores collected for advanced geotechnical testing of Navarin Basin province sediment, 1980 R/V Discoverer cruise.



THIS REPORT IS PRELIMINARY AND HAS
NOT BEEN REVIEWED FOR CONFORMITY
WITH U.S. GEOLOGICAL SURVEY EDITORIAL
STANDARDS

Figure 18. Areal distribution of peak undrained vane shear strength S_v at a subbottom depth of 1 m. Contour interval 5 kPa.



THIS REPORT IS PRELIMINARY AND HAS NOT BEEN REVIEWED FOR CONFORMITY WITH U.S. GEOLOGICAL SURVEY EDITORIAL STANDARDS

Figure 19. Areal distribution of peak undrained vane shear strength S_v at a subbottom depth of 3 m. Contour interval 5 kPa.

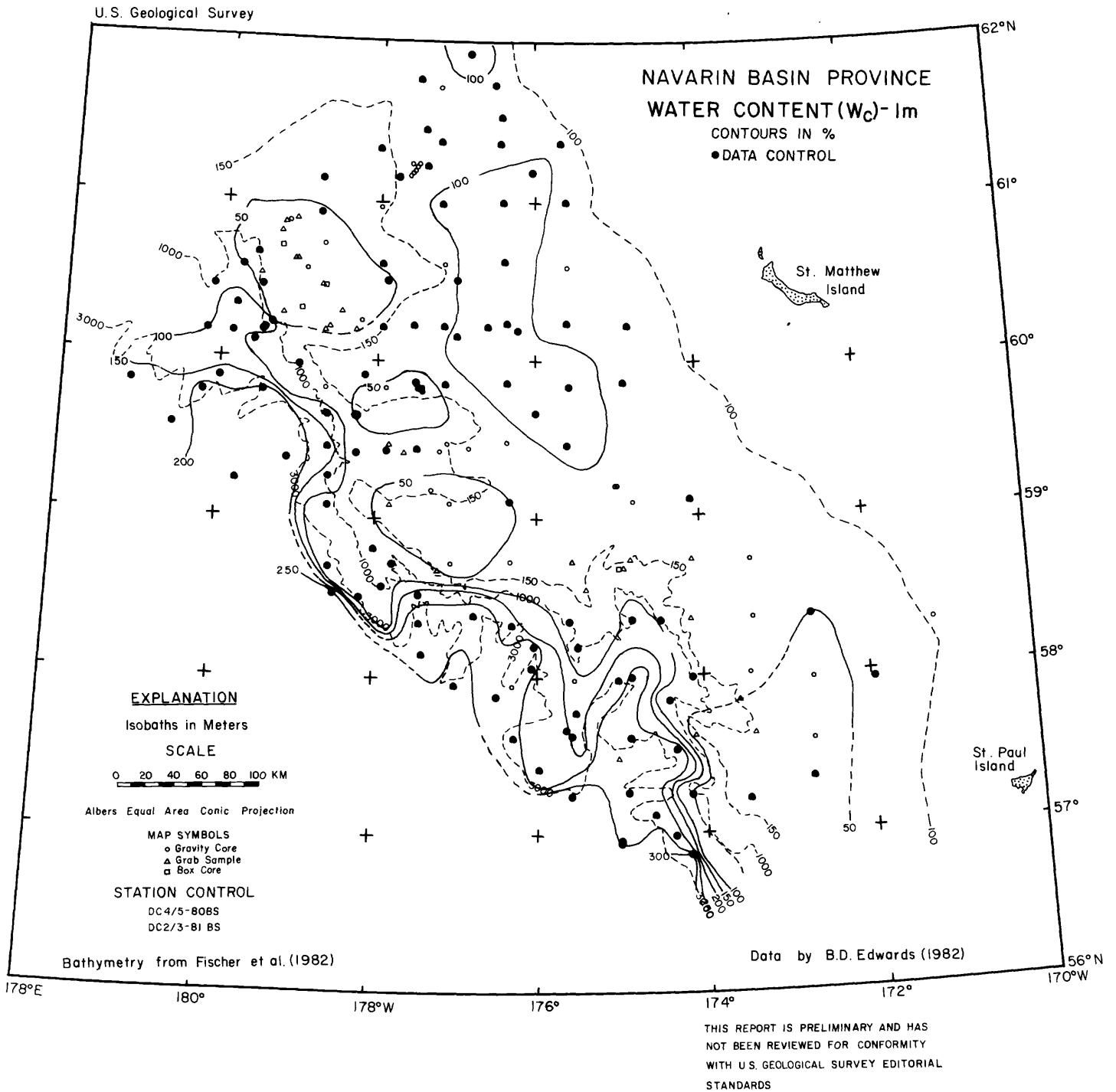


Figure 20. Areal distribution of salt corrected water content (W_C) at a subbottom depth of 1 m. Contour interval 50% by dry weight.

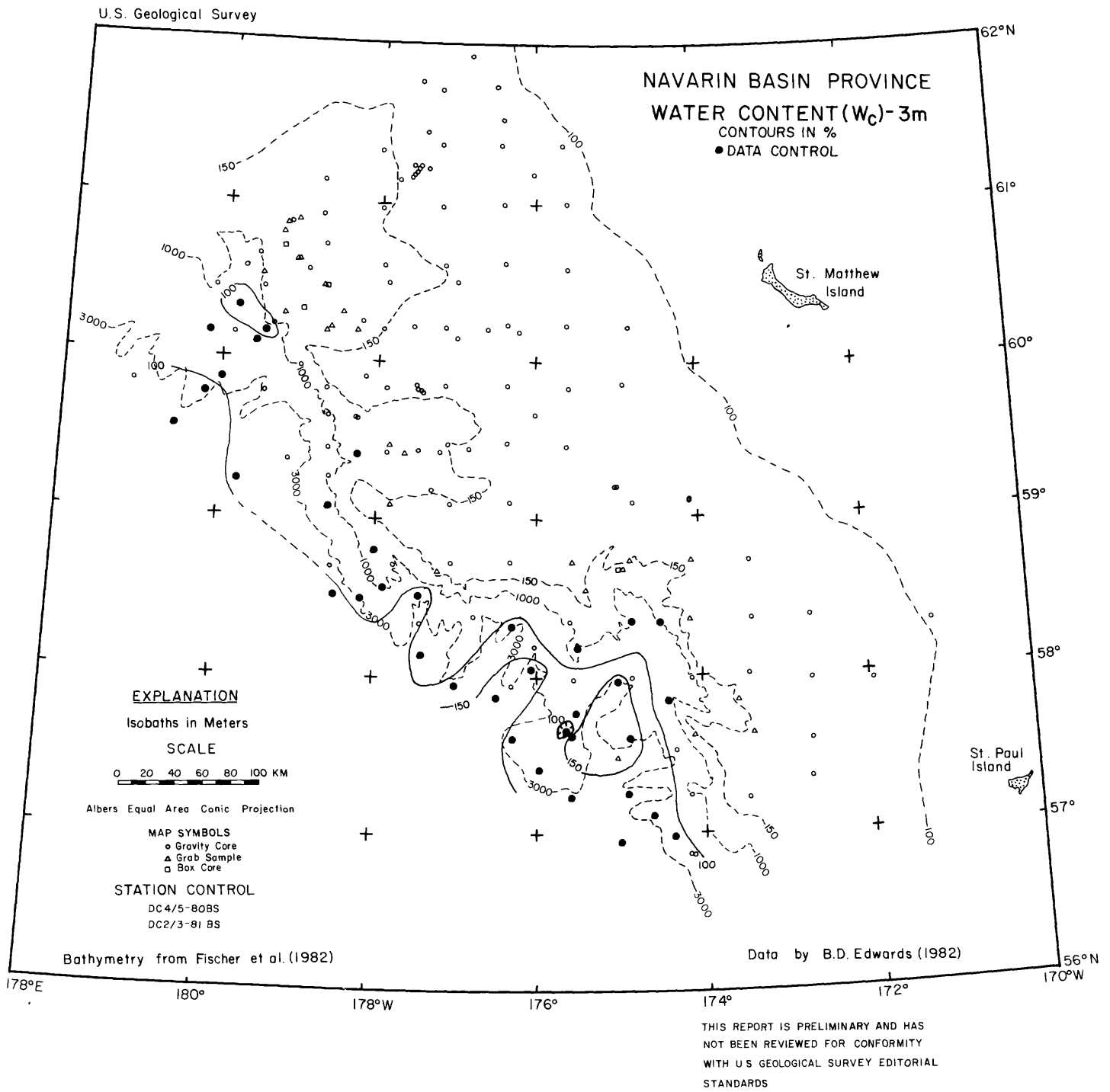


Figure 21. Areal distribution of salt corrected water content (W_c) at a subbottom depth of 3 m. Contour interval 50% by dry weight.

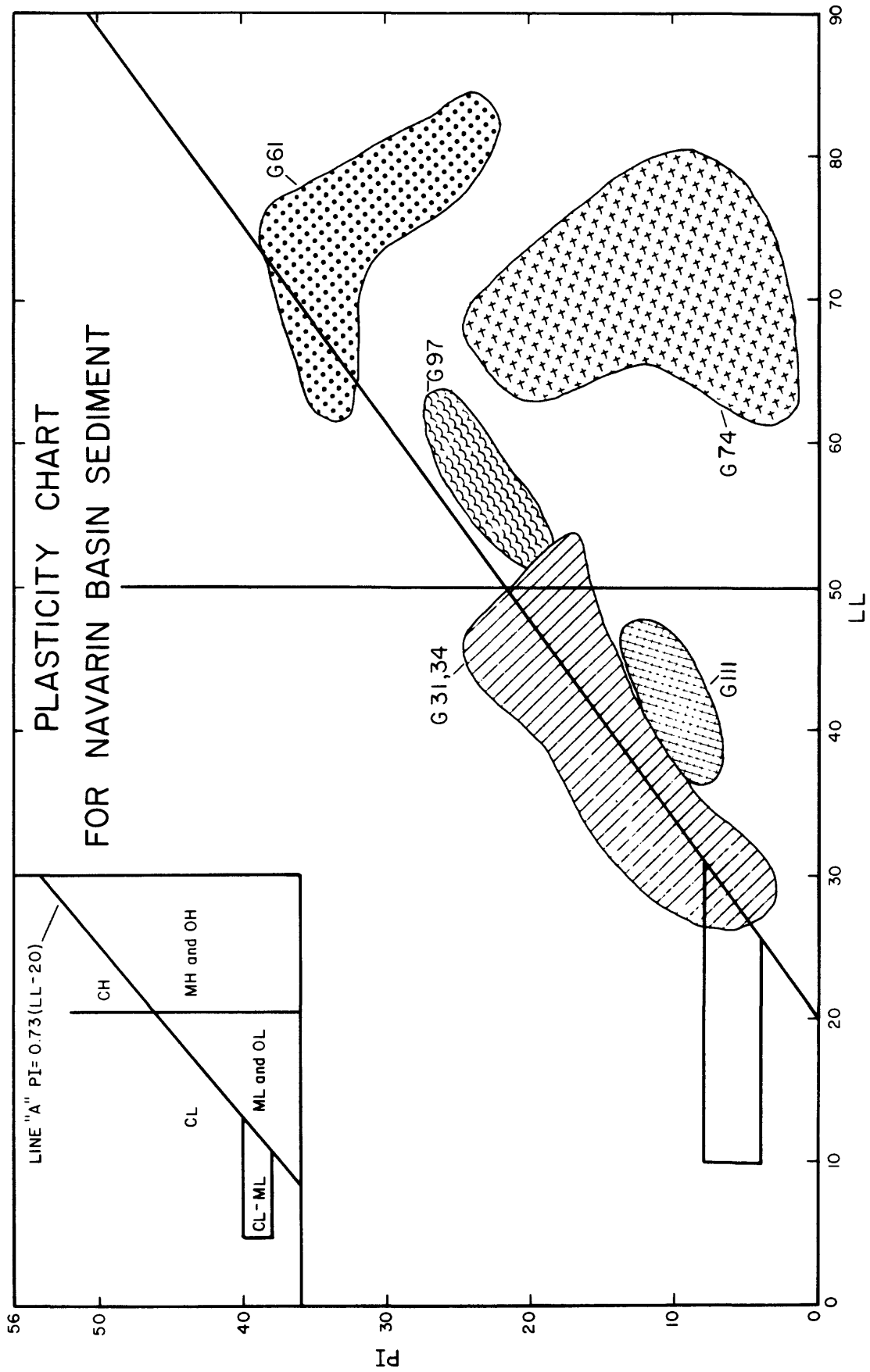


Figure 22. Plasticity chart for Navarin Basin province replicate cores. Data from 1980 R/V Discoverer cruise.

CHAPTER 8: HYDROCARBON GASES IN SEDIMENTS --
RESULTS FROM 1981 FIELD SEASON

by

Margaret Golan-Bac and Keith A. Kvenvolden

INTRODUCTION

This study examines the distribution and origin of the hydrocarbon gases methane (C_1), ethane (C_2), ethene ($C_{2=}$), propane (C_3), propene ($C_{3=}$), isobutane ($i-C_4$), and normal butane ($n-C_4$) in surficial sediments from the shelf, slope, and rise areas of the Navarin Basin province in the Bering Sea. The report covers results obtained on samples collected in 1981. Results for samples collected in 1980 have been reported previously (Vogel and Kvenvolden, 1981).

Methods

Conventional gravity cores were taken from the shelf, slope, and rise areas of the Navarin Basin province from which sediment samples were obtained for gas samples. The 8 cm internal diameter core liner was cut into 10 cm sections at approximately 1 meter intervals (usually 90-100, 190-200, 290-300 cm, etc.). The sediment section was immediately extruded into one liter unlined paint cans which had two septa-covered holes on the side near the top. Each can was filled with helium-purged salt water and 100 ml of water was removed before the can was closed with a double-friction-seal lid. This resulting 100 ml headspace was then purged with helium through the septa, and the cans were immediately inverted and frozen. In the shore-based laboratory, the cans of sediment were brought to room temperature and shaken for 10 minutes by a mechanical shaker to equilibrate the hydrocarbon gases that are released from the sediment and are partitioned into the helium headspace. A sample of gas in this headspace was withdrawn through a septa with a gas-tight syringe. One milliliter of this sample was analyzed by gas chromatography using both flame ionization and thermal conductivity detectors. Concentrations of gases were determined by comparison of the integrated area of each hydrocarbon with the integrated area of a quantitative hydrocarbon standard. These values were then corrected for the different solubilities of the hydrocarbon gases in the interstitial water of the sediment sample by use of partition coefficients (0.8 for methane; 0.7 for ethane, propane, and butanes; 0.6 for ethene and propene).

The method of extraction yields semi-quantitative results; however, because all the samples were processed in the same manner, the results can be compared. The concentrations reported in Table 5 are rounded with respect to limitations of the analytical techniques. The detection limit is approximately 0.1 μ l of methane/liter of wet sediment and 1 nl of gas/liter of wet sediment for the other hydrocarbon gases. Error determined from analytical variation and repeat analysis is less than 20%.

Results

Core locations, concentrations of hydrocarbon gas, and other relevant information for Navarin Basin province are listed in Table 5. This table is divided into three sections, namely, cores taken from the outer shelf (water depths from 100 to 150 m), the slope (water depths from 150 to 2800 m), and the rise (water depths from 2800 to approximately 3600 m). These three areas are delineated by the 150 m and 2800 m contour lines, and in Figure 23 samples are identified by their core number.

Information relative to the ranges of concentrations of hydrocarbon gases found in sediments of the shelf, slope, and rise are summarized in Table 8. Methane is the most abundant hydrocarbon gas in all the sediment samples analyzed and is typically present in concentrations that are 2 to 3 orders of magnitude greater than the concentrations of the other low molecular weight hydrocarbons (LMWH).

Areal distributions of maximum concentrations of C_1 , C_2+C_3 and $n-C_4+i-C_4$ are shown in Figures 24, 25 and 26, respectively. These maximum concentrations generally reflect results of analyses of the deepest samples obtained at a given core location, because the deepest samples usually have the highest concentrations of gas (Table 5). In five cores (11, 13, 14, 15 and 86), all located on the slope, the maximum concentrations of C_1 exceed 1000 $\mu\text{l/l}$ and range from 1400 to 84000 $\mu\text{l/l}$. In each of these cores C_1 concentrations increase 2 to 4 orders of magnitude with depth (Table 5).

Concentrations of C_2 exceed 1000 nl/l in samples from seven cores of slope sediment (15, 19, 38, 58, 66, 71 and 86) and from one core of shelf sediment (62). In these cores, C_2 concentrations increase 1 to 2 orders of magnitude with depth (Table 5). Concentrations of C_3 are usually less than concentrations of C_2 , but the distributions of these gases tend to be parallel. Figure 25 shows locations of eleven cores where the maximum concentrations of $C_2 + C_3$ exceed 1000 nl/l . These cores include numbers 11, 13 and 14 in addition to the eight cores listed above.

Butane ($n-C_4$ and $i-C_4$) are generally the least abundant LMWH in shelf, slope and rise sediment. Wherever detected, $i-C_4$ is generally more abundant than $n-C_4$; in most samples $n-C_4$ could not be measured. The highest concentrations of $n-C_4+i-C_4$ are found in slope sediment. Core 66 had the highest amount of $i-C_4$ (320 nl/l) and core 11 had the most $n-C_4$ (100 nl/l).

The alkenes ($C_{2=}$ and $C_{3=}$) are present in most sediment samples in amounts less than C_2 but generally greater than C_3 . Concentrations of $C_{2=}$ and $C_{3=}$ show no discernable trends with depth. In those samples where C_1 concentrations exceeded about 12000 $\mu\text{l/l}$, $C_{3=}$ could not be measured because of interference resulting from our method of analysis.

Biogenic Methane

The most abundant gas in sediments of Navarin Basin province is C_1 , and in five cores (11, 13, 14, 15, 86), all located in Navarinsky Canyon, maximum concentrations exceed 1000 $\mu\text{l/l}$ (Table 1 and Figure 2). During the 1980 season, the only core (G-37) analyzed with concentrations of C_1 exceeding 1000 $\mu\text{l/l}$ (1900 $\mu\text{l/l}$) was from the rise near the mouth of Navarinsky Canyon (Vogel and Kvenvolden, 1981). Concentrations for four of the five cores (11, 13, 14, and 86) taken during 1981 approach or exceed the saturation of the interstitial water at atmospheric pressure and temperature (about 40 ml of C_1

per liter of seawater according to Yamamoto et al., 1976). Because C_1 solubility increases with increasing pressure, the measured concentrations only represent minimum values; some quantity of gas likely escaped during the sampling procedure. In fact, initial core descriptions for three of the five cores include remarks about cracks attributed to escape of gas. The possibility that C_1 is present at concentrations exceeding its solubility in the interstitial water at depth may lead to high pore-water pressures and hence, sediment instability; seismic evidence indicates slumping of the sediments in the Navarinsky Canyon region (Carlson et al., 1982).

C_1 concentration profiles with depth for these five cores are shown in Figure 27A. The rapid increase in amount of C_1 with depth can be attributed to the presence of C_1 -producing bacteria operating under anoxic conditions. A zone of low C_1 concentration probably exists between the sediment-water interface and about 100 cm depth where the first measurements were made. This zone is generally referred to as the zone of sulfate reduction, where the low C_1 concentrations have been attributed to bioturbation and oxidation by molecular oxygen (Reeburgh, 1969), sulfate inhibition of methanogenesis (Martens and Berner, 1974), and to anaerobic C_1 oxidation by sulfate-reducing bacteria (Barnes and Goldberg, 1976; Reeburgh and Heggie, 1977). Below the zone of sulfate reduction is the zone of C_1 production where high concentration of C_1 occur. Here the C_1 is being generated by the anaerobic microbial decomposition of the organic-rich mud which ranges from 0.7 to 1.43% organic carbon (Fischer, 1981). Those samples having high C_1 concentrations (greater than 1000 $\mu\text{l/l}$) also have large $C_1/(C_2+C_3)$ values ranging from 900 to 43,000 (Table 5). These ratios indicate a biogenic source for C_1 according to criteria defined by Bernard et al. (1977).

At most stations in Navarin Basin the C_1 concentrations are less than 1000 $\mu\text{l/l}$ (Table 5 and Fig. 24). For these stations $C_1/(C_2+C_3)$ values are usually low. In fact, for many samples the ratio is less than 50, which is the upper limit of the range of values assigned by Bernard et al. (1978) to gas from thermogenic sources. However, as pointed out by Kvenvolden and Redden (1980), use of this ratio for assigning source is equivocal where gas concentrations are low. In the case of Navarin Basin, we believe that most of the C_1 and other hydrocarbon gases present are from biogenic sources and not from thermogenic sources. The low $C_1/(C_2+C_3)$ ratios are attributed to preferential loss of C_1 during sampling from sediments in which the original concentrations of C_1 are much lower than 1000 $\mu\text{l/l}$.

Other Biogenic Hydrocarbons

Other LMWH besides C_1 may be biologically produced, as suggested by Emery and Hoggan (1958) and Bernard et al. (1978). The relationship of C_1 to these other hydrocarbon gases may provide a clue to their origin. At the eleven sites with C_2+C_3 concentrations greater than 1000 nl/l (11, 13, 14, 15, 19, 38, 58, 62, 66, 71, and 86), five sites (11, 13, 14, 15, and 86) show a strong correlation between increasing C_1 concentrations and increasing C_2+C_3 concentrations with depth. This correlation suggests that the microbiological processes that produced C_1 may be operating in parallel with the process responsible for C_2 and C_3 . Samples at all five sites also have anomalously

high butane values (Table 5, Fig. 26) which suggest butane may also result from microbiological processes.

The production of alkenes is controlled by biological processes and has been produced by microbes in the laboratory (Davis and Squires, 1954), by marine organisms (Hunt, 1974), and by bacteria in soils (Primrose and Dilworth, 1976). In the Navarin Basin province, alkene concentrations vary with depth but generally remain at about the same level of concentration throughout the area.

Thermogenic Hydrocarbons

Two ratios ($C_1/(C_2+C_3)$ and $C_2/C_{2=}$) were used by Kvenvolden et al. (1981) to attempt to distinguish biogenic and thermogenic hydrocarbon gases in sediments. Extrapolating from the work of Bernard et al. (1976) and from Cline and Holmes (1977) they proposed samples containing gases with $C_1/(C_2+C_3)$ values less than 50 and with $C_2/C_{2=}$ values greater than 1 may have thermogenic sources.

Of the thirteen sites (12, 19, 20, 22, 38, 57, 58, 60, 62, 66, 71, 77, and 88) where $C_1/(C_2+C_3)$ ratios are low and $C_2/C_{2=}$ ratios are high (Table 5), core 66 is of particular interest. The $C_1/(C_2+C_3)$ values in core 66 are 20 and 24 at 200 and 300 cm depth. These values are comparable to the ratios of possible thermogenic gas in cores from St. George Basin (Kvenvolden and Redden, 1980) and core 36 from the 1980 work in Navarin Basin (Vogel and Kvenvolden, 1981). The $C_2/C_{2=}$ ratio of 440 in Core 66 is the highest in the sampling area and in fact, is two orders of magnitude greater than most of the other ratios in the region. The value of the ratio is one order of magnitude greater than the highest value (50) at a minor anomaly observed on the Bering Shelf of St. George Basin (Kvenvolden and Redden, 1980; Kvenvolden et al., 1981). The value of the $C_2/C_{2=}$ ratio in core 66 is almost a factor of three greater than the highest value (160) obtained from the 1980 Navarin Basin study from core 36 (Vogel and Kvenvolden, 1981).

Figure 29 summarizes the cores with anomalous concentrations of C_1 , C_2 , and/or C_3 and with $C_1/(C_2+C_3)$ and $C_2/C_{2=}$ values indicating a possible thermogenic origin. Of the thirteen cores mentioned above, where the $C_1/(C_2+C_3)$ values are less than 50 and the $C_2/C_{2=}$ values are greater than 1, the majority are not of special interest for various reasons. For example, concentrations from core 12 did not increase particularly rapidly with depth. Core 38 has mostly background concentration levels, with only one anomalous concentration (ethane) at the 300-cm depth, the deepest sample analyzed in the core. Core 77 was only sampled at the 90-100 cm depth interval and also had high concentrations of alkenes. Core 88 has background concentrations and cores 22, 57, and 71 have erratic concentration versus depth profiles. Cores 19 and 20 are at almost the same coring location and have mostly high amounts of ethane. A longer core is needed here to determine if these high values continue to increase with depth. Cores 60 and 62 on the shelf and core 58 on the slope are of some interest, but due to the short cores obtained from these locations, it is difficult to predict and interpret the concentration gradient with depth.

RELATIONSHIP TO GEOPHYSICAL ACOUSTIC ANOMALIES

Geophysical evidence shows that extensive areas in the northern shelf areas of the Navarin Basin province may contain gas-charged sediment (Carlson and others, 1982; Carlson and others, this report). Geochemical data from the same areas on the shelf show that gas is present in cores collected where seismic anomalies suggest gas-charged sediment. However, the amount of gas observed is not large enough to be responsible for the seismic anomalies. Actually, the anomalies occur at depths below which sediment samples could be recovered (i.e. greater than about 15 m). Thus, a correlation between our geochemical data and the occurrence of geophysical anomalies attributed to gas-charging of sediment cannot be firmly established.

CONCLUSIONS

Hydrocarbon gases are common in the upper five meters of sediment in the Navarin Basin province. Locations with highest concentrations of gases are found in the slope sediment, followed by sediment of the shelf and rise, respectively. C_1 is the most abundant hydrocarbon gas in all three regions and is generally present in concentrations that are two to three orders of magnitude greater than the higher molecular weight hydrocarbon gases. In four cores, all from the slope, the concentration of C_1 ranged from 12000 to 84000 $\mu\text{l/l}$ and is probably being generated from the microbial decomposition of organics in the anoxic clay mud found in Navarinsky Canyon. Ratios of $C_1/(C_2+C_3)$ are very large for these samples, ranging from 900 to 43000, indicating mainly a biogenic source. These concentrations may be near or exceed the solubility of C_1 in interstitial water at depth and thus the gas may affect the stability of the sediment.

C_2+C_3 concentrations are greater than 1000 nl/l in eleven cores taken at nine locations on the slope and two on the shelf. In seven of these cores, the trends of increasing C_2+C_3 concentration strongly correlate with increasing concentration of C_1 down the core. Therefore, the microbiological processes that account for the C_1 concentrations may be related to the processes producing the high C_2+C_3 concentrations in these cores.

Low concentrations of i- C_4 and n- C_4 are present but are often not detectable in many samples. The highest i- C_4 +n- C_4 concentrations are found in the slope sediment. Anomalously high i- C_4 +n- C_4 concentrations were found in all five cores that had concentrations of $C_2+C_3 > 1000$ nl/l and $C_1 > 1000$ $\mu\text{l/l}$.

The alkenes are generally present in all the samples and are likely the result of biological activity in the sediment. Concentrations are generally low and average about 50 nl/l in the sediment of the shelf and slope and are slightly higher in the rise sediment, averaging about 70 nl/l. Concentrations of the alkenes do not show distinctive trends with depth.

One core in the Navarin Basin province is of particular interest with respect to geochemical prospecting. Core 66 has a mixture of gases that suggest a thermogenic source. The $C_1/(C_2+C_3)$ ratios are 20 and 24 at the 200 and 300 cm depths, respectively, and the $C_2/C_2=$ ratios are 58 and 440. C_2+C_3 has the highest concentration (> 8000 nl/l) of any measured in the 1981 study

area. C₄'s are also present in anomalously high concentrations: for example, the amount of the i-C₄ (320 nl/l) is the highest measured in the study area.

ACKNOWLEDGMENT

We thank T. M. Vogel and D. J. Blunt for collecting the samples and helping with some preliminary analyses.

REFERENCES

- Barnes, R. O., and Goldberg, E. D., 1976, Methane production and consumption in anoxic marine sediments: *Geology*, v. 4, p. 297-300.
- Bernard, B. B., Brooks, J. M., and Sackett, W. M., 1976, Natural gas seepage in the Gulf of Mexico: *Earth and Planet. Sci. Lett.*, 31, p. 48-54.
- Bernard, B. B., Brooks, J. M., and Sackett, W. M., 1977, A geochemical model for characterization of hydrocarbon gas sources in marine sediments: *Proc. 9th Offshore Tech. Conf.*, 1, p. 435-438.
- Bernard, B. B., Brooks, J. M., and Sackett, W. M., 1978, Light hydrocarbons in recent continental shelf and slope sediments: *Jour. Geophys. Res.*, 83, p. 4053-4061.
- Carlson, P. C., Karl, H. A., Fischer, J. M., and Edwards, B. D., 1982, Geological hazards in Navarin Basin Province, Northern Bering Sea: *Proc. 14th Offshore Tech. Conf.*, OTC 4172, p. 73-87.
- Cline, J. D., and Holmes, M. L., 1977, Submarine seepage of natural gas in Norton Sound, Alaska: *Science*, no. 198, p. 1149-1153.
- Davis, J. B., and Squires, R. M., 1954, Detection of microbially produced gaseous hydrocarbons other than methane: *Science*, no. 119, p. 381-382.
- Emery, K. O., and Hoggan, D., 1958, Gases in marine sediments: *Am. Assoc. Petrol. Geol. Bull.*, no. 42, p. 2174-2188.
- Fischer, J. M., 1981, Carbon contents of Navarin Basin sediments: In *Seafloor Geologic Hazards, Sedimentology, and Bathymetry: Navarin Basin Province, Northwestern Bering Sea*: U.S.G.S. Open-File Report 81-1217, Ed. Carlson, P. R., and Karl, H. A., p. 44-57.
- Hunt, J. M., 1974, Hydrocarbon geochemistry of Black Sea: In *The Black Sea - Geology, Chemistry, and Biology*, *Am. Assoc. Pet. Geol. Mem.*, no. 20, p. 499-504.
- Kvenvolden, K. A., and Redden, G. D., 1980, Hydrocarbon gas in sediment from the shelf, slope, and basin of the Bering Sea: *Geochim. Cosmochim. Acta*, vol. 44, p. 1145-1150.
- Kvenvolden, K. A., Vogel, T. M., and Gardner, J. V., 1981, Geochemical prospecting for hydrocarbons in the outer continental shelf, southern Bering Sea, Alaska: *Jour. Geochem. Expl.*, 14, p. 209-219.
- Martens, C. S., and Berner, R. A., 1974, Methane production in the interstitial waters of sulfate-depleted marine sediments: *Science*, 185, p. 1167-1169.
- Primrose, S. B., and Dilworth, M. J., 1976, Ethylene production by bacteria: *Jour. General Microbiology*, no. 93, p. 177-181.

Reeburgh, W. S., 1969, Observations of gases in Chesapeake Bay sediments: *Limnol. Oceanogr.*, no. 14, p. 368-375.

Reeburgh, W. S., and Heggie, D. T., 1977, Microbial methane consumption reactions and their effect on methane distributions in fresh water and marine environments: *Limnol. Oceanogr.*, no. 22, p. 1-9.

Vogel, T. M., and Kvenvolden, K. A., 1981, Hydrocarbon gases in Navarin Basin province sediments: In *Seafloor Geologic Hazards, Sedimentology, and Bathymetry: Navarin Basin Province, Northwestern Bering Sea*: U.S.G.S. Open-File Report 81-1217, Ed. Carlson, P. R., and Karl, H. A., p. 80-99.

Yamamoto, S., Alcauskas, J. B., and Crozier, T. E., 1976, Solubility of methane in distilled water and seawater: *Jour. Chem. and Eng. Data*, vol. 21, no. 1, p. 78-80.

Table 5. Hydrocarbon Gas (C₁-nC₄) Concentrations and Ratios from Sediment Samples

from the Navarin Basin Province (1981)

Core No. and Interval (cm)	Water Depth (m)	Station No.	C ₁ ul/l wet sediment	C ₂ -nC ₄ (nl/l wet sediment)				C ₁ /C ₂ × 10 ³	C ₂ /C ₃ × 10 ³	Location Latitude Longitude
				C ₂	C ₃	C ₃ :1	i-C ₄ n-C ₄			
G1 90-100 202-212	135	1	50	78	44	26	28	n.d.	n.d.	59°28.9' 175°35.7'
			140	690	42	47	250	n.d.	n.d.	
G2 90-100	143	1	47	270	150	170	68	12	33	59°05.6' 176°20.1'
			8.1	47	58	34	95	3	n.d.	
G24 90-100 190-200	104	22	13	100	100	73	130	6	14	61°31.6' 176°25.5'
			79	190	67	39	86	8	4	
G25 90-100 190-200	123	23	210	470	33	82	210	36	6	61°46.2' 177°30.2'
			7.8	43	57	31	81	11	n.d.	
G26 90-100 190-200	122	24	18	66	81	44	200	6	5	61°27.1' 177°25.2'
			11	33	51	28	65	5	4	
G27 90-100 190-200	145	25	19	27	15	9	12	n.d.	n.d.	61°09.0' 177°47.0'
			29	42	66	31	83	4	3	
G28 90-100	128	26	4.8	26	60	27	93	n.d.	5	61°13.5' 177°23.4'
			120	270	94	54	97	8	6	
G31 90-100 190-200	137	28	37	34	44	22	85	4	n.d.	60°12.1' 176°35.5'
			34	120	210	100	130	21	22	
G32 90-100 190-200	130	29	62	70	61	30	20	4	n.d.	60°11.0' 176°13.1'
			47	43	86	26	89	3	n.d.	
G33 90-100 190-200	130	29	180	340	91	80	81	8	13	60°11.1' 176°13.1'
			3.9	42	72	34	120	4	6	
G34 90-100	115	30	7.5	34	39	24	67	4	n.d.	57°20.1' 172°42.7'
			23	270	40	34	34	5	6	
G35 90-100	115	30	11	390	55	62	71	15	n.d.	59°48.3' 177°24.6'
			36	230	30	28	98	n.d.	n.d.	
G60 90-100 190-200	140	56	33	250	38	36	63	4	n.d.	59°49.6' 177°29.8'
			92	1300	56	52	120	6	n.d.	
G61 90-100	141	57	28	180	17	23	65	18	2	59°51.2' 177°29.5'
			28	200	31	20	88	3	n.d.	
G62 90-100 189-199	139	58	33	250	38	36	63	4	n.d.	59°27.1' 176°29.4'
			33	470	270	330	120	25	62	
G63 90-100	135	59	18	420	430	360	190	66	26	59°54.1' 178°09.1'
			56	31	51	15	25	n.d.	n.d.	
G73 90-100	146	69	120	370	130	130	75	13	28	60°13.1' 177°33.1'
			29	31	20	15	35	n.d.	n.d.	
G77 90-100	145	73	140	180	38	31	14	5	n.d.	60°30.1' 176°59.2'
			29	31	20	15	35	n.d.	n.d.	
G78 90-100	139	74	180	540	27	26	57	5	n.d.	60°09.0' 176°59.3'
			57	40	38	18	36	n.d.	n.d.	
G79 90-100 190-200	141	75	180	540	27	26	57	5	n.d.	59°40.0' 175°59.3'
			29	31	20	15	35	n.d.	n.d.	
G105 90-100 191-201	144	95	140	180	38	31	14	5	n.d.	60°09.0' 176°59.3'
			57	40	38	18	36	n.d.	n.d.	
G106 90-100 190-200	135	96	180	540	27	26	57	5	n.d.	59°40.0' 175°59.3'
			29	31	20	15	35	n.d.	n.d.	

n.d. = not detectable

Table 5 (Continued)

Core No. and Interval (cm)	Water Depth (m)	Station No.	C ₁ ul/l wet sediment	C ₂	C ₂ :1	C ₃	n/1			n-C ₄	C ₁ / (C ₂ +C ₃)	C ₂ / C ₂ :1	Location	
							C ₃ :1	1-C ₄	n-C ₄				Latitude	Longitude
Slope Sediment														
G4 90-100	2816	5	8.2	n.d.	n.d.	23	34	n.d.	n.d.	n.d.	360	-	58°31.3'	177°26.0'
190-200			11	67	82	49	36	4	10	0.82	96			
290-300			17	76	46	40	32	n.d.	8	1.6	150			
G7 95-105	173	7	53	420	140	110	55	16	21	3.0	99		59°38.3'	178°15.3'
G11 90-100	980	11	180	230	24	52	3400	170	170	9.8	630		60°39.2'	179°34.6'
190-200			84000	950	110	3400	*	150	180	8.7	19000			
G12 90-100	1683	12	9.6	59	63	32	36	6	4	0.94	110		60°34.3'	179°45.1'
190-200			17	150	41	410	25	180	46	3.6	30			
262-272			25	300	22	610	37	260	46	13	28			
G13 90-100	2080	13	5.8	38	36	34	29	n.d.	n.d.	1.0	81		60°19.3'	179°49.1'
190-200			460	360	14	59	770	46	n.d.	27	1100			
290-300			49000	450	150	700	*	32	36	3.1	43000			
G14 90-100	1826	14	37	160	75	140	39	9	26	2.1	120		60°09.6'	179°50.1'
190-200			230	300	19	610	120	65	49	16	260			
290-300			780	430	22	690	130	84	59	20	700			
390-400			12000	410	39	2700	*	34	26	10	3900			
552-562			44000	270	420	1700	*	55	28	0.63	22000			
G15 90-100	2744	15	25	42	73	24	50	5	3	0.58	370		59°52.4'	179°59.5'
190-200			57	33	74	19	31	4	n.d.	0.44	1100			
290-300			150	640	40	49	33	5	n.d.	16	220			
390-400			1400	1300	22	240	63	20	n.d.	61	900			
G17 90-100	900	17	1.2	26	50	18	29	1	n.d.	0.51	28		60°12.6'	179°21.5'
190-200			4.5	57	45	28	45	4	n.d.	1.2	54			
283-293			6.4	49	30	21	43	6	n.d.	1.6	92			
G18 90-100	884	17	2.8	37	36	18	23	3	n.d.	1.0	50		60°13.1'	179°21.5'
190-200			11	37	35	13	52	3	n.d.	1.1	230			
G19 90-100	1018	18	16	100	41	39	55	3	3	2.4	110		60°10.2'	179°27.9'
190-200			13	270	190	130	70	9	17	1.4	34			
290-300			170	1000	22	210	70	24	2	47	140			
370-380			290	990	39	240	110	52	9	26	230			

n.d. = not detectable

- = not reported

* = concentration not reported due to methane interference

Table 5. (Continued)

Core No. Interval (cm)	Water Station No.	Water Depth (m)	C ₁ ul/l wet sediment	C ₂	C ₂ :1	C ₃	C ₃ :1	i-C ₄	n-C ₄	C ₁ C ₂ +C ₃	C ₂ C ₂ :1	Location Latitude Longitude	
													n/1
Slope Sediment (continued)													
G20	90-100	1005	15	270	180	85	80	8	14	41	1.5	60°10.6'	179°26.9'
	190-200		27	510	200	130	83	12	17	43	2.6		
	290-300		47	710	93	150	48	12	19	55	7.6		
	364-374		52	780	180	270	97	30	36	50	4.3		
G21	90-100	1630	5.7	61	59	36	51	6	n.d.	58	1.0	60°06.1'	179°34.5'
	190-200		8.8	100	170	54	61	7	3	56	0.60		
G22	90-100	1670	5.7	150	200	120	75	12	20	21	0.76	60°06.1'	179°34.5'
	190-200		5.8	140	120	100	52	9	17	24	1.1		
	290-300		7.0	52	44	28	27	5	n.d.	89	1.2		
	390-400		8.5	65	36	26	36	3	n.d.	93	1.8		
G37	190-200	1100	5.7	97	52	32	68	7	n.d.	45	1.8	57°49.6'	174°23.5'
	290-300		8.9	160	130	46	120	9	10	42	1.2		
G38	90-100	1080	1.3	37	41	32	53	3	n.d.	18	0.91	58°10.1'	175°29.2'
	190-200		7.8	81	36	29	85	3	n.d.	71	2.3		
	290-300		130	1600	70	43	130	10	4	77	23		
G39	90-100	915	13	56	66	39	65	7	6	140	0.84	58°20.1'	174°29.1'
	190-200		32	60	56	32	84	8	4	350	1.1		
	290-300		39	250	36	35	31	4	n.d.	140	6.9		
G44	90-100	2530	5.4	20	54	16	86	3	n.d.	150	0.37	56°51.4'	174°08.5'
	190-200		13	26	52	17	61	n.d.	n.d.	310	0.50		
	290-300		14	54	63	39	63	4	n.d.	150	0.86		
	390-400		19	45	56	29	52	3	n.d.	260	0.80		
	490-500		17	41	86	26	67	3	n.d.	250	0.47		
G47	90-100	2760	2.7	36	87	23	81	3	n.d.	45	0.41	56°58.2'	174°21.2'
	190-200		7.5	150	240	120	130	19	20	27	0.64		
	290-300		6.8	39	59	21	86	3	n.d.	110	0.67		
	390-400		7.0	67	100	42	110	7	9	64	0.65		
	490-500		6.2	41	56	28	68	4	n.d.	91	0.73		
G49	90-100	1770	4.8	30	47	26	71	n.d.	n.d.	85	0.64	57°38.5'	175°38.0'
	190-200		7.8	45	75	28	57	n.d.	3	110	0.61		
	290-300		10	31	92	18	57	n.d.	n.d.	210	0.34		
	390-400		14	57	51	23	92	4	n.d.	180	1.1		
	490-500		16	63	71	32	80	4	n.d.	170	0.89		

n.d. = not detectable

Table 5. (Continued)

Core No. and Interval (cm)	Water Depth (m)	Station No.	C ₁ ul/l wet sediment	C ₂	C ₂ :1	C ₃	C ₃ :1	i-C ₄	n-C ₄	C ₁ +C ₂ +C ₃	C ₂ :1	Location	
												Latitude	Longitude
Slope Sediment (continued)													
G52 90-100	1070	46	4.3	48	31	22	21	4	n.d.	61	1.5	58°33.6'	177°53.2'
190-200			4.3	22	20	13	17	n.d.	n.d.	120	1.1		
290-300			5.6	22	22	11	19	3	n.d.	170	1.0		
390-400			5.1	15	28	13	12	n.d.	n.d.	180	0.53		
490-500			5.3	26	17	16	25	n.d.	n.d.	130	1.6		
570-580			5.3	30	23	14	30	3	n.d.	120	1.3		
G53 90-100	2676	47	3.0	53	72	45	32	3	9	31	0.74	58°23.2'	176°25.1'
G55 90-100	2320	49	5.2	27	12	13	10	n.d.	n.d.	130	2.3	57°45.7'	175°30.4'
190-200			18	36	14	11	23	n.d.	n.d.	360	2.5		
290-300			25	55	23	16	21	n.d.	n.d.	350	2.5		
390-400			34	210	22	26	28	1	n.d.	140	9.5		
G58 90-100	179	53	11	44	39	41	22	n.d.	n.d.	130	1.1	59°26.1'	177°28.4'
190-200			19	1400	250	350	110	25	61	11	5.5		
G65 90-100	436	61	6.3	35	24	22	23	3	n.d.	110	1.5	59°25.4'	177°51.2'
190-200			7.3	34	28	24	56	5	n.d.	130	1.2		
G66 90-100	580	62	56	62	31	500	54	200	24	100	2.0	59°24.7'	178°14.5'
190-200			110	4800	83	790	77	260	31	20	58		
290-300			200	7300	17	970	110	320	26	24	440		
G67 90-100	167	63	74	540	71	80	66	8	11	120	7.6	59°38.7'	178°14.2'
G68 90-100	1048	64	19	130	23	20	75	n.d.	n.d.	130	5.7	59°38.6'	178°37.2'
190-200			63	440	13	26	130	n.d.	n.d.	130	34		
G69 90-100	1230	65	1.6	76	62	57	98	n.d.	n.d.	12	1.2	59°15.8'	178°34.4'
190-200			8.8	57	32	32	100	1	n.d.	99	1.8		
G71 90-100	520	67	18	180	38	22	130	7	n.d.	89	4.7	58°48.0'	178°00.0'
190-200			71	1400	37	45	58	10	n.d.	47	39		
290-300			170	93	16	120	57	10	n.d.	790	6.0		
G74 85-95	152	70	30	190	17	18	140	n.d.	n.d.	150	11	59°25.5'	177°11.9'
G80 90-100	152	76	16	180	180	150	73	9	31	48	1.0	60°29.4'	177°53.3'
G82 90-100	860	78	5.6	61	37	23	33	5	n.d.	66	1.6	60°27.2'	179°29.1'
G83 90-100	1120	79	2.4	38	48	27	49	n.d.	4	37	0.8	60°26.2'	179°53.4'
G84 90-100	780	80	23	74	33	31	64	4	n.d.	220	2.2	59°57.9'	178°59.2'
G85 90-100	1745	81	6.4	28	41	21	52	4	n.d.	130	0.68	59°51.9'	179°09.7'
190-200			10	49	41	34	51	5	n.d.	130	1.2		
G86 90-100	2195	82	64	910	150	74	80	5	18	390	0.59	60°09.2'	179°51.4'
190-200			320	930	38	120	170	21	7	310	24		
280-290			34000	19000	54	1700	*	54	n.d.	9400	15		
G88 90-100	205	83	4.8	120	32	52	31	8	8	28	3.6	61°08.1'	178°46.1'
190-200			9.2	290	86	120	47	n.d.	14	23	3.3		

n.d. = not detectable

* = concentration not reported due to methane interference

Core No. and Interval (cm)	Water Depth (m)	Station No.	C ₁ ul/l wet sediment	C ₂				C ₃				i-C ₄	n-C ₄	C ₁ C ₂ +C ₃	C ₂	Location Latitude Longitude
				C _{2:1}	C ₂	C _{2:1}	C ₂	C _{3:1}	C ₃	C _{3:1}	C ₃					
Rise Sediment																
G6	90-100	3395	4.1	39	140	58	49	58	5	11	47	0.29	58°08.3'	177°23.5'		
	190-200		8.5	41	58	34	27	34	5	n.d.	120	0.71				
	290-300		3.5	120	310	120	95	120	8	19	16	0.39				
	390-400		7	29	23	33	8	33	n.d.	n.d.	190	1.3				
G42	90-100	3150	8.4	20	34	50	19	50	1	n.d.	210	0.59	57°57.8'	175°00.0'		
	190-200		17	43	66	32	32	77	3	n.d.	220	0.65				
	290-300		21	48	48	22	22	69	2	n.d.	300	0.99				
G48	90-100	2910	7.7	24	39	81	22	81	n.d.	n.d.	170	0.62	57°06.6'	174°35.5'		
	190-200		13	45	88	26	26	59	3	n.d.	190	0.50				
	290-300		20	37	100	24	24	65	5	n.d.	380	0.44				
	390-400		20	37	100	24	24	65	5	n.d.	320	0.37				
G50	90-100	3430	4.4	21	55	89	22	89	3	n.d.	100	0.39	57°52.2'	176°28.5'		
	190-200		6.3	36	69	28	28	74	2	n.d.	98	0.52				
	290-300		7.9	47	62	30	30	75	3	n.d.	100	0.77				
	390-400		12	26	43	17	17	97	n.d.	n.d.	290	0.60				
	490-500		19	100	91	54	29	29	5	73	120	1.1				
G51	90-100	3220	4.3	18	26	13	13	28	n.d.	n.d.	140	0.71	58°20.4'	177°25.1'		
	190-200		7.5	20	24	16	16	24	n.d.	n.d.	210	0.83				
G54	90-100	3220	10	60	32	24	24	19	n.d.	n.d.	120	1.9	58°08.4'	176°02.9'		
	190-200		18	29	28	15	15	32	n.d.	n.d.	420	1.0				
	290-300		16	30	25	16	16	28	n.d.	n.d.	350	1.2				
G56	90-100	2925	6.0	19	34	14	14	70	n.d.	n.d.	180	0.55	58°11.6'	176°00.1'		
	190-200		16	27	44	16	16	96	4	n.d.	360	0.60				
G57	90-100	3395	3.9	14	25	10	10	25	n.d.	n.d.	160	0.58	57°57.3'	176°58.8'		
	190-200		6.9	24	32	16	16	54	4	n.d.	170	0.77				
	290-300		13	240	270	200	110	15	15	39	30	0.90				
	390-400		12	190	320	170	130	15	15	39	33	0.59				
	470-480		26	520	18	71	22	22	7	n.d.	44	29				
G70	90-100	3390	6.5	13	22	41	22	41	n.d.	n.d.	300	0.61	58°31.6'	178°28.0'		
	190-200		8	18	25	16	16	62	n.d.	n.d.	230	0.72				
	290-300		12	51	38	25	25	89	4	n.d.	160	1.3				
	390-400		8.7	15	20	16	16	46	n.d.	n.d.	280	0.76				
G76	90-100	3210	4.4	36	74	39	39	42	n.d.	n.d.	59	0.49	59°21.5'	179°06.6'		
	190-200		11	130	170	110	110	79	8	19	45	0.72				

n.d. = not detectable

Table 6. Hydrocarbon Gas (C₁-nC₄) Concentration and Ratio Ranges from Sediment Samples from the Navarin Basin Province (1981). Methane (C₁) concentrations are in µl/l; the other hydrocarbon concentrations are in nl/l.

	Shelf	Slope	Rise
C ₁	4 - 200	1 - 84000	4 - 26
C ₂	27 - 1300	n.d.- 7300	13 - 520
C ₃	10 - 360	11 - 3400	8 - 200
C ₂ =	15 - 430	n.d.- 420	18 - 320
C ₃ =	12 - 250	n.d.- 3400	19 - 130
i-C ₄	n.d.- 66	n.d.- 320	n.d.- 15
n-C ₄	n.d.- 62	n.d.- 180	n.d.- 73
C ₁ /C ₂ +C ₃	23 - 1200	11 - 43000	16 - 420
C ₂ /C ₂ =	0.44- 24	0.44- 440	0.29- 29

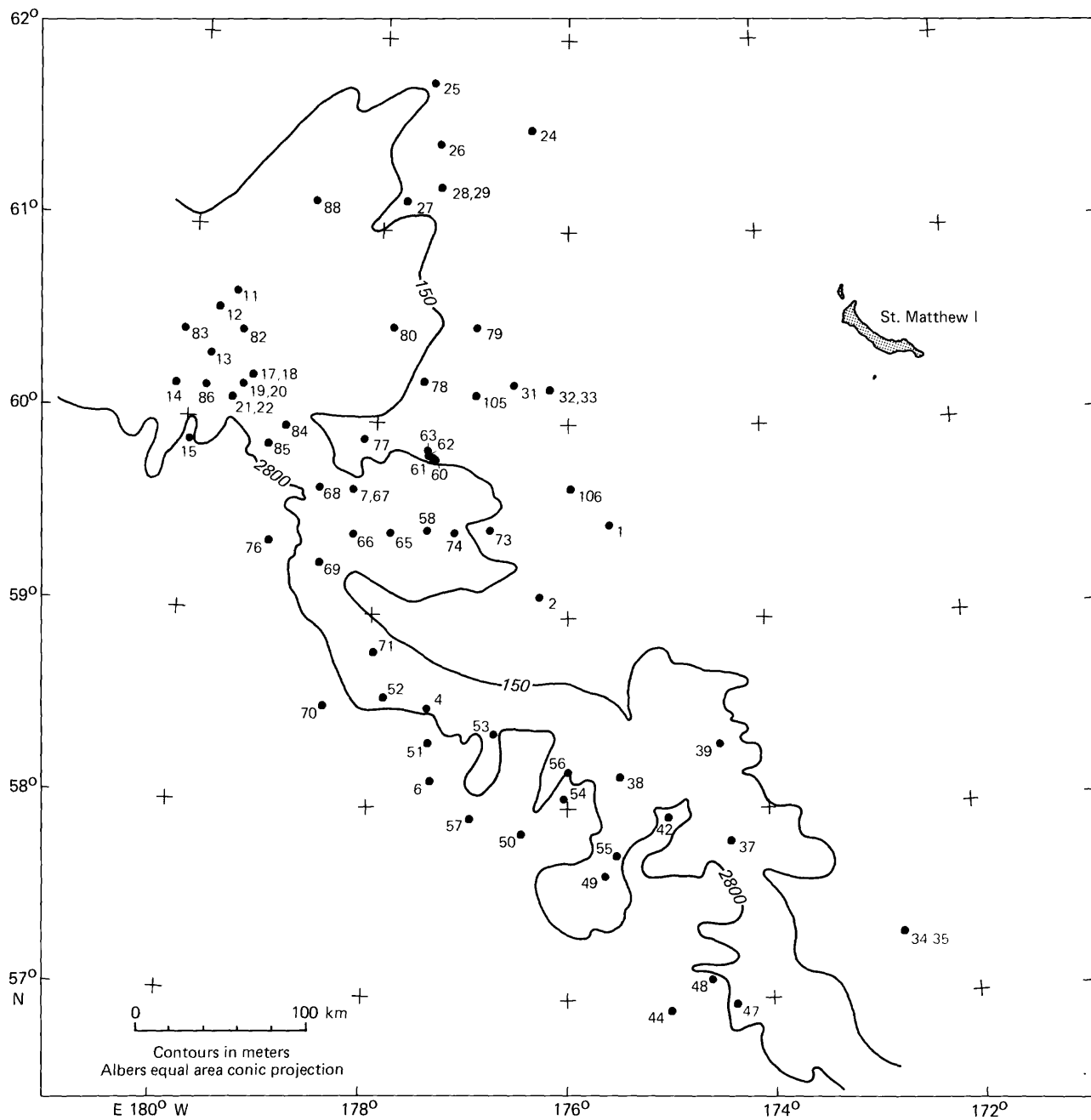


Figure 23. Location of hydrocarbon gas sampling sites in the Navarin Basin province. Sites are designated with core numbers.

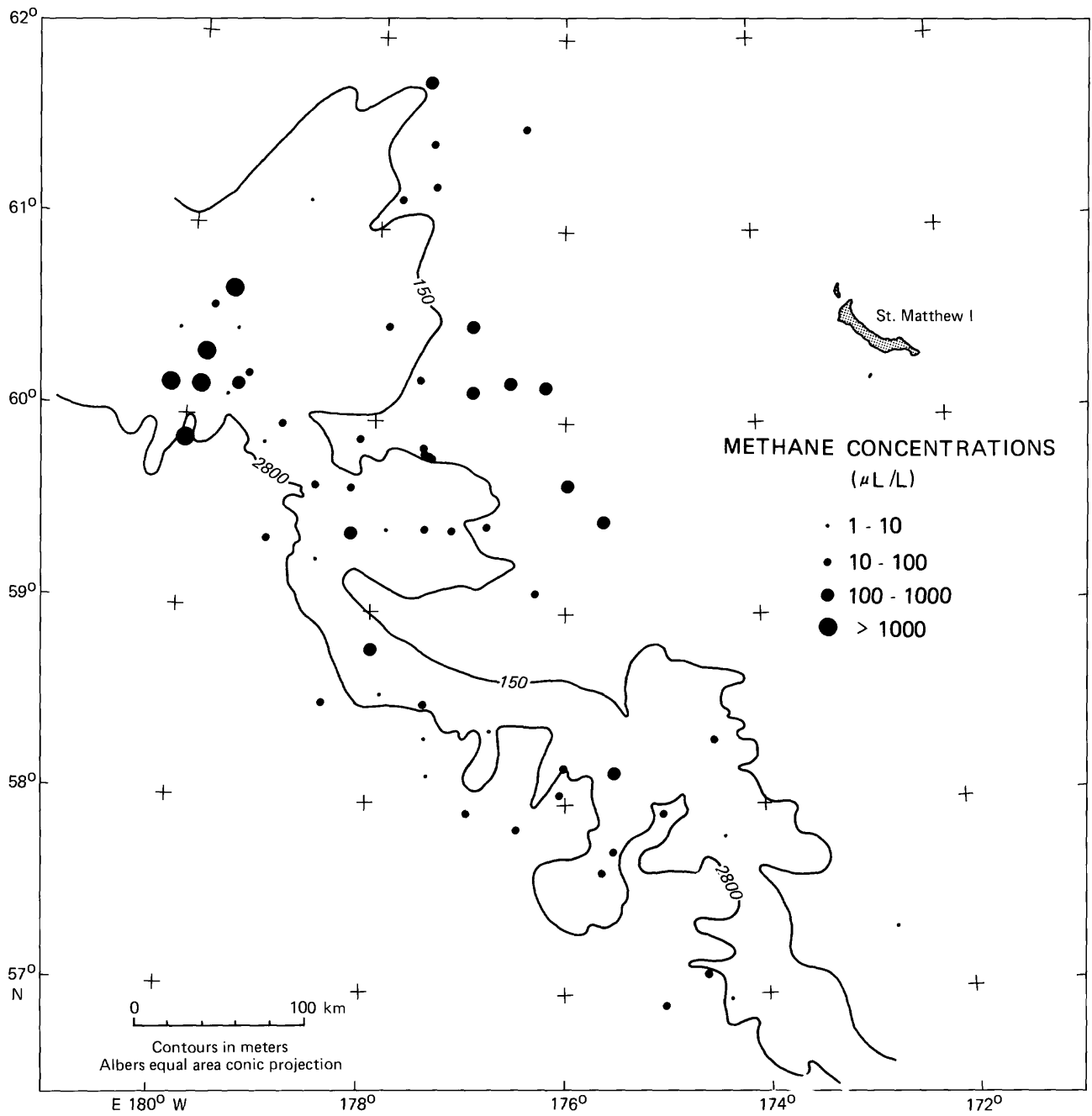


Figure 24. Distribution of maximum concentrations of methane in $\mu\text{l/l}$ of wet sediment.

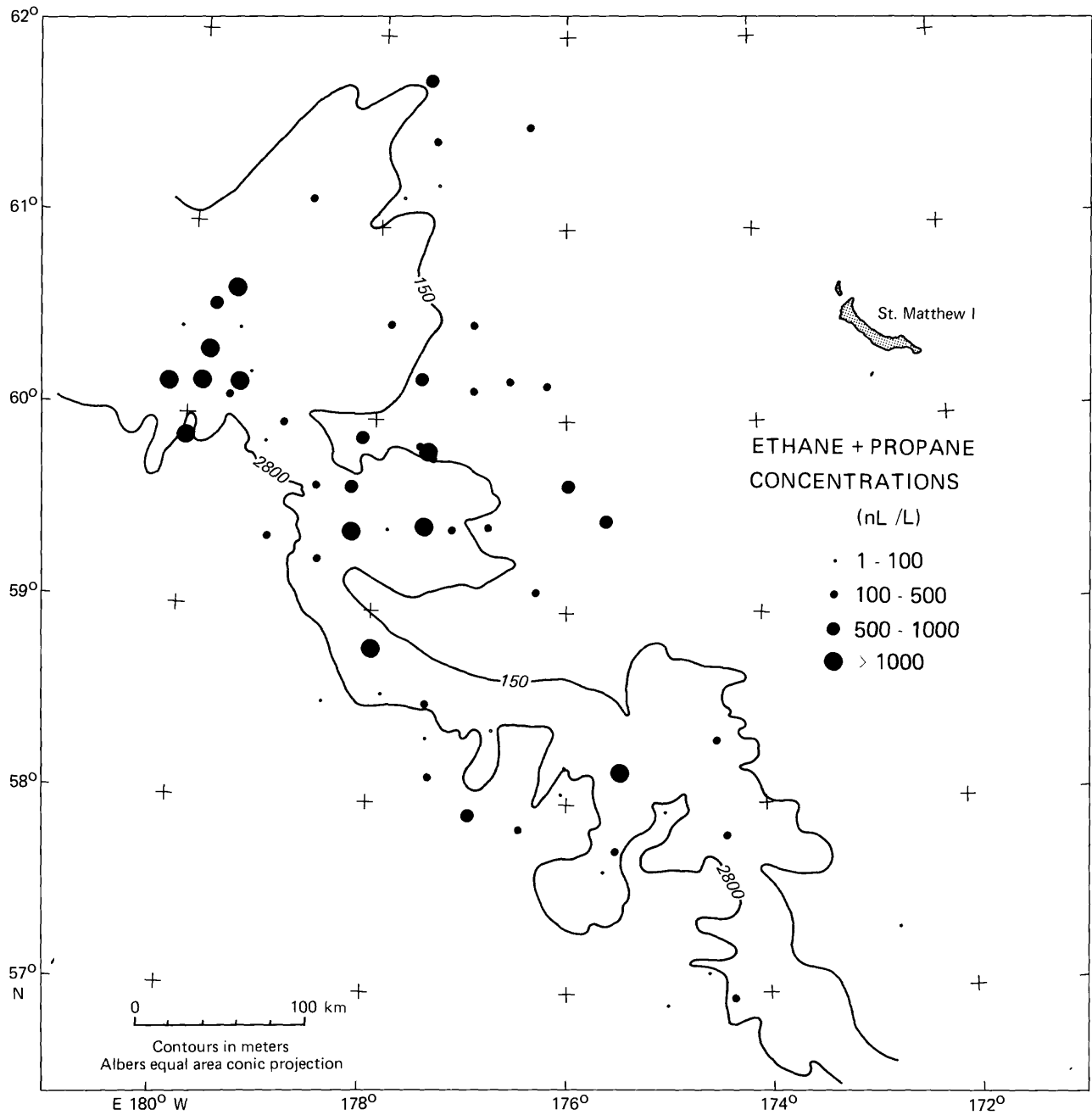


Figure 25. Distribution of maximum concentrations of ethane plus propane in nl/l of wet sediment.

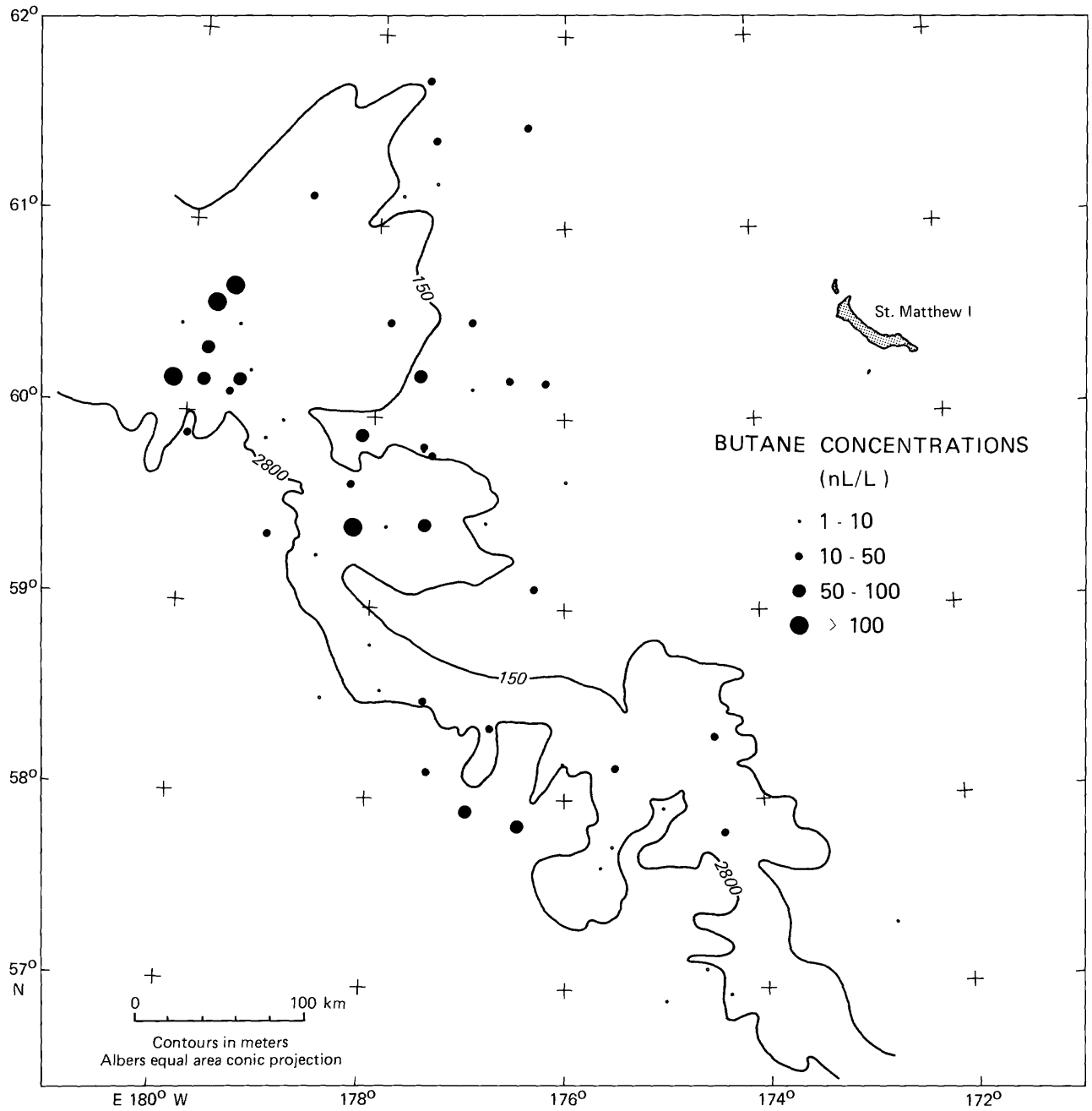


Figure 26. Distribution of maximum concentrations of butane in nl/l of wet sediment.

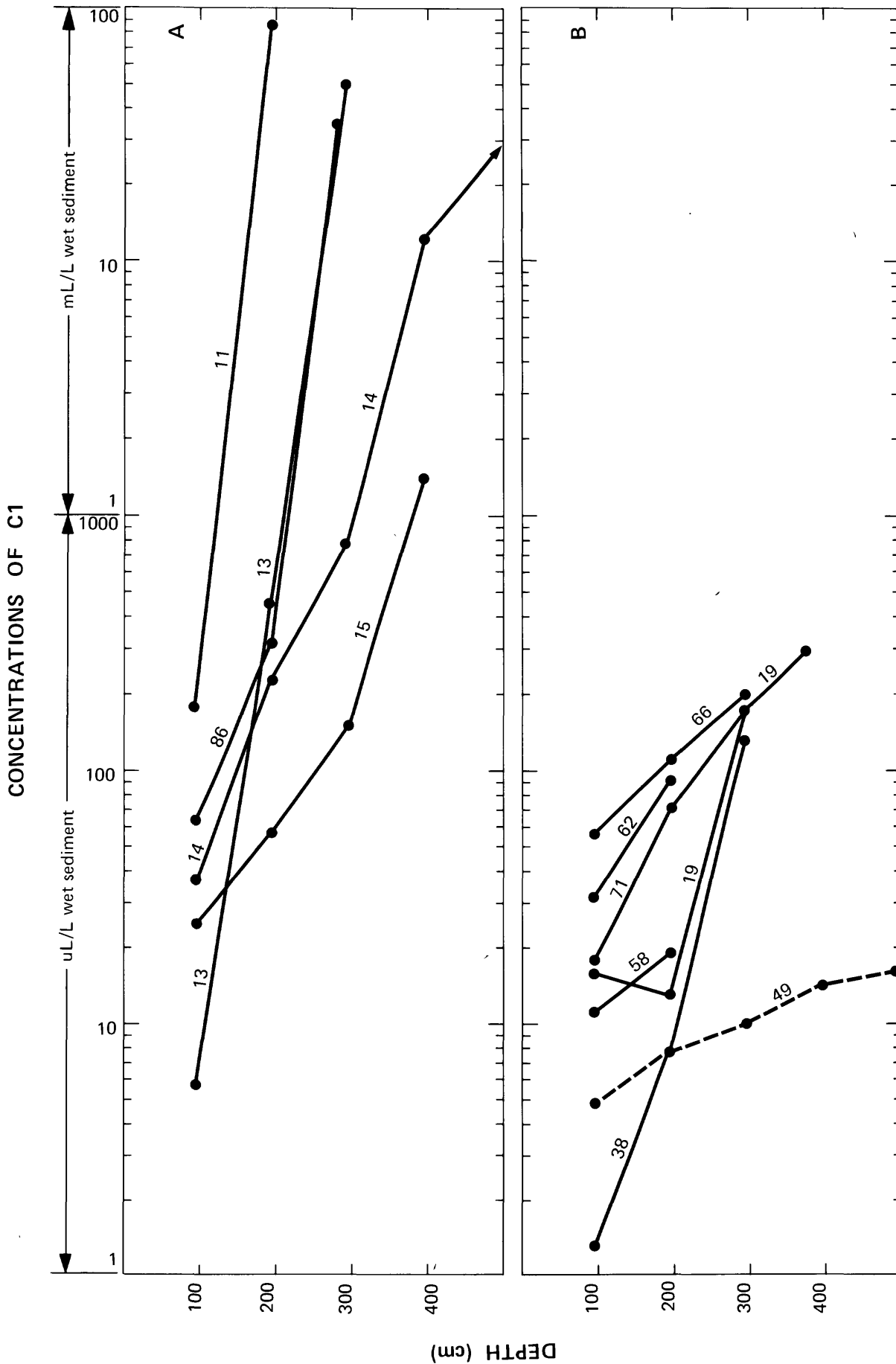


Figure 27. Graph of concentrations of C₁ in µl/l and ml/l wet sediment vs. depth in centimeters for sediment samples from the eleven sites in the Navarin Basin Province where C₂+C₃ concentrations reach or exceed 1 µl/l wet sediment at some depth interval. Figure A groups those profiles whose C₁ concentrations exceed 1 ml/l wet sediment at some depth interval while Figure B groups the remaining cores. The dashed line in Figure B is the profile of a core which represents background concentration levels.

CONCENTRATIONS OF C₂ + C₃

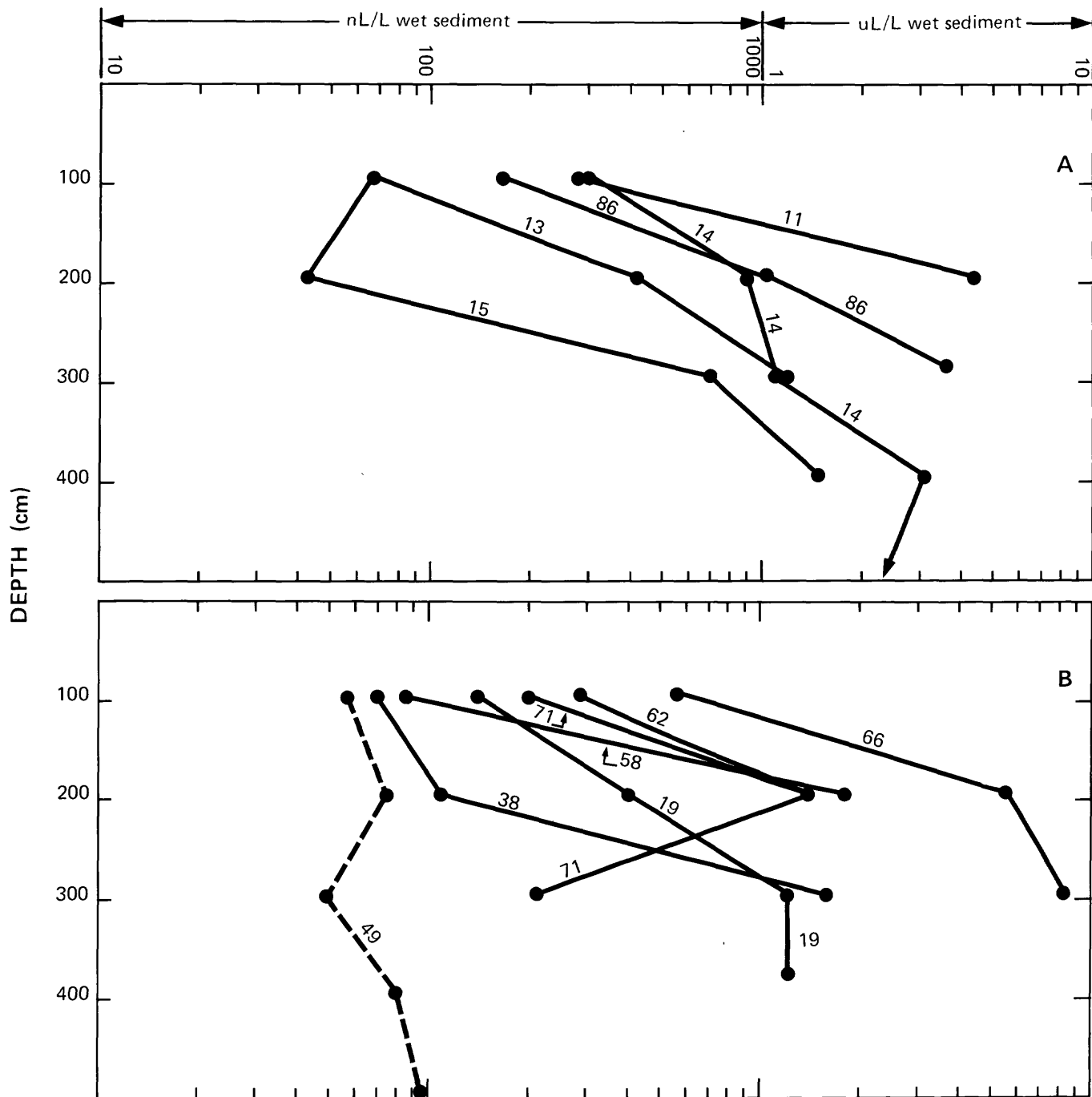


Figure 28. Graph of concentrations of C₂+C₃ in nL/l and μl/l wet sediment vs. depth in centimeters for sediment samples from the eleven sites in the Navarin Basin Province where C₂+C₃ concentrations reach or exceed 1 μl/l wet sediment at some depth interval. Figure A groups those profiles whose C₁ concentrations exceed 1 ml/l wet sediment at some depth interval while Figure B is the profile of a core which represents background concentration levels.

Anomalous* Parameters				Core #		
C1	C2	C3	R	Shelf	Slope	Basin
	•			61,73,79	7,67	
		•		32		6,76
			•		22,88	
•	•			1,25,31,33, 105,106		
•		•			13,14	
	•	•		2,78		
	•		•	60		
		•	•		12	
•	•	•			11,15,86	
•	•		•	62	38,71	
	•	•	•	77	20,58	57
•	•	•	•		19,66	

* Concentrations of C1 (methane), C2 (ethane), C3 (propane) that are above background for the region indicated and R (ratios) that indicate a thermogenic origin (C1/(C2+C3) values that are low and C2/C2= values that are high).

Figure 29. Tally of anomalous parameters for cores in the regions indicated.

CHAPTER 9. BENTHIC FORAMINIFERS

by

Paula Quintero

INTRODUCTION

Samples collected by the U.S. Geological Survey from the Navarin Basin province were analyzed for benthic foraminifers. This study is a continuation of previous work (Quintero, 1981) and includes samples collected during both 1980 and 1981 (Fig. 30).

Other studies of benthic foraminifers in the Bering Sea have been in areas to the north and west (Saidova, 1967; Lisitsyn, 1966) and in shallow waters to the east and northeast of the study area (Anderson, 1963; Knebel and others, 1974).

The purpose of this study is to determine the distribution of benthic foraminifers in the surface sediments and to record faunal changes with depth in the cores.

METHODS

Samples were processed by washing the sediment over a 62 micron-mesh sieve to remove silt and clay fractions. In samples with much sediment, foraminifers were concentrated by floating in carbon tetrachloride. A microsplitter was used to obtain a representative split of approximately 300 benthic foraminifers. The actual number of benthic foraminifers in the splits ranged from 3 to 2,860.

Foraminifers were mounted on cardboard slides, identified, and the relative frequency percentage of each species calculated.

SURFACE DISTRIBUTION

Samples from the approximate upper 2 cm of forty-two gravity cores or grab samples were examined for benthic foraminifers; the relative frequency percentages of the species present are listed in Table 7. Table 8 is the key to abbreviations for species. In order to recognize faunal trends that might be related to water depth, stations were arranged from left to right in order of increasing water depth and the relative frequency percentages of the most abundant species were plotted (Fig. 31). The species abundances for samples having similar water depths were also averaged and plotted. Although percentages fluctuate with depth, some general trends are apparent.

The peak abundances of *Reophax arctica* (35 and 37%) are at depths of 91 and 99 m. At depths greater than 150 m, the abundance decreases to 5% or less

(Fig. 31). Anderson (1963) reports R. arctica in the Bering Sea as dominant in his Central Shelf Fauna (48-100 m) with very low percentages in deeper water. Knebel and others (1974) report the maximum abundance for this species in the Bering Sea between 35-105 m.

Percentages of Elphidium clavatum are low in the samples with the peak abundance of 15% occurring at 99 m depth. This species is absent at most stations having water depths greater than 150 m (Fig. 31). This agrees with previous studies which show that E. clavatum is typical of shelf environments (Knebel and others, 1974; Anderson, 1963; Matoba, 1976).

Peak abundances of Eggerella advena and Spiroplectammina biformis occur in water depths shallower than 150 m; there is a general decrease in abundance with increasing water depth (Fig. 31). Anderson (1963) reports the maximum abundance of E. advena on the Inner Shelf (22-48 m) but finds it present in lesser numbers in the Central and Outer Shelf Faunas (48-200 m).

Epistominella vitrea and Trifarina fluens reach maxima between approximately 150 m and 900 m water depth and disappear below 1,800 m (Fig. 31).

Fursenkoina spp., Reophax spp., Textularia torquata, Bolivina pacifica, and Elphidium batialis are most abundant below 900 m (Fig. 31).

Several species of Fursenkoina were grouped together as Fursenkoina spp., because the tests are extremely small and fragile and are difficult to separate into species. Further subdividing into species might show more clearly-defined depth trends.

Elphidium is usually considered a shelf species with highest abundance in water less than 200 m deep. However, there have been reports of a deep-water species, Elphidium batialis (Saidova, 1961; Matoba, 1976). This large, robust species has a sharp periphery and makes up more than 6% of the fauna at 9 stations with water depths greater than 1,100 m in the Navarin Basin province (Fig. 31). With one exception, (sample 80-110) it is absent in water shallower than 975 m (Table 7).

The depth trends noted above may be dependent on one or more environmental factors (such as salinity, dissolved oxygen, temperature, and sediment type); however, detailed measurements of these parameters are not available at this time. Furthermore, the distribution of some tests has been affected by bottom currents, storm waves, and downslope transport.

DOWN-CORE STUDIES

Relative frequency percentages for benthic foraminiferal species which are present at various intervals in core 81-12 are listed in Table 9, and graphs showing down-core distribution of species are presented in Fig. 32.

Gravity core 81-12 is 262 cm in length and was collected from the floor of Navarinsky Canyon in 1683 m of water. A pronounced faunal and lithologic break exists between 130 cm and 140 cm within the core (Fig. 32). Visual

inspection of the greater than 62 micron portion of sediment from 5 samples above 130 cm shows it to be fine sand. The eleven samples below 130 cm are generally coarser (most contain pebbles or pebble-sized silt aggregates), and contain glauconite and/or iron-stained grains. The sample at 180 cm contains several irregularly-shaped iron-sulfide plates up to 8 mm long.

Relative frequency percentages of the deep-water species Elphidium batialis range from 2-30% in the 5 uppermost samples (0-130 cm) of the core. The shallow-water species E. clavatum is not present in these 5 samples (Fig. 32). However, E. batialis is absent in all eleven samples below 130 cm, whereas E. clavatum is present in abundances ranging from 4-15%. Based on the present-day distribution of E. clavatum with respect to water depth, it is unlikely that this species could live at station 81-12 (1,683 m). Even with glacially lowered sea level, the water depth would be too great. Downslope transport of E. clavatum tests is a possible explanation for the presence of this species in deep water.

The following species have peak abundances above 130 cm in core 81-12 and decrease markedly below: Uvigerina peregrina, Epistominella pacifica, Buccella spp., Trifarina fluens, and Florilus labradoricum. The following species show the opposite trend--low abundances above 130 cm and peak abundances below: Fursenkoina spp., Epistominella vitrea, Nonionella turgida digitata, and large, poorly-preserved specimens of Cassidulina (probably reworked) (Fig. 32).

The pronounced faunal and lithologic break between 130 and 140 cm in core 81-12 may reflect physical and chemical changes in the environment resulting from a change from glacial to interglacial conditions and may represent the Pleistocene/Holocene boundary. With lowered sea level during Pleistocene glaciation, a wide area of the continental shelf was subaerially exposed, and the submerged portion of the shelf was much narrower than at present. During these times, rivers dissected the shelf and transported sediment to the present-day outer shelf (Nelson, Hopkins, and Scholl, 1974). Turbidity currents and debris flows also contributed to down-slope transport (Vallier, Underwood, Gardner, and Barron, 1980; Carlson, Karl, and Quinterno, 1982). Under these conditions of coarser sediment and shallow-water, an organism, such as E. clavatum, could easily be transported into deeper water.

REFERENCES

- Anderson, G. J., 1963, Distribution patterns of Recent foraminifera of the Bering Sea: *Micropaleontology*, v. 9, no. 3, p. 305-317.
- Carlson, P. R., Karl, H. A., and Quintero, Paula, 1982, Sedimentologic processes in world's largest submarine canyons, Bering Sea, Alaska: *Geological Society of America Abstracts with Programs*, v. 14, no. 7, p. 459-460.
- Knebel, H. J., Creager, J. S., and Echols, R. J., 1974, Holocene sedimentary framework, east-central Bering Sea continental shelf, *in* Herman, Y. (ed.), *Marine Geology and Oceanography of the Arctic Seas*: New York, Springer-Verlag, p. 157-172.
- Lisitsyn, A. P., 1966, Recent sedimentation in the Bering Sea (in Russian): *Inst. Okeanol. Akad. Nauk, USSR*, (translated by Israel Program Sci. Transl., Jerusalem), Washington, D.C., U.S. Department of Commerce: National Science Foundation, 614 p.
- Matoba, Yasumochi, 1976, Recent foraminiferal assemblages off Sendai, Northeast Japan, *in* Schafer, C. T. and Pelletier, B. R., *First International Symposium on Benthonic Foraminifera of Continental Margins: Maritime Sediments*, Special Publication no. 1, p. 205-220.
- Nelson, C. H., Hopkins, D. M., and Scholl, D. W., 1972, Cenozoic sedimentary and tectonic history of the Bering Sea, *in* Hood, D. W. and Kelley, E. J. (eds.), *Oceanography of the Bering Sea: Occasional Publication no. 2*, Institute of Marine Science, University of Alaska, Fairbanks, p. 485-516.
- Quintero, P. J., 1981, Preliminary report on benthic foraminifers from Navarin Basin province, Bering Sea, Alaska, *in* Carlson, P. R. and Karl, H. A. (eds.), *Seafloor geologic hazards, sedimentology and bathymetry: Navarin Basin Province, northwestern Bering Sea*: U.S. Geological Survey Open-File Report 81-1217, p. 135-149.
- Saidova, Kh. M., 1961, *Ekologiya foraminifer paleogeografiia dal'nevostochnykh morei* (in Russian): Moscow, Academy of Sciences of the Soviet Union, 232 p., 31 plates.
- _____ 1967, Depth changes in Bering Sea during the Upper Quaternary, as indicated by benthonic foraminifera, *in* Hopkins, D. (ed.), *The Bering Land Bridge*: Stanford University Press, p. 364-368.
- Vallier, T. L., Underwood, M. B., Gardner, J. V., and Barron, J. A., 1980, Neogene sedimentation on the outer continental margin, southern Bering Sea: *Marine Geology*, v. 269-287.

SAMPLE	80-14 (91m)	80-59 (99m)	80-50 (110m)	80-16 (120m)	81-25 (123m)	81-26 (125m)	81-01 (135m)	80-70 (142m)	81-02 (143m)	81-77 (145m)	81-27 (145m)	80-41 (150m)	80-32 (150m)	81-74 (152m)	80-10 (164m)	80-39 (220m)	80-40 (220m)	81-81 (269m)	81-09 (290m)	81-65 (436m)	80-03 (524m)	81-18 (884m)	81-11 (975m)	81-83 (1120m)
ADRGLO	1	3	8	10	90	100	50	60	40	90	40	70	90	70	110	30	120	70	0	4	40	0	0	10
ALVSP	0	0	0	0	1	0	0	0	0	0	20	0	20	0	10	0	0	0	0	0	0	0	0	0
AMOBAC	0	0	0	0	0	0	0	0	0	0	0	0	0	0	0	0	0	0	0	0	0	0	0	0
AMDSPP	0	0	0	0	0	0	0	0	0	0	0	0	0	0	0	0	0	0	0	0	0	0	0	0
AMSSPP	0	0	0	0	0	0	0	0	0	0	0	0	0	0	0	0	0	0	0	0	0	0	0	0
AMTCAS	4	0	10	0	40	20	10	3	0	2	10	8	6	0	0	0	0	0	0	0	0	0	0	0
ASTSPP	0	0	0	0	0	0	0	0	0	1	0	0	0	0	0	0	0	0	0	0	0	0	0	0
BTYSIP	0	0	0	0	0	0	0	0	0	0	0	0	0	0	0	0	0	0	0	0	0	0	0	0
BOLDEC	0	0	0	0	0	0	0	0	0	0	0	0	0	0	0	0	0	0	0	0	0	0	0	0
BOLPAC	0	1	20	0	20	10	50	30	0	10	40	20	20	3	0	10	20	120	0	110	2	50	0	40
BOLPSE	0	0	0	0	0	0	0	0	0	0	0	0	0	0	0	0	0	0	0	0	0	50	0	0
BOLSEM	0	0	0	0	0	0	0	0	0	0	0	0	0	0	0	0	0	0	0	0	0	70	0	0
BOLSPI	0	0	0	0	0	0	0	0	0	0	0	0	0	0	0	0	0	0	0	0	0	0	0	0
BOLSPP	0	0	0	0	0	0	0	0	0	0	0	0	0	0	0	0	0	0	0	0	0	0	0	0
BUCSPP	0	10	20	1	10	20	10	10	10	20	30	10	40	30	30	30	5	5	0	10	10	2	2	30
BULELE	0	0	0	0	0	0	0	0	0	0	0	0	0	0	0	0	0	0	0	0	0	0	0	0
BULTEN	0	0	0	0	0	0	0	0	0	0	0	0	0	0	0	0	0	0	0	0	0	290	0	0
CALSPI	0	0	0	0	0	0	0	0	0	0	0	0	0	0	0	0	0	0	0	0	0	0	0	0
CASCAL	0	0	0	0	0	0	0	0	0	0	0	0	0	0	0	0	0	0	0	0	0	0	0	0
CASDEL	0	0	0	0	0	0	0	0	0	0	0	0	0	0	0	0	0	0	0	0	0	0	0	0
CASLIM	0	0	0	0	0	0	0	0	0	0	0	0	0	0	0	0	0	0	0	0	0	70	0	0
CASLRG	0	0	0	0	0	0	0	0	0	0	0	0	0	0	0	0	0	0	0	0	0	0	0	0
CASMIN	0	40	20	0	0	30	30	10	0	10	20	20	40	10	40	40	10	2	0	20	0	0	0	40
CASSPP	0	0	0	1	3	0	0	0	0	0	0	0	0	0	0	0	0	0	0	0	10	3	0	2
CSDSPP	0	0	0	0	0	0	0	0	0	0	0	0	0	0	0	0	0	0	0	0	0	5	0	0
CHISPP	0	0	0	0	0	0	0	0	0	0	0	0	0	0	0	0	0	0	0	0	0	0	0	0
CHNFIM	0	0	0	0	0	0	0	0	0	0	0	0	0	0	0	0	0	0	0	0	0	20	0	0
CIBLOB	0	0	0	0	0	0	0	0	0	0	0	0	0	0	0	0	0	0	0	0	0	0	0	0
CIBSPP	0	0	0	0	0	0	0	0	10	0	0	0	0	0	0	0	0	0	0	0	0	0	0	0
CRBSPP	40	0	0	4	0	0	0	0	0	0	0	0	0	0	0	0	0	0	0	0	0	0	0	0

Table 7. Relative frequency percentages of benthic foraminifers in surface samples.

SAMPLE	80-14 (91m)	80-59 (99m)	80-50 (110m)	80-16 (120m)	81-25 (123m)	81-26 (125m)	81-01 (135m)	80-70 (142m)	81-02 (143m)	81-27 (145m)	80-41 (150m)	80-32 (150m)	81-74 (152m)	80-39 (220m)	80-40 (220m)	81-81 (269m)	81-09 (290m)	81-65 (436m)	80-03 (524m)	81-18 (884m)	81-11 (975m)	81-83 (1120m)
CYCSP	0	0	0	0	0	0	0	0	0	0	0	0	0	0	0	0	0	0	0	0	0	0
DENSP	0	0	0	0	0	0	0	0	0	0	0	0	0	0	0	0	0	0	0	0	0	0
EGGADV	350	20	260	730	200	250	180	230	650	360	230	240	30	70	170	170	0	30	10	10	50	0
EGGSCR	0	0	10	0	0	20	0	10	0	0	40	30	10	0	30	40	0	10	0	0	10	0
EGGSUB	0	0	0	0	0	0	0	0	0	0	0	0	0	0	0	0	0	0	0	0	0	0
ELPBAT	0	0	0	0	0	0	0	0	0	0	0	0	0	0	0	0	0	0	0	0	0	0
ELPCLA	0	150	90	5	20	10	70	30	0	20	80	100	10	3	0	0	0	0	0	10	40	0
ELPSP	0	4	0	4	0	0	0	0	0	0	0	3	0	0	2	1	0	4	10	2	0	0
EPIPAC	0	0	0	0	0	0	0	0	0	0	0	0	0	0	0	0	0	0	0	0	0	0
EPIVIT	0	0	30	30	50	30	70	50	0	120	70	100	100	170	70	50	0	10	240	80	0	0
EPOLEV	0	0	0	0	0	0	0	0	0	4	0	0	20	10	10	4	0	0	10	10	40	0
EPOSP	0	0	0	1	3	0	0	0	0	0	0	0	0	0	0	0	0	0	0	0	0	0
FISSP	0	1	0	0	0	0	0	0	0	1	0	0	0	0	0	0	0	0	1	0	0	0
FLOLAB	0	2	10	0	10	20	70	20	0	10	20	20	20	3	20	10	0	3	40	2	10	0
FURSP	0	220	30	0	10	30	60	20	0	20	20	30	6	3	45	40	0	600	10	10	90	0
GLOSP	0	0	10	2	0	10	10	20	0	14	20	10	6	0	0	0	0	3	2	10	30	0
GYRSP	0	0	0	0	0	0	0	0	0	0	0	0	0	0	0	0	0	0	0	0	0	0
HAPBRA	0	0	0	0	0	0	0	0	0	1	0	0	0	0	10	30	170	1	5	0	20	0
HAPCOL	0	0	0	0	0	0	0	0	0	0	0	0	0	0	0	0	0	0	1	5	0	0
HAPSP	0	0	3	2	0	0	3	0	0	0	0	0	3	0	2	0	170	0	0	0	0	0
HYPSP	0	0	0	0	0	0	0	0	0	0	0	0	0	0	0	0	0	0	0	0	0	0
ISTRNR	0	0	20	4	10	0	20	10	20	30	40	20	40	20	10	0	0	0	0	0	0	0
KARBAC	0	0	0	0	0	0	0	0	0	0	0	0	0	0	0	0	0	0	0	0	0	0
LAGSP	0	0	3	2	0	0	10	0	0	1	0	1	3	3	2	1	0	3	2	2	10	0
MAROB	0	0	0	0	0	0	0	0	0	0	0	0	0	0	0	0	0	0	0	0	0	0
MARSP	0	0	0	0	0	0	0	0	0	0	0	0	0	0	0	0	0	0	0	0	0	0
MELPOM	0	0	0	0	0	0	0	0	0	0	0	0	0	0	0	0	0	0	0	0	0	0
NONPUL	0	0	0	0	0	0	0	0	0	0	0	0	0	0	0	0	0	0	0	0	0	0
NONTGD	0	0	0	0	0	0	20	0	0	2	0	0	0	0	20	5	0	10	70	40	0	30
NONSP	0	0	0	1	0	0	0	0	0	0	0	0	20	0	0	0	0	0	0	0	0	0

Table 7. (continued).

SAMPLE	80-14 (91m)	80-59 (99m)	80-50 (110m)	80-16 (120m)	81-25 (123m)	81-26 (125m)	81-01 (135m)	80-70 (142m)	81-02 (143m)	81-77 (145m)	81-27 (145m)	80-41 (150m)	80-32 (150m)	81-74 (152m)	80110 (164m)	80-39 (220m)	80-40 (220m)	81-81 (269m)	81-09 (290m)	81-65 (436m)	80-03 (524m)	81-18 (884m)	81-11 (975m)	81-83 (1120m)
OOLSPP	0	0	0	0	0	0	0	0	0	0	0	0	0	0	0	0	0	0	0	0	0	0	0	0
PATCOR	0	0	0	0	0	0	0	0	0	0	0	0	0	0	0	0	0	0	0	0	0	0	0	0
PELVAR	0	0	0	0	0	0	0	0	0	0	0	0	0	0	0	0	0	0	0	0	0	0	0	0
PRTORB	0	0	0	0	0	0	0	0	0	0	0	0	0	0	0	0	0	0	0	0	0	0	0	0
PSENON	0	0	0	0	0	0	0	0	0	0	0	0	0	0	0	0	0	0	0	0	0	0	0	0
PULSPP	0	0	0	0	0	0	0	0	0	0	0	0	0	0	0	0	0	0	0	0	0	0	0	0
PYRSPP	0	0	0	0	0	0	0	0	0	0	0	0	0	0	0	0	0	0	0	0	0	0	0	0
QNGSPP	0	0	0	0	0	0	0	0	0	0	0	0	0	0	0	0	0	0	0	0	0	0	0	0
RECSPP	0	30	20	0	10	20	10	0	0	1	30	3	20	3	10	10	3	3	0	0	0	0	0	0
REOARC	35	37	40	20	90	80	70	140	0	2	10	40	20	10	10	0	2	10	0	10	0	0	0	20
REOCUR	3	0	20	2	0	20	0	3	0	30	0	20	20	10	0	0	10	20	0	0	0	0	0	0
REODIF	0	0	0	0	110	50	0	0	0	20	50	20	30	0	0	0	0	0	0	0	0	0	0	10
REOFUS	0	0	70	0	0	0	70	90	0	0	0	0	0	30	0	0	0	0	0	0	0	0	0	0
REOSCO	0	1	0	0	0	0	0	0	0	5	0	0	0	0	0	10	0	0	0	0	0	0	0	0
REOSPP	0	2	0	2	0	0	3	0	0	2	0	0	0	0	0	0	0	0	0	0	0	0	0	2
RHSBPP	0	0	0	0	0	0	0	0	0	0	0	0	0	0	0	0	0	0	0	0	0	0	0	10
SACSPH	0	0	0	0	0	0	0	0	0	0	0	0	0	0	5	0	0	0	0	0	0	0	0	0
SPRBIF	220	10	110	80	230	160	100	180	90	100	110	140	130	130	50	30	130	70	0	60	50	0	0	60
SPRSPP	0	0	0	0	0	0	0	0	0	0	0	0	0	0	0	0	0	13	0	23	0	20	0	0
TEXTOR	20	50	60	20	60	80	20	20	20	30	20	20	60	50	80	20	80	150	0	40	0	20	20	20
TEXSPP	0	0	0	0	0	0	0	0	0	0	0	0	0	0	0	0	0	0	0	0	10	0	0	10
TRIFLU	0	0	20	40	10	3	10	10	70	70	20	20	30	90	200	320	100	70	330	10	20	20	20	20
TRLTRI	0	0	0	0	0	0	0	0	0	0	0	0	0	0	0	0	0	0	0	0	0	0	0	4
TROGLO	0	0	0	0	0	0	0	0	0	0	0	0	0	0	0	0	0	0	0	0	0	0	0	0
TRONIT	0	0	0	0	0	0	0	0	0	0	0	10	0	0	0	0	0	0	0	0	0	0	0	0
TROPAC	0	0	0	0	3	0	0	0	0	0	0	0	0	0	0	0	0	0	0	0	0	10	0	0
TROSPP	0	0	0	0	3	0	0	0	10	0	0	0	0	6	20	0	0	10	170	0	10	0	0	0
UVGPRG	0	0	10	20	0	20	50	40	40	10	40	20	10	50	50	90	10	20	0	10	10	20	20	40
UVGSEN	0	0	0	0	0	0	0	0	0	0	0	0	0	0	0	0	0	0	0	0	0	0	0	0
UVGSPP	0	0	0	0	3	0	0	0	0	0	0	0	0	0	0	0	0	0	0	0	0	0	0	0

Table 7 (continued).

SAMPLE	80-65 (1609m)	81-21 (1640m)	81-12 (1683m)	81-85 (1745m)	81-14 (1826m)	81-13 (2080m)	80-17 (2481m)	81-46 (2530m)	81-15 (2750m)	81-47 (2760m)	80-22 (2842m)	81-48 (2910m)	80-13 (2962m)	80-04 (3222m)	81-76 (3230m)	80-26 (3373m)	81-57 (3395m)	81-06 (3395m)
ADRGLO	2	0	0	0	0	0	0	0	0	0	0	0	0	0	0	0	0	0
ALVSP	4	2	0	20	0	0	0	0	0	0	0	0	0	0	0	0	0	0
AMOBAC	0	0	0	0	0	0	0	0	0	0	0	0	0	0	0	0	0	0
AMDSP	0	0	0	0	0	0	0	0	0	0	0	0	0	0	0	0	0	0
AMSPP	0	0	0	0	0	0	0	0	0	0	0	0	0	0	0	0	0	0
AMTCAS	0	0	0	0	0	0	0	0	0	0	0	0	0	0	0	0	0	0
ASTSPP	2	0	0	0	0	0	0	0	0	0	0	0	0	0	0	0	0	0
BTYSIP	0	0	0	0	0	0	0	0	0	0	0	0	0	0	0	0	0	0
BOLDEC	0	0	0	0	0	0	0	0	0	0	0	4	0	0	0	0	0	0
BOLPAC	30	0	30	70	100	3	170	0	80	170	420	230	420	420	180	50	130	50
BOLPSE	0	0	0	0	0	0	0	0	0	0	0	0	0	0	0	0	0	0
BOLSEM	0	0	0	0	0	0	0	0	0	0	0	0	30	0	0	0	0	0
BOLSPI	0	0	0	0	0	0	0	0	0	0	0	0	0	0	0	0	20	0
BOLSPP	2	0	0	0	0	0	0	0	0	0	0	0	0	0	0	0	20	0
BUCSPP	2	0	6	2	3	0	0	0	0	0	0	4	0	0	0	0	3	0
BULELE	0	0	0	0	4	0	0	0	0	0	0	4	0	0	0	0	0	0
BULTEN	0	0	0	0	140	0	0	0	0	0	0	0	0	0	0	0	50	0
CALSPI	0	0	0	0	0	0	0	0	0	0	0	0	0	0	0	0	0	0
CASCAL	0	0	0	0	0	0	0	0	0	0	0	0	0	0	0	0	0	0
CASDEL	0	0	0	0	0	0	0	0	0	0	0	0	0	0	0	0	0	0
CASLIM	0	0	0	0	0	0	0	0	0	0	0	0	0	0	0	0	0	0
CASLRG	0	0	0	0	0	0	0	0	0	0	0	0	0	0	0	0	0	0
CASMIN	60	60	20	60	10	40	20	0	10	20	0	20	0	30	10	10	3	10
CASSPP	2	0	0	0	0	0	0	0	0	4	0	0	0	0	0	0	0	0
CSDSPP	0	10	0	0	10	0	0	0	0	0	0	0	0	0	0	0	10	0
CHISPP	10	0	0	2	10	0	0	0	0	0	0	0	0	0	0	0	0	0
CHNFIM	10	0	3	4	70	10	0	0	0	10	40	0	30	0	0	0	20	0
CIBLOB	0	0	0	0	0	0	10	0	0	0	0	0	0	0	0	0	0	0
CIBSPP	2	0	0	0	0	0	0	0	0	0	0	0	0	0	20	0	0	0
CRBSPP	0	10	0	0	0	0	3	0	0	0	0	0	0	0	0	0	0	0

Table 7 (continued).

SAMPLE	80-65 (1609m)	81-21 (1640m)	81-12 (1683m)	81-85 (1745m)	81-14 (1826m)	81-13 (2080m)	80-17 (2481m)	81-46 (2530m)	81-15 (2750m)	81-47 (2760m)	80-22 (2842m)	81-48 (2910m)	80-13 (2962m)	80-04 (3222m)	81-76 (3230m)	80-26 (3373m)	81-57 (3395m)	81-06 (3395m)
CYCSPP	0	0	0	0	0	0	0	0	0	0	0	0	0	0	0	0	0	0
DENSPP	0	0	0	0	0	0	0	0	0	0	0	0	0	0	0	0	0	0
EGGADV	70	60	130	40	2	30	10	80	30	50	0	60	0	20	30	0	10	10
EGGSCR	20	10	10	4	0	0	0	0	0	0	0	0	0	0	0	0	0	0
EGGSUB	60	140	20	190	0	0	60	0	140	20	10	40	0	150	0	20	10	10
ELPBAT	0	0	0	0	20	0	0	0	50	0	0	0	0	0	0	0	0	0
ELPCLA	0	0	0	0	0	0	0	0	0	0	0	0	0	0	0	0	0	0
ELPSP	0	0	0	0	2	0	0	0	0	0	0	0	0	0	0	0	0	0
EPIPAC	0	0	0	0	2	0	0	0	0	0	0	0	0	0	0	0	0	0
EPIVIT	20	3	0	0	20	3	0	0	20	90	190	10	4	0	10	90	10	30
EPOLEV	4	0	0	0	0	0	70	0	0	0	0	10	0	20	0	10	0	0
EPOSPP	0	0	0	0	0	0	0	0	0	0	0	0	0	0	0	0	0	0
FISSPP	0	3	0	0	0	0	0	0	10	14	20	4	0	0	0	0	3	3
FLOLAB	20	30	3	100	70	40	10	0	10	70	0	50	30	50	10	0	50	20
FURSPP	430	190	130	250	391	110	250	0	124	130	110	290	260	20	130	10	60	15
GLOSPP	24	10	8	70	40	10	10	0	4	40	0	10	50	50	0	0	43	12
GYRSPP	0	0	0	0	0	0	10	0	0	0	0	0	0	0	0	0	0	0
HAPBRA	0	3	0	0	0	0	0	0	4	10	0	10	0	0	0	0	0	10
HAPCOL	0	0	0	0	0	0	0	0	0	0	0	0	0	0	0	0	0	0
HAPSP	0	10	0	0	1	0	0	0	0	0	0	0	0	0	0	0	0	0
HYPSP	0	0	0	0	0	0	0	0	0	0	0	0	0	0	0	0	0	0
ISTRNR	0	0	0	2	1	40	0	50	20	10	0	0	0	0	0	0	3	0
KARBAC	0	0	0	0	0	0	0	0	0	7	0	0	0	0	0	0	0	2
LAGSPP	2	0	3	0	4	3	3	0	10	0	0	0	0	0	0	10	0	2
MAROB	0	0	0	0	0	0	0	0	0	0	0	0	0	0	0	0	0	0
MARSPP	0	0	0	0	0	0	0	0	0	0	0	0	0	0	0	0	0	0
MELPOM	0	0	0	0	0	0	3	0	0	10	0	4	0	0	0	0	0	0
NONPUL	0	0	0	0	0	0	0	0	0	0	0	0	0	0	0	0	0	0
NONTGD	40	20	0	40	40	20	120	0	10	40	50	80	0	0	60	0	40	10
NONSP	0	0	70	0	0	0	0	0	0	0	0	0	0	0	0	0	0	0

Table 7 (continued).

SAMPLE	80-65 (1609m)	81-21 (1640m)	81-12 (1683m)	81-85 (1745m)	81-14 (1826m)	81-13 (2080m)	80-17 (2481m)	81-46 (2530m)	81-15 (2750m)	81-47 (2760m)	80-22 (2842m)	81-48 (2910m)	80-13 (2962m)	80-04 (3222m)	81-76 (3230m)	80-26 (3373m)	81-57 (3395m)	81-06 (3395m)
OOLSPP	0	0	0	0	0	0	0	0	0	0	0	0	0	0	0	0	0	0
PATCOR	0	0	0	0	0	0	0	0	0	0	0	0	0	0	0	0	0	0
PELVAR	0	0	0	0	0	0	0	0	0	0	0	0	0	0	0	0	0	0
PRTORB	0	0	0	0	0	0	0	0	0	0	0	0	0	0	0	0	0	0
PSENON	0	0	40	0	0	0	0	0	0	0	0	0	30	0	10	0	10	2
PULSPP	0	0	0	0	0	0	0	0	0	4	0	0	0	0	0	0	0	0
PYRSPP	0	0	0	0	0	0	0	0	0	0	0	0	0	0	0	10	0	2
QNSQSP	0	0	0	0	0	0	0	0	0	0	0	0	0	0	0	10	10	0
RECSPP	0	0	0	0	0	0	0	0	0	0	0	0	0	0	0	0	0	0
REOARC	0	0	20	0	0	50	0	0	10	0	0	0	0	0	10	10	10	0
REOCUR	2	80	10	30	1	20	50	490	20	0	0	0	0	0	140	230	120	210
REODIF	4	0	0	0	0	0	2	30	30	160	50	40	0	0	100	50	10	20
REOFUS	0	0	0	20	0	0	0	0	40	0	0	0	0	0	0	20	30	20
REOSCO	0	0	0	0	0	10	0	0	0	0	0	0	0	0	0	0	0	0
REOSPP	0	20	13	0	0	10	0	110	88	34	0	0	20	0	60	30	90	0
RHSBPP	0	0	0	0	0	0	0	0	0	0	0	0	0	0	0	0	0	0
SACSPH	0	0	0	0	0	0	3	0	0	10	0	0	0	0	0	0	0	30
SPRBIF	60	0	50	0	0	60	10	0	0	0	0	10	30	0	10	0	0	0
SPRSPP	0	30	80	10	0	0	0	190	0	10	0	0	30	0	20	0	0	0
TEXTOR	70	170	230	30	3	50	20	30	0	10	40	0	0	0	0	0	0	20
TEXSPP	10	0	0	0	0	0	0	0	0	0	0	0	0	0	0	0	0	0
TRIFLU	10	0	5	0	0	0	0	0	0	0	0	0	0	0	0	0	0	0
TRLTRI	0	0	0	0	3	0	0	0	0	0	0	0	0	0	0	0	0	0
TROGLO	0	0	0	0	0	0	3	0	0	0	0	0	0	0	0	10	0	0
TRONIT	0	0	0	2	0	0	0	0	0	0	0	0	0	0	0	0	0	0
TROPAC	0	0	50	0	0	30	0	0	50	40	0	20	0	50	100	40	20	40
TROSPP	2	23	0	0	0	0	13	0	60	0	30	10	0	50	10	0	0	0
UVGPRG	30	50	20	30	40	10	0	0	0	0	10	4	0	0	0	50	0	0
UVGSEN	0	10	0	0	0	0	0	0	0	10	10	0	0	0	0	10	0	0
UVGSPP	0	0	0	0	0	0	0	0	0	0	0	0	0	0	0	0	0	5

Table 7 (continued).

SAMPLE	80-65 (1609m)	81-21 (1640m)	81-12 (1683m)	81-85 (1745m)	81-14 (1826m)	81-13 (2080m)	80-17 (2481m)	81-46 (2530m)	81-15 (2750m)	81-47 (2760m)	80-22 (2842m)	81-48 (2910m)	80-13 (2962m)	80-04 (3222m)	81-76 (3230m)	80-26 (3373m)	81-57 (3395m)	81-06 (3395m)
SPECIES																		
VALCON	0	0	0	0	0	0	0	0	0	0	0	0	0	0	0	0	0	0
VALGLA	0	0	0	1	0	0	3	0	0	4	0	0	0	0	0	0	3	2
VIRSP	0	0	0	0	0	0	0	0	0	14	0	10	0	0	0	0	0	0
OTHAGG	4	0	30	0	0	20	0	0	60	20	0	0	0	0	0	0	30	5
OTHCAL	4	10	0	20	1	3	9	0	10	10	10	74	50	20	70	40	13	72
OTHMIL	0	3	0	2	0	0	0	0	0	0	0	4	0	0	10	0	0	30

Table 7 (continued).

Table 8. List of Benthic Foraminiferal Species.

ADRGLO	<i>Adercotryma glomeratum</i>
ALVSPP	<i>Alveolophragmium</i> spp.
AMOBAC	<i>Ammobaculites</i>
AMDSPP	<i>Ammodiscus</i> spp.
AMSSPP	<i>Ammoscalaria</i> spp.
AMTCAS	<i>Annotium cassis</i>
ASTSPP	<i>Astrononion</i> spp.
BTYSIP	<i>Bathysiphon</i>
BOLDEC	<i>Bolivina decussata</i>
BOLPAC	<i>Bolivina pacifica</i>
BOLPSE	<i>Bolivina pseudobeyrichi</i>
BOLSEM	<i>Bolivina seminuda</i> and <i>B. seminuda</i> var. <i>foraminata</i>
BOLSPI	<i>Bolivina spissa</i>
BOLSPP	<i>Bolivina</i> spp.
BUCSPP	<i>Buccella</i> spp.
BULELE	<i>Buliminella elegantissima</i>
BULTEN	<i>Buliminella tenuata</i>
CALSP1	small, transparent calcareous foram
CASCAL	<i>Cassidulina californica</i>
CASDEL	<i>Cassidulina delicata</i>
CASLIM	<i>Cassidulina limbata</i>
CASLRG	<i>Cassidulina lomitensis</i> and <i>C. l. elegantula</i>
CASMIN	<i>Cassidulina minuta</i>
CASSPP	<i>Cassidulina</i> spp.
CSDSPP	<i>Cassidulinoides</i> spp.
CHISPP	<i>Chilostomella</i> spp.
CHNFIM	<i>Chilostomellina fimbriata</i>
CIBLOB	<i>Cibicides lobatulus</i>
CIBSPP	<i>Cibicides</i> spp.
CRBSPP	<i>Cribrostomoides</i> spp.
CYCSPP	<i>Cyclammina</i> spp.
DENSPP	<i>Dentalina</i> spp.
EGGADV	<i>Eggerella advena</i>
EGGSCR	<i>Eggerella scrippsi</i>
EGGSUB	<i>Eggerella subadvena</i>
ELPBAT	<i>Elphidium batialis</i>
ELPCLA	<i>Elphidium clavatum</i>
ELPSPP	<i>Elphidium</i> spp.
EPIPAC	<i>Epistominella pacifica</i>
EPIVIT	<i>Epistominella vitrea</i>
EPOLEV	<i>Eponides leviculus</i>
EPOSPP	<i>Eponides</i> spp.
FISSPP	<i>Fissurina</i> spp.
FLOLAB	<i>Florilus labradoricum</i>

FURSPP	<i>Fursenkoina</i> spp.
GLOSPP	<i>Globobulimina</i> spp.
GYRSPP	<i>Gyroidina</i> spp.
HAPBRA	<i>Haplophragmoides bradyi</i>
HAPCOL	<i>Haplophragmoides columbiense</i>
HAPSPP	<i>Haplophragmoides</i> spp.
HYPSP	<i>Hyperammina</i> spp.
ISTRNR	<i>Islandiella teretis/norcrossi</i>
KARBAC	<i>Karrerriella baccata</i>
LAGSPP	<i>Lagena</i> spp.
MAROB	<i>Marginulina obesa</i>
MARSPP	<i>Martinottiella</i> spp.
MELPOM	<i>Melonis pompiliodes</i>
NONPUL	<i>Nonionella pulchella</i>
NONTGD	<i>Nonionella turgida digitata</i>
NONSPP	<i>Nonionella</i> spp.
OOLSPP	<i>Oolina</i> spp.
PATCOR	<i>Patellina corrugata</i>
PELVAR	<i>Pelosina variabilis</i>
PRTORB	<i>Protelphidium orbiculare</i>
PSENON	<i>Pseudononion</i> spp.
PULSPP	<i>Pullenia</i> spp.
PYRSPP	<i>Pyrgo</i> spp.
QNQSPP	<i>Quinqueloculina</i> spp.
RECSPP	<i>Recurvoidea</i> spp.
REOARC	<i>Reophax arctica</i>
REOCUR	<i>Reophax curtus</i>
REODIF	<i>Reophax difflugiformis</i>
REOFUS	<i>Reophax fusiformis</i>
REOSCO	<i>Reophax scorpiurus</i>
REOSPP	<i>Reophax</i> spp.
RHBSPP	<i>Rhabdammina</i> spp.
SACSPH	<i>Saccammina sphaerica</i>
SPRBIF	<i>Spiroplectammina biformis</i>
SPRSPP	<i>Spiroplectammina</i> spp.
TEXTOR	<i>Textularia torquata</i>
TEXSPP	<i>Textularia</i> spp.
TRIFLU	<i>Trifarina fluens</i>
TRLTRI	<i>Triloculina</i> spp.
TROGLO	<i>Trochammina globigerinaformis</i>
TRONIT	<i>Trochammina nitida</i>
TROPAC	<i>Trochammina pacifica</i>
TROSPP	<i>Trochammina</i> spp.
UVGPRG	<i>Uvigerina peregrina</i>
UVGSEN	<i>Uvigerina senticosa</i>
UVGSPP	<i>Uvigerina</i> spp.
VALCON	<i>Valvulina conica</i>
VALGLA	<i>Valvulineria glabra</i>
VIRSPP	<i>Virgulina</i> spp.
OTHAGG	Other agglutinated species
OTHCAL	Other calcareous species
OTHMIL	<i>Miliollids</i>

SPECIES	81-12		40-42cm	80-82cm	120-122cm	129-132cm	140-142cm	160-162cm	175-177cm	180-183cm	210-212cm	220-222cm	235-237cm	240-242cm	248cm	257-260cm	core catcher
	Sample number and depth interval within core	TOP (~2cm)															
ADRGLO		30	0	0	0	0	0	0	0	0	0	0	0	0	0	0	0
ALVSPP		0	0	0	0	0	0	0	0	0	0	0	0	0	0	0	0
AMOBAC		0	0	0	0	0	0	0	0	0	0	0	0	0	0	0	0
AMDSPP		0	0	0	0	0	0	0	0	0	0	0	0	0	0	0	0
AMSSPP		0	0	0	0	0	0	0	0	0	0	0	0	0	0	0	0
AMTCAS		0	0	0	0	0	0	0	0	0	0	0	0	0	0	0	0
ASTSPP		0	0	0	2	0	0	3	0	1	0	0	0	0	0	2	0
BTYSIP		0	0	0	0	0	0	0	0	0	0	0	0	0	0	0	0
BOLDEC		0	0	20	0	6	10	10	10	4	3	5	0	10	20	20	20
BOLPAC		30	20	10	20	20	40	60	30	20	40	30	20	40	50	40	30
BOLPSE		0	0	0	2	6	3	0	2	0	0	0	0	1	0	0	0
BOLSEM		0	0	0	0	3	0	0	0	2	0	0	0	0	0	1	0
BOLSPI		0	0	0	0	0	3	0	0	0	0	0	0	0	0	0	0
BOLSPP		0	0	0	0	0	0	0	0	0	0	0	0	0	0	0	0
BUCSPP		6	50	30	50	90	10	10	4	1	6	10	10	10	0	20	20
BULELE		0	0	0	10	3	3	1	0	0	10	0	10	1	0	0	10
BULTEN		0	3	0	10	6	40	4	4	10	10	10	10	20	10	20	20
CALSPI		0	0	0	0	0	0	0	0	0	0	0	0	0	0	0	0
CASCAL		0	0	0	0	0	20	30	0	0	0	0	0	0	0	0	0
CASDEL		0	0	0	2	0	0	0	0	0	0	0	0	0	0	2	0
CASLIM		0	0	0	0	0	0	0	0	0	0	0	0	0	0	0	0
CASLRG		0	0	0	0	0	0	0	4	20	3	50	10	4	0	20	40
CASMIN		20	30	90	20	70	30	0	30	30	40	60	50	60	30	50	70
CASSPP		0	0	0	0	0	0	0	0	0	0	0	0	0	10	0	0
CDSPP		0	0	0	50	30	0	0	2	1	0	0	0	0	0	0	0
CHISPP		0	0	0	0	0	0	0	0	0	0	0	0	0	0	0	0
CHNFIM		3	0	0	10	10	10	4	10	10	0	20	30	10	5	20	10
CIBLOB		0	0	0	0	0	0	10	0	0	0	5	0	0	10	10	20
CIBSPP		0	0	3	10	0	10	1	0	2	3	0	0	10	0	1	0
CRBSPP		0	0	0	0	0	0	0	0	0	0	0	0	0	0	0	0

Table 9. Relative frequency percentages of benthic foraminiferal species in core 81-12.

SPECIES	81-12		4C-42cm	80-82cm	120-122cm	129-132cm	140-142cm	160-162cm	175-177cm	180-183cm	210-212cm	220-222cm	235-237cm	240-242cm	248cm	257-260cm	core catcher
	depth interval	number and TOP (~2cm)															
CYCSPP	0	0	0	0	0	0	0	0	0	0	0	0	0	0	0	0	0
DENSPP	0	0	0	0	0	0	0	0	0	0	0	0	0	0	0	0	0
EGGADV	130	60	0	5	0	3	10	0	0	0	10	10	10	0	0	0	0
EGGSCR	10	0	0	0	0	0	0	0	0	0	0	0	0	0	0	0	0
EGGSUB	0	0	0	0	0	0	0	0	0	0	0	0	0	0	0	0	0
ELPBAT	20	130	30	0	50	40	0	0	0	0	0	0	0	0	0	0	0
ELPCLA	0	0	0	0	0	6	50	100	120	60	40	60	140	110	60	90	150
ELPSPP	0	0	0	0	0	6	0	3	10	2	6	3	0	10	0	20	20
EPIPAC	0	50	5	40	100	30	10	10	10	0	3	10	3	10	4	20	30
EPIVIT	0	10	40	10	80	450	350	440	310	360	310	360	340	370	290	310	0
EPOLEV	0	0	10	0	3	3	3	0	10	1	0	0	0	0	0	1	0
EPOSPP	0	0	0	0	0	0	0	0	0	0	0	0	0	0	0	0	0
FISSPP	0	0	0	0	2	3	0	2	2	2	3	4	0	1	10	5	0
FLOLAB	3	50	100	210	170	30	30	2	0	10	10	5	10	20	2	2	10
FURSP	130	10	70	30	20	63	280	250	412	323	260	170	202	330	261	140	0
GLOSPP	8	10	10	30	20	40	20	10	10	3	10	3	10	20	10	10	30
GYRSPP	0	0	0	0	0	0	0	0	0	0	0	0	0	0	0	0	0
HAPBRA	0	0	0	0	0	0	0	0	0	0	3	0	0	0	0	0	0
HAPCOL	0	0	0	0	0	0	0	0	0	0	0	0	0	0	0	0	0
HAPSPP	0	0	0	0	0	0	0	0	0	0	0	0	0	0	0	0	0
HYPSP	0	0	0	0	0	0	0	0	0	0	0	0	0	0	0	0	0
ISTRNR	0	0	0	0	5	10	3	4	4	2	10	10	10	10	4	10	20
KARBAC	0	0	0	0	0	0	0	0	0	0	0	0	0	0	0	0	0
LAGSPP	3	6	0	3	5	15	0	4	2	0	0	0	0	0	2	1	0
MAROB	0	0	0	0	0	0	0	0	0	0	0	0	0	0	0	0	0
MARSPP	0	0	0	0	0	0	0	0	0	0	0	0	0	0	0	0	0
MELPOM	0	0	0	0	0	0	0	0	0	0	0	0	0	0	0	0	0
NONPUL	0	0	0	0	0	0	0	0	0	0	0	0	0	0	0	0	0
NONTGD	0	10	0	0	10	0	10	0	10	40	40	80	70	20	20	0	30
NONSP	70	0	0	0	0	0	0	10	0	0	0	0	0	10	10	0	0

Table 9. (continued).

SPECIES	Sample number and depth interval within core															
	81-12 TOP (~2cm)	40-42cm	80-82cm	120-122cm	129-132cm	140-142cm	160-162cm	175-177cm	180-183cm	210-212cm	220-222cm	235-237cm	240-242cm	248cm	257-260cm	core catcher
OOLSPP	0	0	0	0	0	0	0	0	0	0	0	0	0	0	0	0
PATCOR	0	0	0	0	0	0	0	0	0	0	0	0	0	0	0	0
PELVAR	0	0	0	0	0	0	0	0	0	0	0	0	0	0	0	0
PRTORB	0	0	0	0	0	0	0	0	0	0	0	0	0	0	0	0
PSENON	10	0	0	2	2	3	0	0	1	0	1	1	0	1	0	1
PULSPP	0	0	0	0	0	0	0	0	0	0	0	0	0	0	0	0
PYRSPP	0	0	0	0	0	0	0	0	0	0	0	0	0	0	0	0
GNQSPP	0	0	0	0	0	0	0	0	0	0	0	0	0	0	0	0
RECSPP	0	0	0	0	0	0	0	0	0	0	0	0	0	0	0	0
REOARC	20	0	0	0	0	0	0	0	5	0	0	0	0	0	0	0
REOCUR	10	3	0	0	0	0	0	0	0	0	0	0	0	0	0	0
REODIF	0	0	0	0	0	0	0	0	0	0	0	0	0	0	0	0
REOFUS	0	0	0	0	0	0	0	0	0	0	0	0	0	0	0	0
REOSCO	0	0	0	0	0	0	0	0	0	0	0	0	0	0	0	0
REOSPP	13	0	0	0	0	0	0	0	0	0	0	0	0	0	0	0
RHBSPP	0	0	0	0	0	0	0	0	0	0	0	0	0	0	0	0
SACSPH	0	0	0	0	0	0	0	0	0	0	0	0	0	0	0	0
SPRBIF	50	10	0	0	0	0	0	0	2	6	1	2	3	4	3	0
SPRSPP	80	0	0	0	0	0	0	0	1	0	0	0	0	0	0	0
TEXTOR	230	0	0	0	0	0	0	0	0	0	0	0	0	0	0	0
TEXSPP	0	0	0	0	0	0	0	0	0	0	0	0	0	0	0	0
TRIFLU	5	10	8	5	6	3	1	1	2	0	0	0	0	0	1	0
TRLTRI	0	0	0	0	0	0	0	0	0	0	0	0	0	0	0	0
TROGLO	0	0	0	0	0	0	0	0	0	0	0	0	0	0	0	0
TRONIT	0	0	0	0	0	0	0	0	0	0	0	0	0	0	0	0
TROPAC	50	0	0	0	0	0	0	0	0	0	0	0	0	0	0	0
TROSPP	0	3	3	0	3	0	0	0	0	0	0	0	0	0	0	0
UVGPRG	20	45	21	35	18	7	1	4	1	6	1	1	0	2	2	0
UVGSEN	0	0	0	0	0	0	0	0	0	0	0	0	0	0	0	0
UVGSPP	0	0	0	0	0	0	0	0	0	0	0	0	0	0	0	0

Table 9. (continued).

SPECIES	81-12									
	TOP (~2cm)									
Sample number and depth interval within core	VALCON	VALGLA	VIRSP	OTHAGG	OTHCAL	OTHMIL	0	0	0	0
40-42cm	0	0	0	0	0	0	0	0	0	0
80-82cm	0	0	0	0	0	0	0	0	0	0
120-122cm	0	0	0	0	0	0	0	0	0	0
129-132cm	0	0	0	0	0	0	0	0	0	0
140-142cm	0	0	0	0	0	0	0	0	0	0
160-162cm	1	0	0	0	0	0	0	0	0	0
175-177cm	0	0	0	0	0	0	0	0	0	0
180-183cm	0	0	0	0	0	0	0	0	0	0
210-212cm	0	0	0	0	0	0	0	0	0	0
220-222cm	0	0	0	0	0	0	0	0	0	0
235-237cm	0	0	0	0	0	0	0	0	0	0
240-242cm	0	0	0	0	0	0	0	0	0	0
248cm	0	0	0	0	0	0	0	0	0	0
257-260cm	0	0	1	0	0	0	0	0	0	0
core catcher	0	0	0	0	0	0	0	0	0	0

Table 9. (continued)

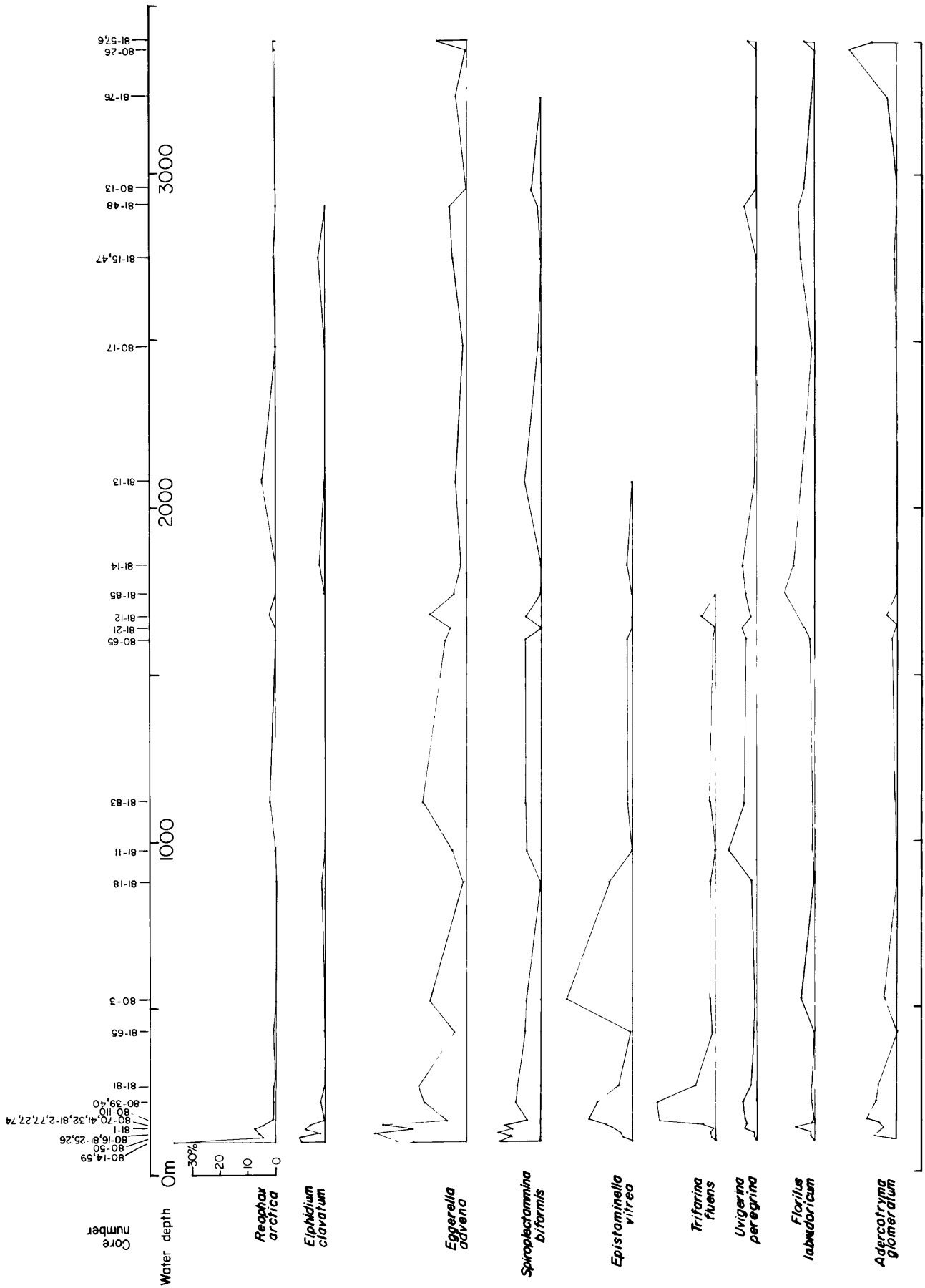


Figure 31. Relative frequency percentages of the most abundant species in surface samples plotted against increasing water depth.

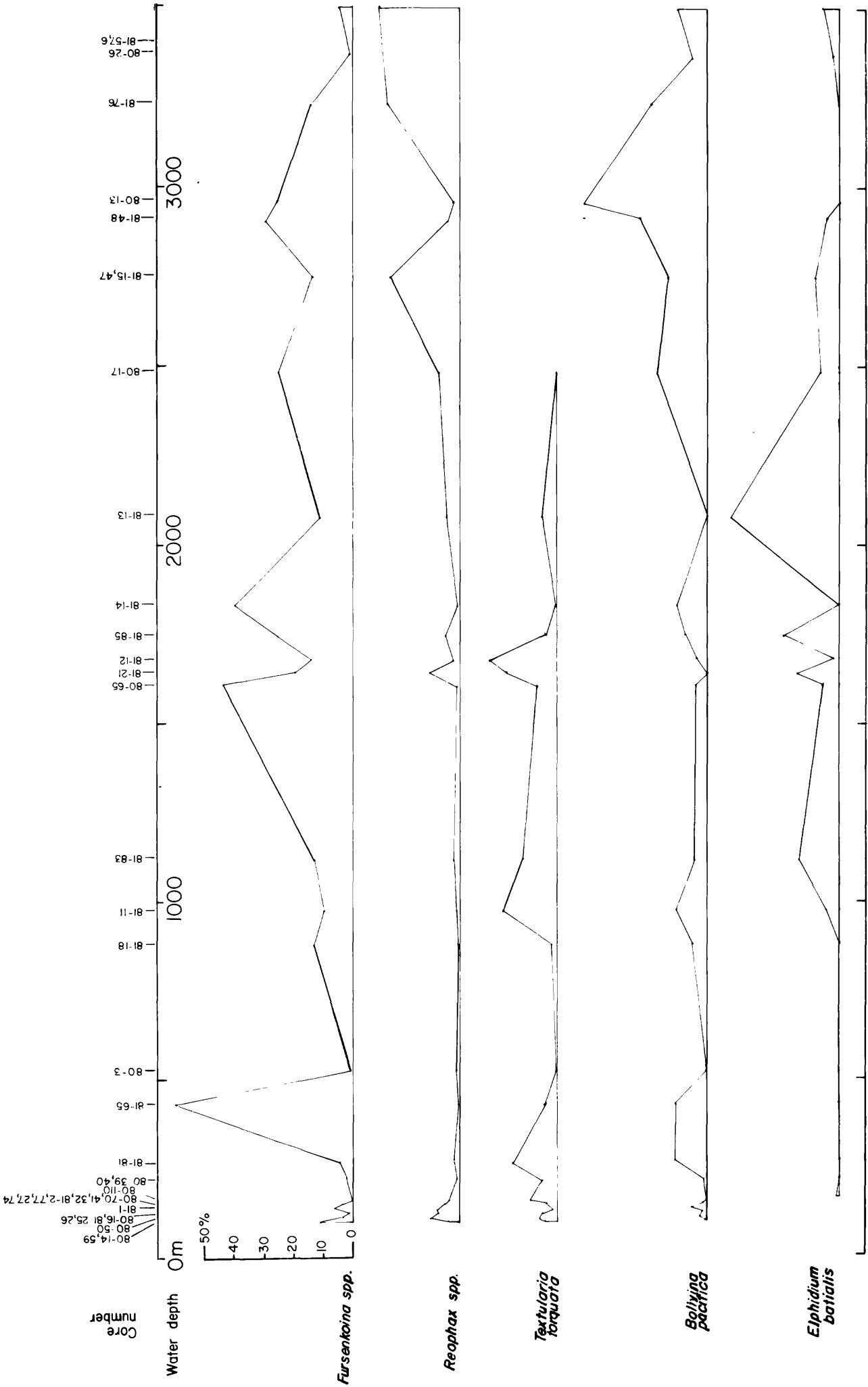


Figure 31. (continued).

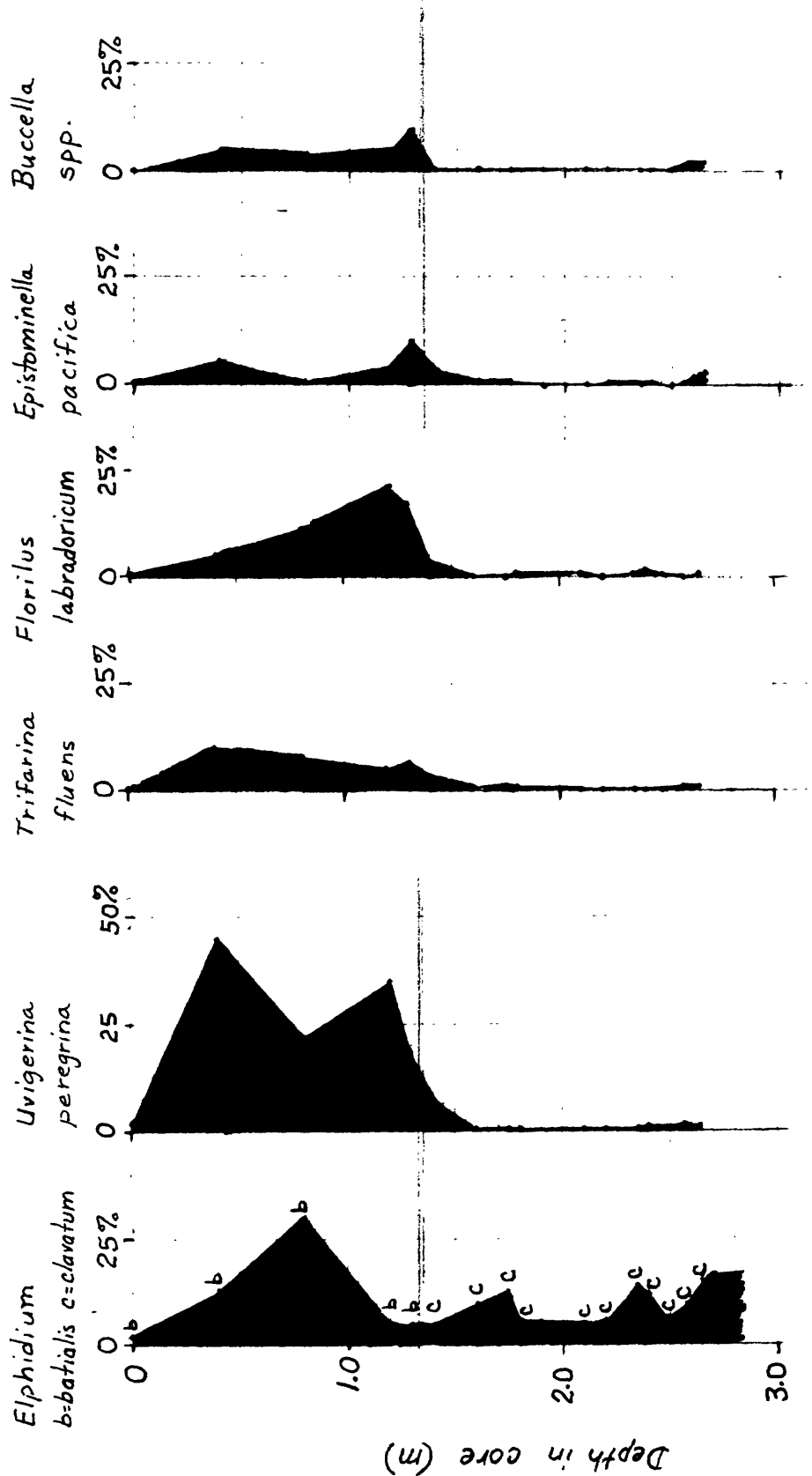


Figure 32. Relative frequency percentages of the most abundant benthic foraminiferal species plotted against depth in core 81-12.

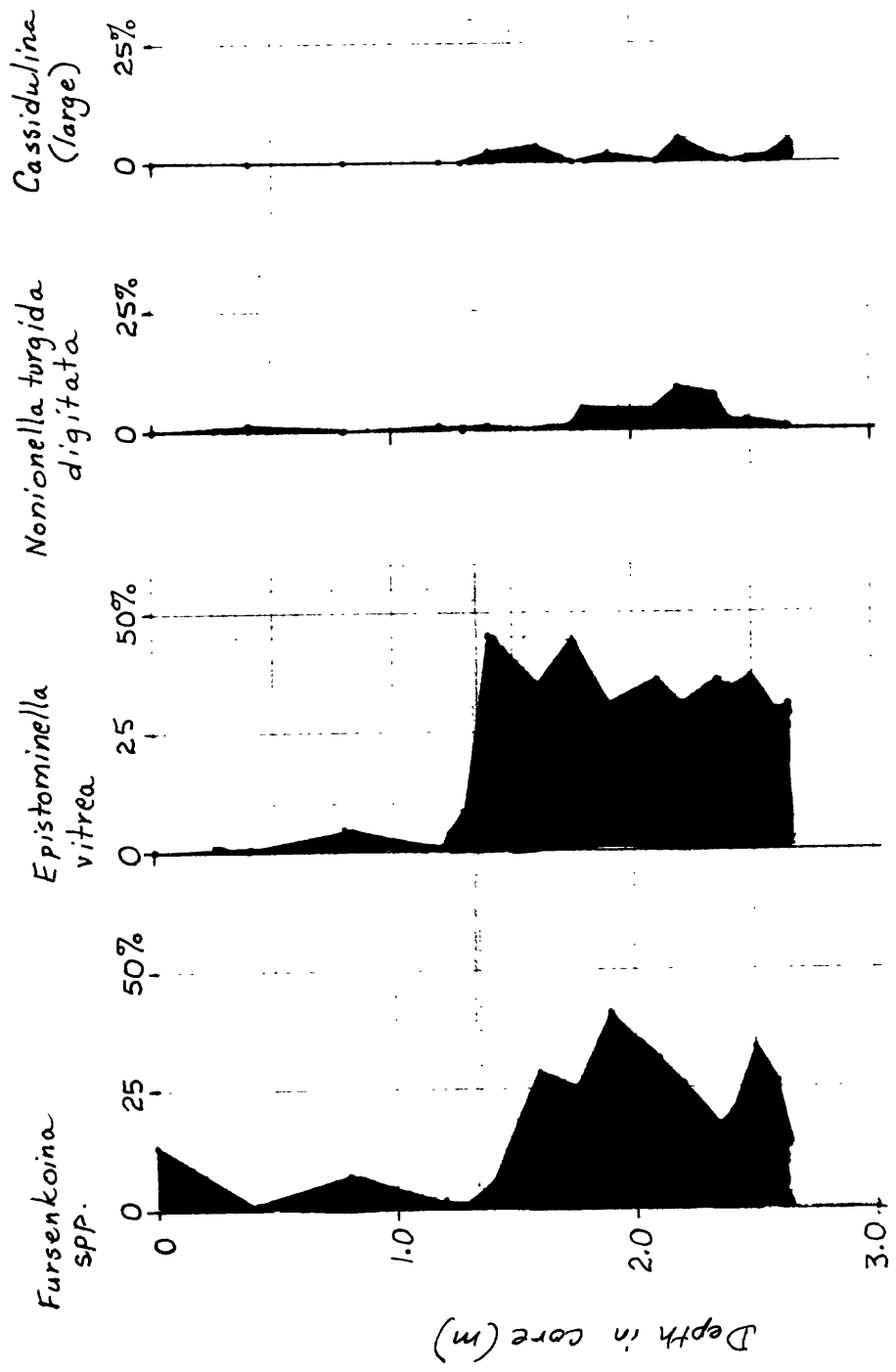


Figure 32. (continued).

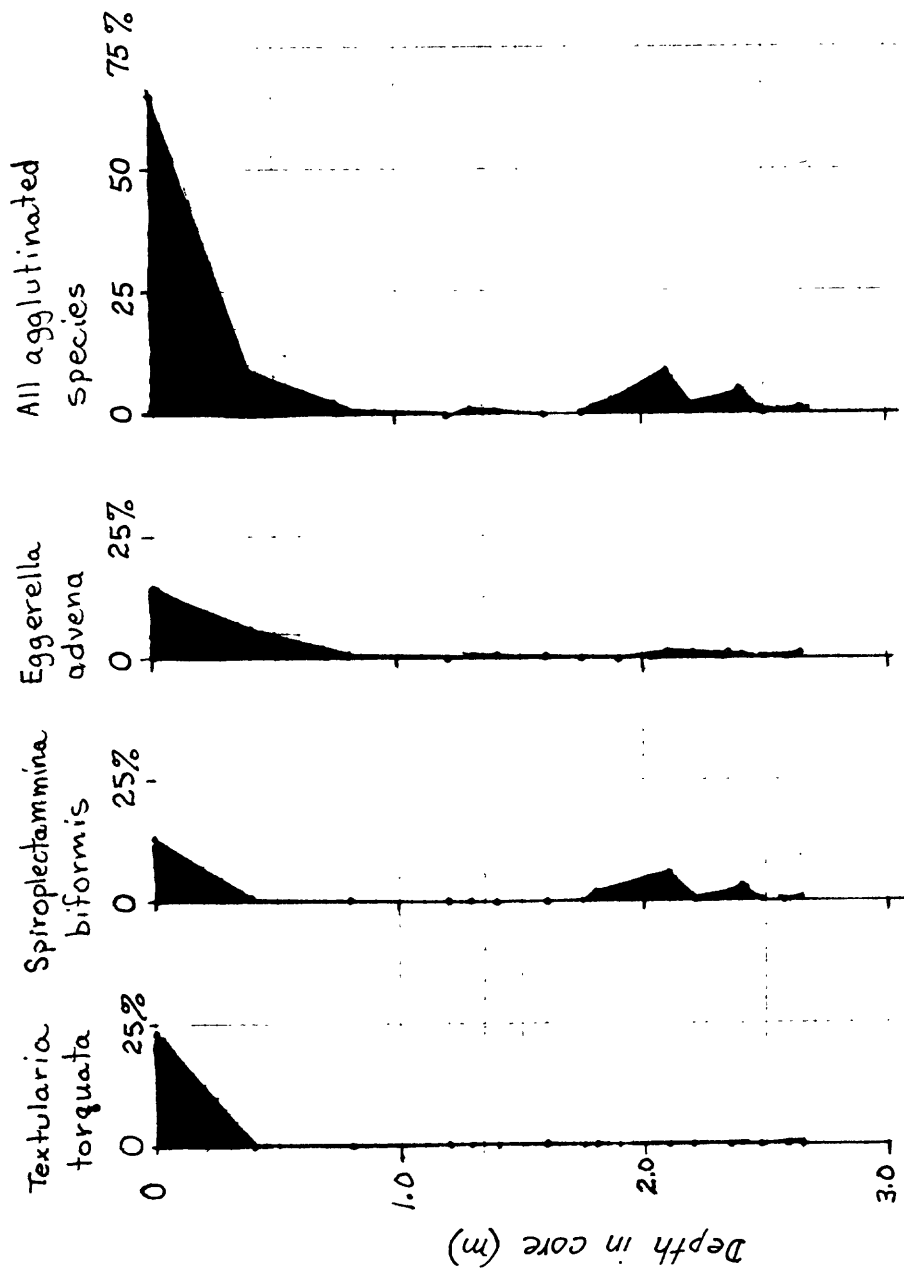


Figure 32. (continued).

CHAPTER 10: DIATOM ANALYSIS OF SURFACE SAMPLES
RECOVERED FROM PERVENETS CANYON

by

Jack G. Baldauf

INTRODUCTION

The Navarin basin province within the Bering Sea (Fig. 33) is geographically divided into a flat shallow shelf, a relatively steep slope, and a deep marginal basin. Five major submarine canyons (Zhemchug, Pervenets, St. Matthew, Middle, and Navarinsky) occur within this region (Fisher and others, 1982).

Previously, Baldauf (1982) analyzed thirty surface samples from this region and documented the existence of two distinct diatom assemblages separated from each other by the shelf-slope break. The basin-slope assemblage is characterized by the species Denticulopsis seminae which typically comprises 20-40 percent of the entire assemblage. Other species within this group include; Oscinodiscus marginatus, Oscinodiscus oculus-iridis, Rhizosolenia hebatata forma hebatata, and Thalassiosira oestrupii. Most basin-slope species, although most abundant in the deeper waters, are present on the shelf. For example, Denticulopsis seminae composes less than 10 percent of the overall assemblage on the continental shelf compared to 20-40 percent in the basin-slope region.

The shallow water assemblage is dominated by Nitzschia grunowii (previously referred to as Nitzschia oceanica in Baldauf (1981, 1982)) which composes greater than 20 percent of the shelf assemblage. Additional species in this assemblage includes; Nitzschia cylindrus, Thalassiosira nordenskioldii, and an increase in abundance of both benthonic and brackish water species.

The presence of these two assemblages within the surface sediment may be useful in determining the effect that secondary processes such as sediment transport or winnowing have on surface sediment within the canyon and slope regions of the Navarin basin province. The very abundant occurrence of shelf species within the surface samples examined from the canyon regions would suggest the erosion and transportation of sediment from the shelf and deposition of these sediments in the canyons.

To examine the usefulness of diatoms for interpreting the effect of sedimentary processes, thirty-seven surface samples were examined within the region of Pervenets Canyon (Fig. 34). Pervenets Canyon was selected for this preliminary study due to its relatively small. An additional motive for selecting Pervenets Canyon, was the occurrence of Rhizosolenia curvirostris and Thalassiosira nidulus in sample G-80-66 recovered from within this canyon. The presence of these species suggests that sample G-80-66 has an age greater than 0.26 Ma, the age cited by Donahue (1970) and Schrader (1976) for the last occurrence of Rhizosolenia curvirostris.

Pervenets Canyon, located within the central portion of the Navarin Basin province, is approximately 125 kilometers long and heads in a water depth of approximately 150 meters. The mouth of this canyon occurs at an approximate water depth of 3000 meters. Pervenets Canyon is approximately 30 kilometers wide at the shelf break, which is narrow when compared to both Zhemchug and Navarinsky Canyons which have an approximate width of 100 kilometers. Two main tributaries which form a right angle at the head of Pervenets Canyon are 80-90 kilometers long and have an approximate gradient of 0.30 degrees.

METHODS AND PROCEDURES

In addition to samples previously examined (Baldauf 1981, 1982), thirty-three surface samples were obtained from cores collected in and around Pervenets Canyon by the NOAA research vessel DISCOVERER during the summers of 1980, 1981, and from the U.S. Geological Survey vessel S.P. LEE during the summer of 1982. Strewn slides of unprocessed sediment were prepared for each sample and examined at 500x for age diagnostic species. Samples of Quaternary age were further examined at 1250x with the first 300 specimens tabulated to determine the abundance of individual species within each sample.

The preservational quality of each sample is based on the presence and absence of delicate forms such as Thalassiosira hyalina, Pseudopodosira elegans, and Asteromphalus robustus and heavily silicified forms such as Coscinodiscus marginatus, Rhizosolenia hebatata forma hebatata, Stephanopyxis turris, Bacteriosira fragilis, and Thalassiosira gravida. The occurrence of both robust and delicate species suggests well preserved samples whereas the presence of only robust forms indicated poorly preserved samples.

RESULTS

With the exception of samples G-82-18, G-82-20 and G-81-66 all samples examined are latest Quaternary in age. Samples G-82-18 and G-82-20 are equivalent in age with previously examined sample G-81-66, based on the presence of Rhizosolenia curvirostris and Thalassiosira nidulus. The occurrence of these two species suggests that these samples are older than 0.26 Ma. Samples G-81-66, G-82-18, and G-82-20 are located in Pervenets Canyon at a water depth of 580, 625, and 739 meters, respectively (Fig. 34).

Sample G-82-19, which is located between samples G-82-18 and G-82-20 (Fig. 34) at a water depth of 852 meters, is latest Quaternary in age, as it lacks both Rhizosolenia curvirostris and Thalassiosira nidulus. This suggests that modern sediment is swept clean of the canyon walls and deposited on the canyon floor. However, the sediment associated with core G-82-19 also could be transported from the adjacent continental shelf directly to the canyon floor.

A seismic profile perpendicular to the canyon's axis (Fig. 35) shows surface exposures of stratigraphically older seismic reflectors within the upper canyon walls. A portion of these reflectors occur in proximity of samples G-81-66, G-82-18, and G-82-20 which suggests an age greater than 0.26 Ma for these reflectors. Although exact correlation between these samples and specific seismic reflectors is uncertain, the water depth of each sample

allows approximate correlation and suggests that the reflectors of interest are exposed surficially between the depths of 580-739 meters.

Table 10 shows the occurrence of species encountered during the examination of the latest Quaternary age surface sediment from Pervenets Canyon. The over-all species distribution agrees well with the previous conclusions of Baldauf (1982) in which two assemblages separated by the shelf-slope break were observed. The deeper water assemblage is dominated by Denticulopsis seminae, whereas the shallow water assemblage is dominated by Nitzschia grunowii.

The latest Quaternary age samples from the Pervenets Canyon area (Fig. 34) range in water depth from 145 meters to 3230 meters. One major transect from the shelf (sample G-80-79, 128 meters) to the basin (sample G-81-76, 3230 meters; Fig. 34 transect 1) shows an increase in the abundance of Denticulopsis seminae from the shelf, to mid slope, to lower slope and basin (Fig. 36). In sample G-80-65, water depth 1609 meters, D. seminae composes approximately 33 percent of the assemblage. This unusually high concentration of D. seminae is the probable result of either high productivity within a very restricted microenvironment or down slope sediment transport. The abundance of other species within this sample is equivalent to their abundance within nearby samples.

The abundance of Denticulopsis seminae in samples from transect 2 (Figs. 34 and 35) perpendicular to the canyon axis (samples G-82-16, 17, 19, and G-81-67; Fig. 36) is similar to the above results. D. seminae composes approximately 15-17 percent of the assemblage at a depth between 100-500 meters, and increases in abundance to 23-26 percent of the assemblage at a water depth greater than 500 meters. Although samples G-80-76, 77 are exceptions to this trend for presently unknown reasons, the conformity of all other samples to this trend suggest that depth either directly or as a secondary factor is responsible for the distribution of D. seminae within the Navarin Basin province.

To determine the abundance of shelf species in the surface sediments of Pervenets Canyon, the same samples used in the transects for determining the distribution of Denticulopsis seminae, were also used to compare the abundance of the shelf species Nitzschia grunowii.

The abundance of Nitzschia grunowii within surface samples from Pervenets Canyon (Fig. 37) shows more irregularities than that observed in the distribution pattern of Denticulopsis seminae. As a general trend, Nitzschia grunowii increases in abundance as one proceeds from the slope region to the inner shelf (see Baldauf, 1982).

The abundance of Nitzschia grunowii within Pervenets Canyon, however, disagrees with this pattern. N. grunowii in most samples within the canyon between the depths of 150-2400 meters constitutes approximately 10-17 percent of the entire assemblage. No trend in abundance vs. depth is observed. Furthermore, in sample G-80-26, Nitzschia grunowii composes 19 percent of the assemblage which is equivalent elsewhere in the Navarin Basin to its abundance within water depths of less than 125 meters.

The difference in abundance patterns of N. grunowii between samples within Pervenets Canyon and elsewhere within the Navarin Basin (see Baldauf, 1982) suggests that sediments within the canyon may be under the influence of post depositional processes of which sediment transport of shelf sediments in to the canyon may be a primary factor.

However, further studies are required to determine all factors which influence this process as well as to examine in detail additional distribution patterns of species not only restricted to shelf environments but also to the slope and basin regions as well.

REFERENCES

- Baldauf, J. G., 1981, Diatom analysis of late Quaternary sediments from the Navarin Basin Province, Bering Sea. In Carlson, P. R. and Karl, H. A. (eds.), Seafloor geologic hazards, Sedimentology, and Bathymetry: Navarin Basin Province, Northwestern Bering Sea. U.S. Geological Survey Open-File Report 82-1217, p. 100-113.
- Baldauf, J. G., 1982, Identification of the Holocene-Pleistocene Boundary in the Bering Sea by diatoms. *Boreas*, volume 11, p. 113-118.
- Donahue, J. G., 1970, Pleistocene diatoms as climatic indicators in North Pacific sediments. *Geological Society of America Memoir* 126, p. 121-138.
- Fischer, J. M., Carlson, P. R., and Karl, H. A., 1982, Bathymetric map of Navarin Basin province, northern Bering Sea; U.S. Geological Survey Open-File Report 82-1038, 11 p., 1 map, scale 1:1,000,000.
- Schrader, H. J., 1973, Cenozoic diatoms from the Northeastern Pacific, Leg 18. In Kulm, D., von Huene, R., et al., Initial Reports of the Deep Sea Drilling Project, Volume 18, Washington (U.S. Government Printing Office), p. 673-797.

Table 10. Abundance (in percent) of species encountered during the experimentation of surface sediments from the Pervenets Canyon region

SPECIES	80-04	80-12	80-13	80-22	80-25	80-26	80-28	80-30	80-35	80-36	80-50	80-51	80-52	80-56	80-65	80-77	80-79	80-81	80-82	80-83	80-84	80-85
<i>Actinocyclus curvatus</i>	-	-	0.3	-	0.6	-	-	-	-	-	-	-	-	0.6	1.0	-	-	-	-	-	-	-
<i>A. divinus</i>	0.6	0.6	0.3	0.3	1.6	0.3	2.6	0.3	1.0	0.6	1.0	1.0	0.3	1.6	-	0.6	0.6	2.0	2.3	-	0.6	0.3
<i>A. ochotensis</i>	-	-	1.0	-	-	-	-	0.6	0.6	-	-	-	-	1.0	1.6	-	-	-	-	-	2.3	1.0
<i>Actinoptychus undulatus</i>	-	-	-	-	0.6	-	0.3	-	-	-	0.6	-	-	-	0.3	-	0.3	0.3	0.6	-	-	-
<i>A. vulgaris</i>	-	0.3	-	-	-	-	-	-	-	0.3	-	-	-	-	-	-	-	-	-	-	-	-
<i>Asteromphalus robustus</i>	-	0.6	-	-	-	-	-	-	0.6	-	-	-	-	-	-	-	-	-	-	-	-	-
<i>Barbarosira fragilis</i>	6.0	6.6	2.6	3.0	4.3	4.3	7.3	7.3	3.3	6.0	9.3	9.0	10.6	7.0	3.0	7.6	7.0	7.3	6.0	5.3	3.0	3.0
<i>Biddulphia aurita</i>	3.0	1.6	2.6	1.0	1.0	2.0	1.0	1.6	2.3	1.3	2.0	1.3	1.6	1.3	0.3	1.3	0.6	1.0	1.6	2.3	2.3	2.3
<i>Coscinodiscus lacustris</i>	-	-	-	0.3	-	-	-	0.3	-	-	0.6	-	-	-	-	0.3	0.3	-	-	-	-	-
<i>C. marginatus</i>	0.6	2.0	0.3	0.6	-	1.6	1.0	0.3	1.3	0.3	-	0.3	1.6	1.3	2.3	0.3	2.0	1.0	1.3	1.3	1.6	1.6
<i>C. oculis-iridis</i>	1.0	1.3	1.3	0.3	-	1.3	0.6	0.3	1.3	1.3	0.6	1.6	0.6	0.3	2.6	-	0.6	0.6	0.3	1.6	2.0	2.0
<i>C. radiatus</i>	-	-	-	-	-	-	-	-	-	-	-	-	-	-	-	-	-	-	-	-	-	-
<i>C. stellaris</i>	-	-	-	-	-	-	-	-	-	-	-	-	-	-	-	-	-	-	-	-	-	-
<i>C. tabularis</i>	0.3	0.3	-	-	-	0.6	-	-	0.3	-	0.3	0.6	0.3	-	-	-	-	-	-	0.3	0.3	0.6
<i>Denticulopsis seminae</i>	28.0	27.0	31.3	38.3	4.0	26.0	7.3	3.0	17.0	29.0	7.0	6.3	6.0	14.3	33.0	27.6	10.0	10.6	13.0	11.3	37.0	37.0
<i>Melosira "GROUP"</i>	1.0	1.0	0.6	1.0	9.3	1.0	2.6	5.3	4.0	2.6	3.6	5.3	4.0	4.6	1.6	2.3	5.3	11.6	-	9.0	2.3	2.3
<i>Melosira sp. 1.</i>	0.3	0.3	-	0.3	2.0	0.6	5.0	4.3	1.6	0.6	3.3	2.6	2.3	0.3	1.0	0.3	1.6	2.3	0.3	1.3	0.3	0.3
<i>Mavicula sp. 2.</i>	-	0.3	0.3	0.3	1.0	-	0.6	-	1.3	1.6	0.6	1.3	0.6	0.6	0.6	-	0.6	-	-	0.3	1.0	0.6
<i>Mavicula sp. 3.</i>	0.3	0.3	-	-	-	-	-	-	0.6	0.3	0.3	0.3	1.0	0.3	-	-	0.3	1.0	1.0	-	0.3	0.3
<i>Mitschia cylindrus</i>	4.0	3.0	3.6	3.1	9.0	5.6	10.6	13.6	10.0	7.0	9.0	10.3	10.6	8.3	7.3	6.6	9.3	6.0	6.6	7.6	1.0	1.0
<i>M. grunowii</i>	16.3	10.6	9.6	11.0	26.3	19.0	19.3	36.0	18.6	15.0	25.6	24.3	20.6	20.3	11.3	16.6	16.6	17.6	15.3	9.0	5.6	5.6
<i>Pleurosigma sp.</i>	-	-	-	0.3	-	-	0.6	-	-	0.3	-	0.3	-	-	-	-	0.6	-	-	0.3	-	-
<i>Porosira glacialis</i>	1.0	2.0	1.3	1.6	2.3	3.0	4.6	2.6	3.6	3.6	2.0	1.3	6.0	3.3	4.0	1.3	3.3	1.3	3.3	4.0	2.6	2.6
<i>Pseudopodosira elegans</i>	1.3	3.0	-	1.3	1.3	0.6	0.6	-	0.6	-	-	1.0	-	2.6	-	2.0	1.0	0.6	0.3	1.0	-	-
<i>Raphoneis sachalinensis</i>	-	-	-	0.3	0.6	-	-	-	1.0	0.3	-	0.3	-	-	0.3	0.3	1.3	0.3	0.6	-	-	-
<i>R. surirella</i>	-	0.3	-	-	1.3	-	-	1.3	2.3	-	0.6	-	0.3	-	0.3	-	-	-	-	2.0	-	-
<i>Rhizolenia hebatata</i>	2.6	3.0	4.6	3.0	1.6	3.3	1.6	0.3	2.0	1.6	0.3	1.6	2.6	2.3	2.3	2.3	3.0	2.0	0.3	1.3	2.3	2.3
<i>R. styliformis</i>	1.3	2.3	-	1.0	0.3	-	-	0.6	0.3	0.3	0.3	1.3	1.6	0.6	2.6	1.6	1.3	0.3	1.3	2.3	2.0	2.0
<i>Stephanopyxis turris</i>	-	-	-	-	-	0.6	-	-	0.3	-	-	-	-	-	0.3	-	-	-	-	-	-	-
<i>Thalassionema nitsochoides</i>	-	-	1.6	1.0	3.6	0.3	2.0	2.6	2.6	1.0	1.3	0.6	3.0	2.6	2.0	0.6	1.6	-	-	2.6	4.6	4.0
<i>Thalassiosira decipiens</i>	2.3	3.3	2.0	2.0	1.3	2.6	2.6	1.6	2.6	1.0	3.3	2.3	2.6	3.3	2.0	3.3	4.3	2.3	3.3	3.6	1.6	1.6
<i>T. eccentrica</i>	-	-	-	-	-	-	-	-	-	-	-	-	-	-	-	-	-	-	-	-	-	-
<i>T. gravida</i>	7.3	6.6	2.3	3.0	3.6	2.3	4.6	8.6	1.6	4.3	10.0	12.3	3.0	2.6	2.6	5.6	6.3	10.0	7.0	1.0	2.3	2.3
<i>T. hyalina</i>	10.0	8.0	11.0	5.6	5.6	7.6	8.6	0.6	6.6	5.0	7.0	5.0	5.0	6.0	5.3	3.0	5.3	5.0	3.6	4.0	6.3	6.3
<i>T. leptopus</i>	1.0	-	0.3	-	0.6	-	0.3	0.3	0.3	-	0.3	1.0	0.6	0.3	-	-	-	0.3	-	0.3	-	-
<i>T. nordenskioldii</i>	3.0	-	6.0	5.6	3.6	4.6	8.0	4.6	1.6	6.3	4.0	3.6	5.3	4.3	4.0	6.0	4.6	4.6	1.6	5.3	4.0	4.0
<i>T. oestrupii</i>	-	1.3	2.0	2.0	-	1.3	2.0	-	2.6	2.6	-	1.0	-	2.6	0.3	2.0	2.0	1.3	2.3	2.6	1.0	1.0
<i>T. trifalta</i>	6.6	8.3	10.0	7.3	4.6	10.3	3.3	2.0	5.3	6.0	3.3	3.0	3.3	5.3	7.3	6.6	5.6	6.0	8.3	10.3	10.3	10.3
<i>T. undulosa</i>	-	1.6	1.0	1.6	0.6	1.6	-	-	0.6	1.3	0.6	0.6	1.0	1.6	1.6	1.6	1.6	1.6	1.6	0.6	1.3	0.3
<i>Thalassiothrix longissima</i>	1.0	0.6	3.0	1.6	1.0	1.6	1.0	0.6	1.6	0.3	0.3	-	0.6	1.0	0.3	-	-	-	1.0	0.6	1.3	1.3
<i>Xathopyxis ovalis</i>	0.6	0.3	0.3	0.6	-	0.3	-	-	0.3	-	-	-	-	0.6	0.6	0.6	-	-	-	0.3	-	-
FRESH WATER SPECIES	-	-	-	-	-	-	-	-	-	-	-	-	-	-	-	-	-	-	-	-	-	-

Table 10. cont'd

SPECIES	SAMPLE	80-98	80-99	80100	80101	80105	80-10	80110	80112	81-3	81-2	81-1	81-51	81-58	81-59	81-60	81-61	81-62	81-64	81-65	81-66	81-67	81-68
<i>Actinocyclus curvatus</i>		1.0	0.3	-	0.6	0.6	-	-	-	-	-	-	0.3	-	0.3	0.6	-	-	-	-	-	-	-
<i>A. divius</i>		0.6	0.6	1.0	1.0	1.0	3.0	2.0	2.3	-	-	-	0.6	-	0.3	0.6	-	-	-	-	-	-	-
<i>A. ochotensis</i>		0.6	2.0	0.3	-	1.0	1.0	0.6	0.6	0.6	-	0.6	-	-	0.3	1.3	-	0.3	-	-	-	-	0.3
<i>Actinoptychus undulatus</i>		0.6	1.0	-	-	0.3	-	-	-	-	-	-	-	-	-	-	-	-	-	-	-	-	-
<i>A. vulgaris</i>		-	-	-	-	-	-	-	-	-	-	-	0.3	-	-	0.3	-	-	-	0.3	0.3	-	-
<i>Astaromphalus robustus</i>		-	-	0.6	-	-	-	-	-	0.3	-	-	-	0.3	-	-	-	-	-	-	-	-	0.3
<i>Bacteriosira fragilis</i>		7.0	6.0	4.3	3.6	4.6	4.3	6.6	5.6	4.3	8.0	6.6	1.3	5.0	6.0	5.0	4.6	7.3	5.6	2.3	3.6	5.0	5.0
<i>Biddulphia aurita</i>		1.3	1.3	1.0	0.3	2.3	2.0	1.6	3.3	0.6	2.3	0.6	1.6	2.3	2.0	1.0	1.6	0.3	2.3	3.3	1.0	0.6	0.6
<i>Coccinodiscus lacustris</i>		-	-	-	-	0.3	-	0.3	-	0.3	0.3	-	-	-	0.6	0.3	0.6	-	-	1.0	-	-	-
<i>C. marginatus</i>		0.3	0.6	1.3	1.6	0.6	1.6	-	1.0	2.0	0.3	1.3	0.3	-	0.3	2.6	1.0	-	1.3	0.3	2.3	1.3	1.3
<i>C. oculus-iridis</i>		1.0	1.0	0.6	1.3	1.3	1.3	0.6	1.0	1.0	-	1.0	-	1.3	-	0.6	-	-	0.3	2.6	2.0	-	-
<i>C. radiatus</i>		-	-	-	-	-	-	-	-	-	0.6	-	-	-	-	1.0	-	-	-	-	-	-	-
<i>C. stellaris</i>		-	-	0.3	1.3	-	1.0	-	0.3	-	-	-	0.3	0.6	-	-	-	-	0.3	1.0	-	-	0.9
<i>C. tabularis</i>		-	-	-	-	-	-	-	-	-	-	-	-	-	-	-	-	-	-	-	-	-	1.3
<i>Denticulopsis seminiae</i>		9.6	10.3	17.6	28.0	24.0	22.3	33.3	15.0	14.6	11.3	17.6	40.6	15.7	6.6	14.0	9.6	9.6	14.0	16.3	24.3	24.0	24.0
<i>Melosira</i> GROUP		12.0	6.0	4.6	2.0	2.6	7.0	1.0	4.0	10.3	2.3	5.3	2.0	0.3	5.5	4.0	3.3	3.6	3.6	3.6	1.0	1.3	2.0
<i>Mavicula</i> sp. 1.		1.0	3.0	1.6	1.0	0.3	2.0	-	-	-	4.3	0.3	1.3	0.6	-	1.3	1.0	0.3	2.0	1.3	2.0	1.0	0.3
<i>Mavicula</i> sp. 2.		0.3	-	1.3	-	-	-	-	-	-	0.6	-	-	-	-	-	1.0	0.3	-	-	0.3	0.3	-
<i>Mavicula</i> sp. 3.		-	0.3	0.3	-	-	0.3	-	-	-	0.3	0.3	0.6	-	-	0.6	0.3	-	1.3	-	1.3	-	0.3
<i>Nitzschia cylindrus</i>		8.0	9.6	9.3	3.0	3.0	6.6	4.6	5.6	4.3	5.6	4.3	9.0	1.3	6.0	9.3	4.3	9.6	8.0	6.0	9.0	6.6	8.8
<i>M. grunovii</i>		21.0	15.6	17.6	13.0	11.0	13.0	7.0	21.0	21.6	8.2	12.0	12.3	6.6	11.0	17.3	16.0	16.6	14.6	16.3	16.6	8.6	13.6
<i>Pleurosigma</i> sp.		-	-	-	0.3	-	-	-	-	-	0.6	-	-	-	-	-	-	-	0.6	-	-	-	-
<i>Podocira glacialis</i>		4.0	3.3	3.6	2.0	2.6	1.6	4.0	1.6	2.0	5.0	1.6	2.6	1.3	1.3	3.3	1.7	1.0	1.0	1.0	1.6	1.0	-
<i>Pseudopodocira elegans</i>		2.6	-	-	1.0	1.6	0.6	0.6	1.0	0.6	1.6	1.0	1.0	0.3	1.0	0.6	0.3	2.0	0.6	0.6	0.6	0.6	0.6
<i>Rhaphoneis sachalinensis</i>		0.3	0.3	-	-	-	-	-	-	-	0.3	-	0.6	-	0.3	1.3	0.3	-	1.3	-	-	0.3	1.0
<i>Rh. surirella</i>		2.0	1.3	2.0	-	0.3	0.6	-	1.6	-	-	0.3	-	-	-	0.6	-	-	-	-	-	-	-
<i>Rhizocolenia hebetata</i>		2.3	0.6	2.3	2.6	5.3	1.3	3.0	1.3	2.3	4.6	3.6	1.6	7.3	1.6	1.0	5.0	1.3	3.6	2.3	1.0	2.0	2.0
<i>R. styliformis</i>		1.6	0.6	2.0	3.3	1.6	2.0	0.6	0.3	-	0.6	-	0.3	0.3	-	0.3	-	-	-	-	-	-	-
<i>Stephanopyxis turris</i>		-	-	-	-	-	-	-	-	-	-	-	-	-	-	-	-	-	-	-	-	-	-
<i>Thalassionema nitzschoides</i>		2.3	4.0	3.0	0.6	3.0	3.3	1.6	0.6	4.0	8.3	2.6	7.3	4.3	6.6	10.0	4.6	7.6	8.3	7.6	10.3	7.6	6.0
<i>Thalassiosira decipiens</i>		1.3	2.6	3.0	3.0	1.0	2.3	1.2	2.3	2.3	1.0	0.6	-	-	1.6	3.3	0.3	2.3	0.6	1.0	1.0	0.6	-
<i>T. eccentrica</i>		-	-	-	-	-	-	-	-	-	3.0	2.6	0.6	1.0	1.6	3.0	-	1.0	3.0	1.6	0.6	1.6	4.3
<i>T. gravida</i>		3.6	4.3	1.3	2.6	4.0	3.3	4.3	5.3	3.0	3.0	12.0	11.6	5.6	8.2	3.0	12.6	8.0	7.6	5.6	3.6	7.3	6.6
<i>T. hyalina</i>		2.6	4.0	7.6	7.6	5.3	7.0	7.3	4.6	6.0	9.0	3.0	4.6	4.3	5.3	9.6	4.0	6.6	5.0	5.0	6.0	9.3	5.3
<i>T. leptopus</i>		0.3	-	0.3	0.3	-	0.5	0.6	-	-	0.3	1.0	0.6	0.3	-	0.3	-	-	0.6	0.3	-	0.3	-
<i>T. nordenskioldii</i>		3.0	5.6	1.6	6.6	6.0	4.3	3.6	3.3	5.6	9.4	6.6	2.3	2.6	6.3	8.0	6.0	6.3	5.0	6.6	8.0	5.0	5.3
<i>T. ostrupii</i>		1.0	1.6	0.6	1.0	0.3	1.3	2.6	0.6	0.6	-	0.3	0.3	0.6	-	0.6	-	1.0	1.0	0.3	0.6	1.3	1.3
<i>T. trifurcata</i>		5.0	6.0	6.0	7.3	17.0	6.3	8.3	2.6	4.3	3.3	4.3	5.0	7.3	2.3	3.3	2.3	5.0	3.6	4.0	6.6	4.0	4.0
<i>T. undulosa</i>		0.6	1.3	0.6	0.6	0.3	1.6	1.6	0.6	1.3	2.3	-	2.3	-	3.0	1.0	3.0	2.3	1.3	-	2.3	2.3	3.3
<i>Thalassiothrix longissima</i>		1.0	1.0	0.6	1.6	0.6	1.3	1.0	0.3	0.6	1.0	0.6	1.0	-	2.0	1.3	1.3	2.3	2.0	2.3	0.3	1.6	-
<i>Xanthopyxis ovalis</i>		-	-	-	0.3	0.6	0.3	1.0	0.3	0.3	-	-	0.3	0.3	-	0.3	-	0.3	-	0.3	0.6	-	0.3
FRESH WATER SPECIES		-	-	-	-	-	-	-	-	0.6	0.3	-	-	-	0.3	-	-	0.3	-	0.3	-	-	-

Table 10. cont'd

SPECIES	SAMPLE	72-18	73-18	74-18	76-18	77-18	81-18	82-19	82-28	82-22	82-23	82-24	82-26	82-28
<i>Actinocyclus curvatus</i>		0.3	-	-	-	-	-	-	0.6	-	1.0	1.0	1.3	-
<i>A. diviseus</i>		-	-	-	-	-	0.3	-	-	0.3	-	-	-	-
<i>A. octanerus</i>		-	-	0.3	-	-	-	-	-	-	-	0.3	-	-
<i>Actinopterychus undulatus</i>		-	-	-	-	-	0.6	-	0.3	-	-	-	0.3	-
<i>A. vulgaris</i>		-	-	-	-	-	0.3	0.3	-	-	-	0.3	-	0.3
<i>Asteromphalus robustus</i>		-	-	-	-	0.6	0.3	0.3	0.3	-	0.3	0.6	-	-
<i>Bacteriosira fragilis</i>		5.0	9.6	5.0	6.0	5.0	2.3	2.0	2.6	4.3	7.3	5.0	5.3	4.6
<i>Biddulphia aurita</i>		1.3	1.3	2.0	0.6	1.0	3.0	1.0	1.6	3.0	1.6	0.6	2.3	1.0
<i>Coccinodiscus lacustris</i>		-	-	-	-	-	0.3	1.0	0.3	0.3	0.3	-	-	0.6
<i>C. marginatus</i>		0.6	1.0	2.3	-	1.3	2.6	2.3	2.0	2.3	2.3	2.6	1.0	2.0
<i>C. oculus-iridis</i>		0.3	0.3	1.0	-	-	1.0	-	1.6	1.3	0.3	2.0	0.6	1.0
<i>C. radiatus</i>		0.6	-	-	-	-	0.6	-	1.6	0.3	0.6	-	0.3	-
<i>C. stellaris</i>		-	-	0.3	0.3	0.3	-	-	-	-	-	-	-	0.3
<i>C. tabularis</i>		-	-	-	-	0.3	-	0.3	0.3	0.3	-	0.3	-	0.3
<i>Denticulopsis seminae</i>		9.3	12.4	14.3	22.3	14.0	23.3	26.3	18.6	20.6	13.3	18.3	23.3	20.3
<i>Melosira "GROUP"</i>		2.0	3.6	1.6	1.3	3.3	2.0	2.6	2.3	2.6	2.3	3.6	3.0	2.3
<i>Mavicula sp. 1.</i>		0.3	1.3	2.3	0.6	0.6	1.3	1.0	-	-	1.6	0.3	0.6	-
<i>Mavicula sp. 2.</i>		-	-	0.3	1.0	0.3	0.6	0.6	-	-	-	-	-	0.3
<i>Mavicula sp. 3.</i>		-	0.3	0.6	-	0.3	1.0	-	0.3	-	-	-	-	0.3
<i>Mitschia cylindrus</i>		5.0	8.3	5.0	5.6	6.3	2.3	3.0	4.0	5.0	3.6	7.6	4.3	3.6
<i>M. grunowii</i>		6.3	17.3	14.0	15.6	17.0	10.3	10.0	16.6	16.6	10.6	18.0	15.6	15.3
<i>Pleurosigma sp.</i>		0.3	-	-	-	-	0.6	-	-	-	-	-	-	-
<i>Podocira glacialis</i>		3.0	0.6	1.3	-	1.3	1.6	2.0	2.6	1.3	3.0	2.6	1.0	1.3
<i>Pseudopodosira elegans</i>		-	0.6	0.6	0.3	1.3	1.3	2.6	-	-	-	0.3	0.3	1.0
<i>Raphoneis sachalinensis</i>		-	0.3	0.3	0.3	0.6	0.3	1.0	1.3	1.0	0.3	-	-	-
<i>R. surirella</i>		0.3	0.6	0.6	-	-	0.6	1.3	-	0.3	0.3	-	0.3	0.3
<i>Rhizosolenia hebetata</i>		-	2.6	2.3	1.3	1.3	1.6	3.3	4.3	4.6	3.6	2.3	5.3	3.0
<i>R. styliformis</i>		1.3	-	-	-	0.3	-	-	-	0.3	-	-	-	0.3
<i>Stephanopyxis turris</i>		-	-	-	-	-	-	-	-	0.3	-	-	-	-
<i>Thalassiosira nitsochoides</i>		2.6	5.6	8.0	10.6	13.0	3.0	5.0	4.3	4.0	4.3	4.0	5.3	6.0
<i>Thalassiosira decipiens</i>		1.0	0.6	0.3	1.0	0.3	0.6	1.6	-	1.0	0.6	1.3	0.3	1.3
<i>T. eccentrica</i>		-	0.3	2.0	0.6	1.3	3.3	3.0	1.0	-	1.0	0.3	1.6	2.6
<i>T. gravida</i>		9.6	7.0	9.3	2.6	6.0	7.6	6.0	9.6	8.6	10.0	5.6	7.3	9.0
<i>T. hyalina</i>		5.0	3.6	5.3	6.0	2.6	5.6	4.0	4.0	3.6	4.6	5.0	3.3	7.6
<i>T. leptopus</i>		0.3	-	-	1.0	-	0.6	0.3	0.3	-	0.6	-	0.3	0.6
<i>T. nordenfalkioidii</i>		7.0	6.6	6.0	6.6	5.6	4.3	6.0	5.0	4.0	4.6	3.6	3.0	3.3
<i>T. ostrupii</i>		1.0	0.6	0.3	0.3	0.6	0.6	1.3	1.0	0.6	0.6	0.3	1.0	0.6
<i>T. trifurca</i>		5.0	6.3	6.0	4.0	4.6	7.6	6.6	4.6	6.6	7.3	4.0	4.3	3.0
<i>T. undulosa</i>		2.0	3.6	2.0	0.6	2.3	2.3	1.6	3.0	3.3	5.0	3.0	1.6	2.6
<i>Thalassiothrix longissima</i>		1.0	1.0	1.0	1.6	1.3	1.3	2.0	0.6	1.0	1.3	1.0	1.3	0.6
<i>Xanthopyxis ovalis</i>		0.6	-	0.3	-	-	-	-	0.6	-	-	-	-	-
FRESH WATER SPECIES		0.3	1.0	-	-	-	-	-	-	-	-	-	-	-

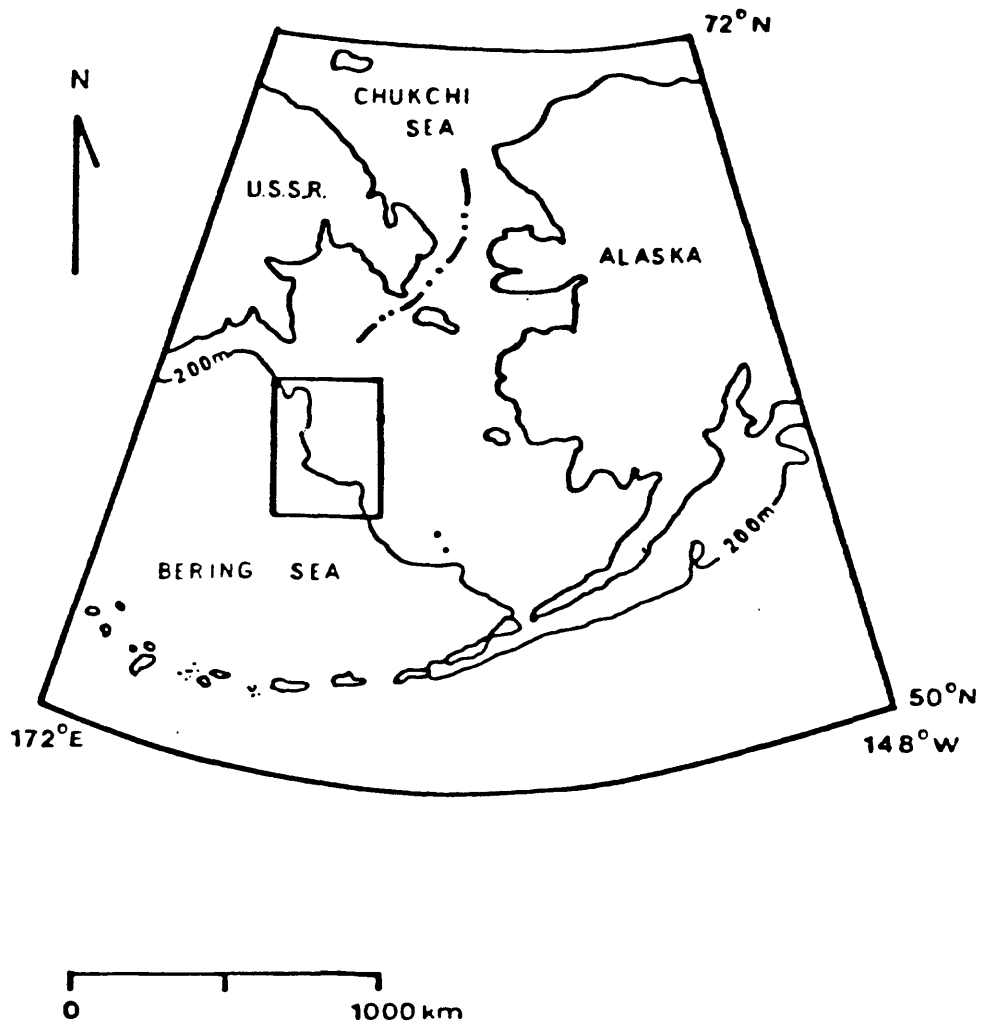


Figure 33. Index map of the Navarin Basin Province, Bering Sea.

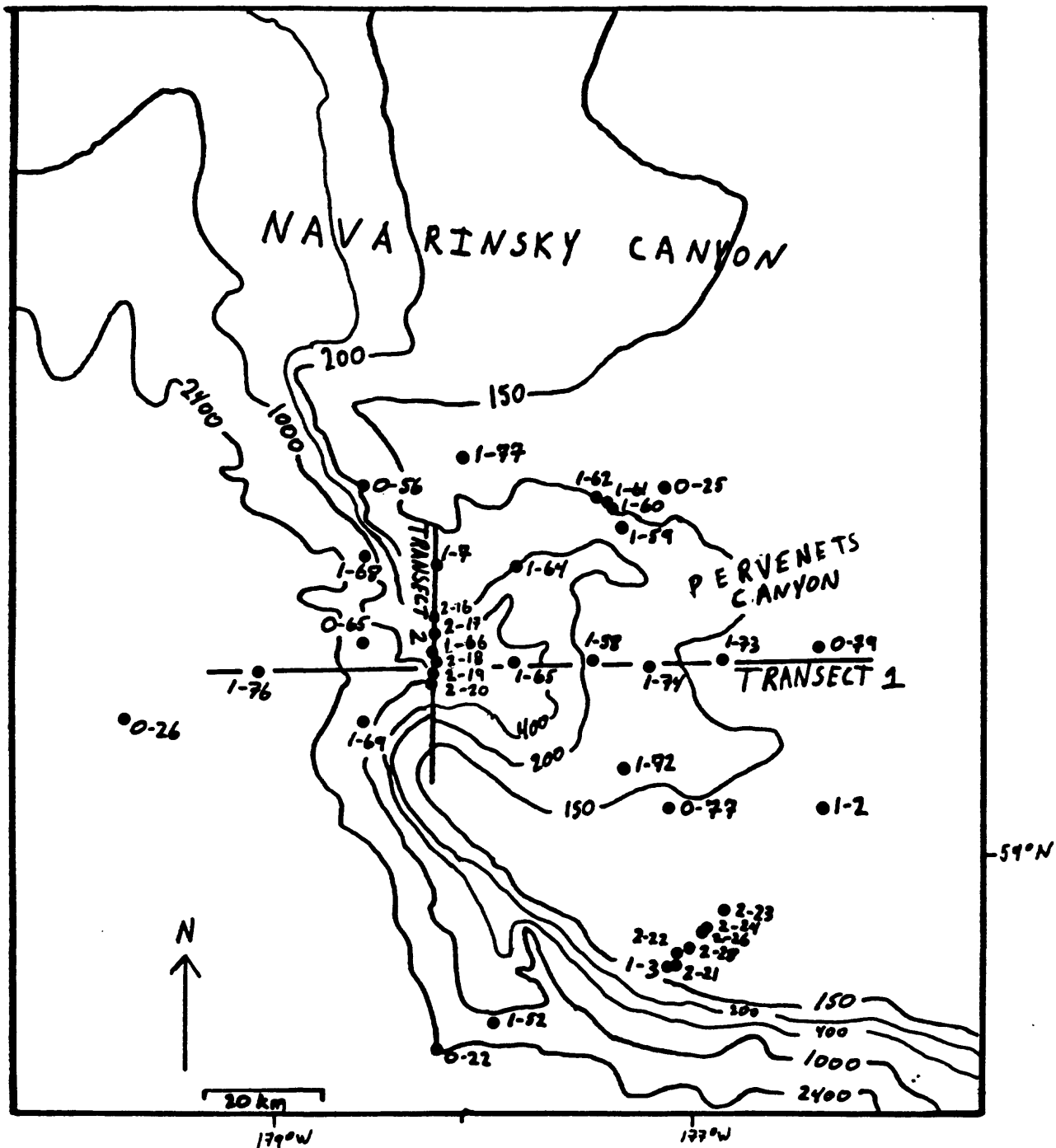


Figure 34. Location of surface samples collected from Pervenets Canyon (10 - 1980; 1 - 81; 2 = 82).

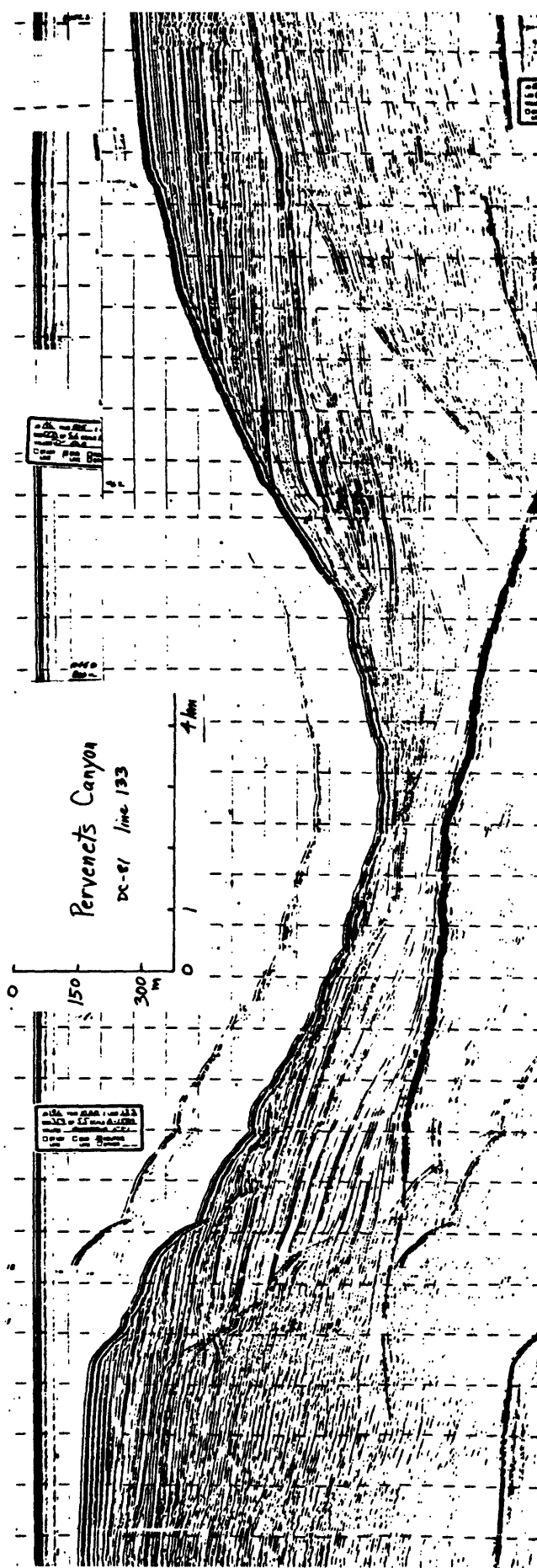


Figure 35. Seismic reflection profile across Pervenets Canyon showing surface exposures of stratigraphically older reflectors. Line 33, DC4-81-BS/NB. See Fig. 47, transect 2 for profile location.

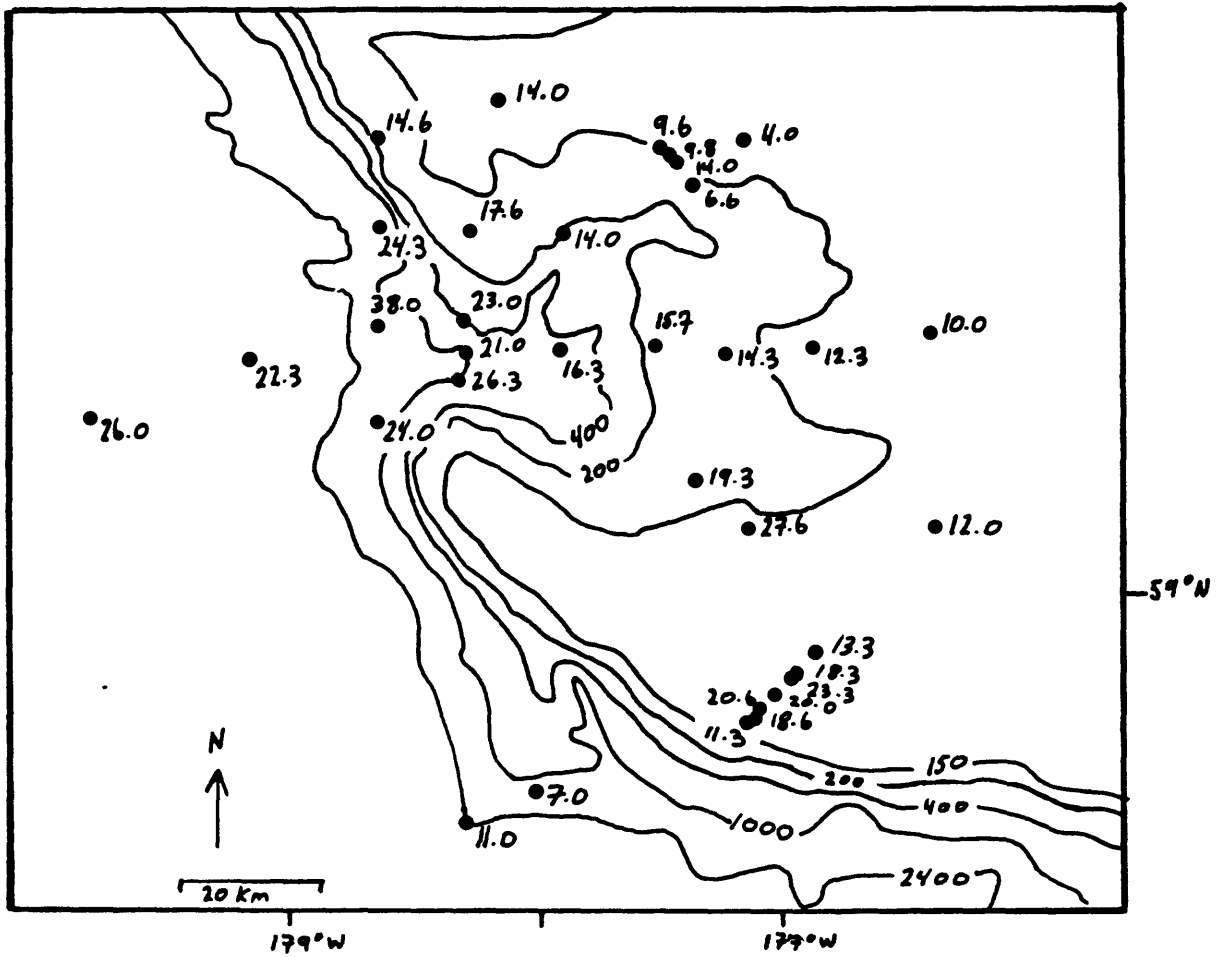


Figure 36. Distribution of *Denticulopsis seminae* in the surface sediments (values are in percent).

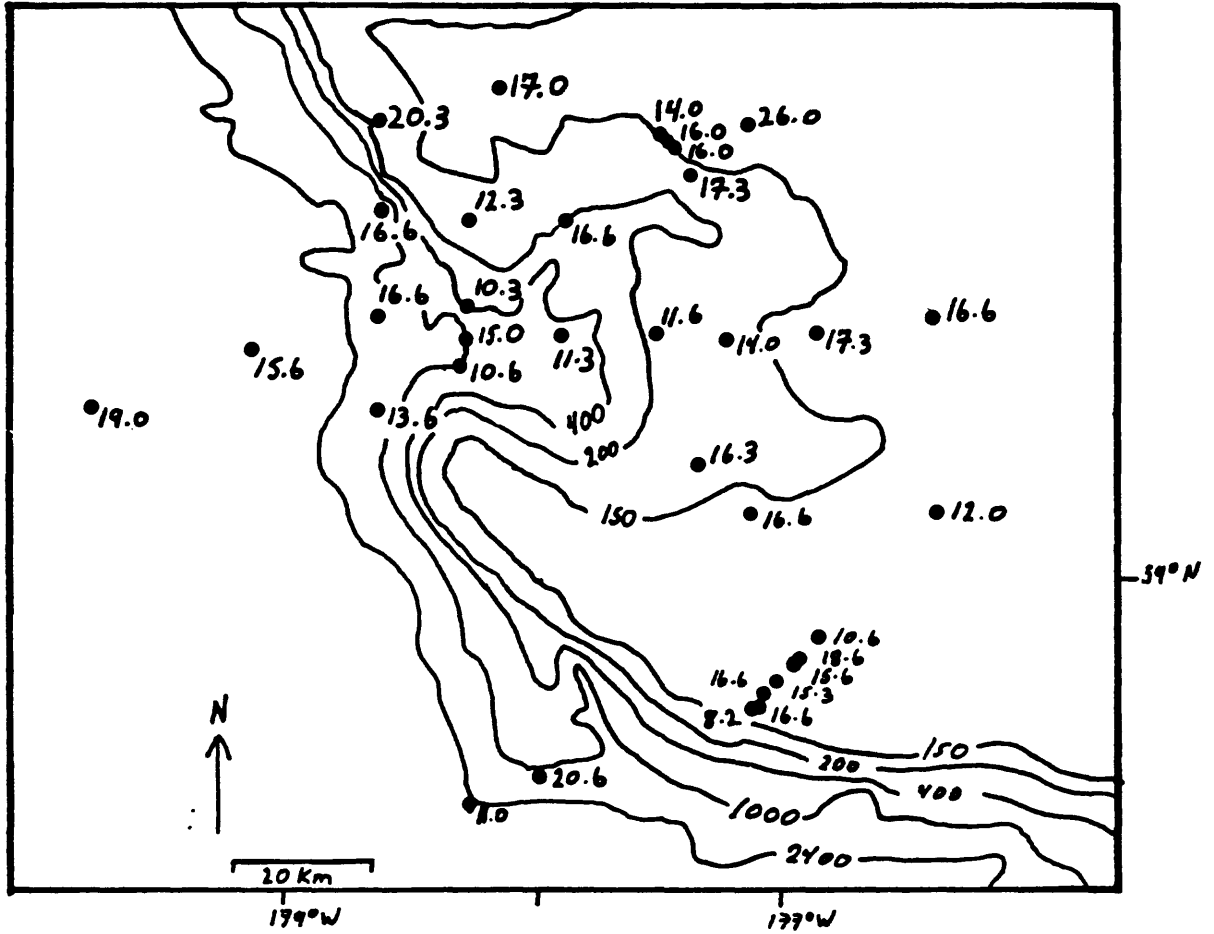


Figure 37. Distribution of *Nitzschia grunowii* in the surface sediment (values are in percent).

CHAPTER 11: ASPARTIC ACID GEOCHRONOLOGY OF MOLLUSCS

by

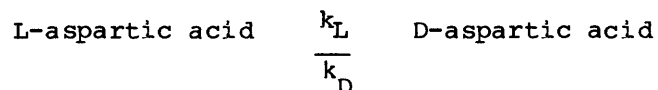
David J. Blunt and Keith A. Kvenvolden

INTRODUCTION

This report considers relative and absolute ages of fossil molluscs from the Navarin Basin Province, Bering Sea, as estimated by the method of amino-acid geochronology. Blunt and Kvenvolden (1981) first reported leucine geochronology of fossil molluscs from the Navarin Basin province. In the present study, aspartic acid is used for the purpose of establishing the age of fossil molluscs. The location of cores containing molluscs investigated in this study include both shelf and slope environments (Fig. 38).

THEORY

Individual amino acids that are no longer being biologically reproduced in the protein of shell matrix undergo a stereochemical change from the L-enantiomeric to a mixture of the L- and D-enantiomeric configurations during natural hydrolysis. The process of interconversion of enantiomers is called racemization and takes place over geologic time. The kinetics of racemization can be expressed as a reversible first-order reaction:



where k_L and k_D are the respective reaction rate constants for the L- and D-aspartic acid enantiomers. The integrated rate expression for the racemization reaction as derived by Bada and Schroeder (1972) is:

$$\ln \left(\frac{1 + D/L}{1 - D/L} \right) - \ln \left(\frac{1 + D/L}{1 - D/L} \right)_{t=0} = 2kt \quad (1)$$

where k is the racemization rate constant, D/L is the ratio of D- and L-aspartic acid enantiomers, and t is time. The logarithmic term at $t = 0$ is evaluated by measuring the D/L value obtained from modern specimens. Aspartic acid has a D/L value of about 0.06 in modern molluscs (Kvenvolden and others, 1980; Blunt, unpublished data).

RESULTS

Fossil molluscs recovered from the Bering Sea have been analyzed for aspartic acid D/L values by the method of Kvenvolden and others (1979). Further characterization of the amino acid content in some of the molluscs is reported by Blunt and Kvenvolden (1981). Twenty-four specimens from ten genera of mollusc (nine pelecypods and one gastropod, *Neptunea*) are reported on Table 13. These specimens occur within the top two meters of the sedimentary column. The aspartic acid values range from 0.06 in *Panomya* (DC-5-80, G-

71) to 0.43 in Neptunea (DC-5-80, G-98). Radiocarbon analyses of organic carbon in the bulk sediments range from 7,500 to 33,990 years.

DISCUSSION
Relative Age

Relative ages for the same genera of mollusc are inferred by the order of extent of aspartic acid racemization (column six on Table 11). Older fossils have progressively larger D/L values. For example, Macoma of DC-4-80 G-6 has an aspartic acid D/L value of 0.07 at 10 cm depth, whereas, Macoma of DC-5-80 G-44 has an aspartic acid D/L value of 0.23 at 203 cm depth. Yoldia from DC-3-81 V.V.-75 and DC-5-80 G-66 has aspartic acid D/L values that range from 0.07 at 0.2 cm to 0.30 at 60 cm, respectively.

In several instances, however, samples with similar D/L values occur at quite different sediment-depths. For example, Macoma specimens from DC-3-81 G-105 and DC-2-81 G-31 have aspartic acid D/L values of 0.14 and sample depths of 100 cm and 38-39 cm, respectively. Specimens of Yoldia from DC-5-80 G-26 and DC-5-80 G-66 have D/L values and depth relationships of $0.23 \pm .01$ at 223-230 cm and 0.30 at 60 cm, respectively. Possible explanations for samples having relatively high D/L values and shallow sample depths are: 1) specimens may have been reworked; 2) sediment accumulation rates may be different at the sites.

Absolute Ages

Absolute ages of specimens are determined with equation 1, the expression of linear first-order racemization kinetics. Samples which have radiocarbon ages measured immediately next to them are used for the calculation of a calibrated rate constant (Bada and Protoch, 1973). The measured aspartic acid D/L value, radiocarbon age and correction at $t = 0$ are inserted into equation (1), and the equation is solved for k , the calibrated rate constant. The calibrated rate constant represents the integrated temperature history of the mollusc over the radiocarbon span of time. A calibrated rate constant cannot be calculated for Macoma, because radiocarbon ages are not available adjacent to these specimens. Calibrated rate constants for four genera of mollusc are:

<u>Nuculana</u>	$k_{asp} = 1.53 \pm 0.30 \times 10^{-5} \text{ yr}^{-1}$
<u>Neptunea</u>	$k_{asp} = 9.69 \times 10^{-6} \text{ yr}^{-1}$
<u>Yoldia</u>	$k_{asp} = 1.29 \times 10^{-5} \text{ yr}^{-1}$
<u>Clinocardium</u>	$k_{asp} = 1.90 \times 10^{-5} \text{ yr}^{-1}$

These rate constants permit age estimations to be made for other specimens of the same genera that lack radiocarbon age control (Table 11). The age of Nuculana in G-26 from DC-5-80 is calculated to be 22,000 years by this method. This value is in agreement with the range of 10,880 to 33,990 years based on radiocarbon dates that bracket an erosional surface close to where the Nuculana was recovered. Yoldia from the same interval in G-26 gives an age of 14,000 years which also is in agreement with the radiocarbon range of 10,880 to 33,990 years. In core G-42 from DC-5-80 Clinocardium at 97 cm has an age of 8,000 years which is in general agreement with the radiocarbon date of 13,650 at 170-183 cm depth. Neptunea from DC-3-81 G-80 has a calibrated age of 21,000 years. The Neptunea from DC-5-80 G-98 has an age of 41,000

years at a depth of 140 cm. This is the oldest sample measured in this investigation.

SUMMARY

Aspartic acid enantiomeric ratios were used to establish the age of five mollusc samples collected from sediment cores from the Navarin Basin Province. These samples range in age from 8,000 to 41,000 years old. In general the ages given by the amino acid method agree with radiocarbon dates.

REFERENCES

- Bada, J. L. and Protsch, R., 1973, Racemization reaction of aspartic acid and its use in dating fossil bones: Proceedings of the National Academy of Science, v. 70, p. 1331-1334.
- Bada, J. L. and Schroeder, R. A., 1972, Racemization of isoleucine in calcareous marine sediments: kinetics and mechanism: Earth and Planetary Science Letters, v. 15, p. 223-231.
- Blunt, D. J. and Kvenvolden, K. A., 1981, A preliminary report on amino acid diagenesis in fossil mollusks recovered from the Navarin Basin Province, Bering Sea: in Carlson, P. R. and Karl, H. A. (eds) Seafloor Geologic Hazards, Sedimentology, and Bathymetry: U.S. Geological Survey Open-File Report 81-1217, p. 138-149.
- Kvenvolden, K. A., Blunt, D. J., and H. E. Clifton, 1979, Amino acid racemization in Quaternary shell deposits at Willapa Bay, Washington: Geochimica Cosmochimica, Acta, v. 43, p. 1505-1520.
- Kvenvolden, K. A., Blunt, D. J., McMenamin, M. A., and Strahan, S. E., 1980, Geochemistry of amino acids in shells of the clam Saxidomus; in Douglas, A. G., and Maxwell, J. R. (eds), Advances in Organic Geochemistry 1979: Pergamon Press, Oxford, p. 321-332.

Table 11.--Summary of aspartic acid D/L values in molluscs from the Navarin Basin Province.

Specimen ¹	Cruise ²	Station	Core No. ³	Depth (cm)	D/L	Age	¹⁴ C	Comment ⁵
<u>Macoma</u> sp.	DC-4-80	3	G-6	10	0.07			
<u>Macoma</u> sp.	DC-3-81	58	G-62	18	0.07			
<u>Macoma</u> sp.	DC-5-80	47	G-59	13-14	0.08			
<u>Macoma calcarea</u>	DC-3-81	95	G-105	100	0.14		8,385 ± 310	160-190 cm
<u>Macoma</u> sp.	DC-2-81	28	G-31	38-39	0.14		8,815 ± 355	160-190 cm
<u>Macoma brota</u>	DC-5-80	49	G-62	214-220	0.21			
<u>Macoma</u> cf. <u>M. obliqua</u>	DC-5-80	34	G-44	203	0.23		14,980 ± 110	125-145 cm
<u>Nuculana fossa</u>	DC-2-81	22	G-24	205	0.23			
<u>Nuculana radiata</u>	DC-5-80	39	G-50	219-230	0.23			
<u>Nuculana fossa</u>	DC-5-80	34	G-44	125	0.24	*	14,980 ± 110	125-145 cm
<u>Nuculana fossa</u>	DC-5-80	32	G-42	170	0.30	*	13,650 ± 100	170-183 cm
<u>Nuculana radiata</u>	DC-5-80	20	G-26	223-230	0.30	22,000	10,880 ± 80 to 33,900 ± 610	188-222 cm 235-260 cm
<u>Neptunea</u> sp.	DC-3-81	76	G-80	164	0.26	21,000		
<u>Neptunea neptunea</u>	S-4-76	-	G-116	90-98	0.33	*	29,197 ± 320	90-98 cm on shell ⁶
<u>Neptunea</u> sp.	DC-5-80	79	G-98	140	0.43	41,000		
<u>Yoldia myalis</u>	DC-3-81	71	V.V.-75	0-2	0.07			
<u>Yoldia myalis</u>	DC-5-80	20	G-26	223-230	0.23 ± .01	14,000	10,880 ± 80 to 33,990 ± 610	188-222 cm 235-260 cm
<u>Yoldia myalis</u>	DC-5-80	53	G-66	60	0.30	*	19,370 ± 160	65-84 cm
<u>Clinocardium</u> sp.	DC-2-81	29	G-32	220	0.20	*	7,500 ± 305	160-190 cm
<u>Clinocardium nuttallii</u>	DC-5-80	32	G-42	97	0.21	8,000	13,650 ± 100	170-103 cm
<u>Cyclocardia crebricostata</u>	DC-5-80	21	G-28	8	0.10			
<u>Mya truncata</u>	DC-5-80	19	G-25	173	0.21			
<u>Serripes groenlandicus</u>	DC-2-81	36	BC-41	0-2	0.08			
<u>Panomya</u> sp.	DC-5-80	60	G-71	1-6	0.06			

¹ Fossil molluscs are identified by L. Marincovich, USGS, Menlo Park

² DC, NOAA Research Vessel DISCOVERER; S, USGS Research Vessel SEA SOUNDER

³ G, gravity core; V.V., Van Veen sampler; B.C., box core

⁴ ASP, D-aspartic acid/L-aspartic acid

⁵ Depths of radiocarbon analysis differ from depths of mollusc occurrence

⁶ Sample from southern Bering Sea, radiocarbon analysis on shell carbonate (Jim Gardner, personal communication)

* Sample used for determination of calibrated rate constant for amino acid dating

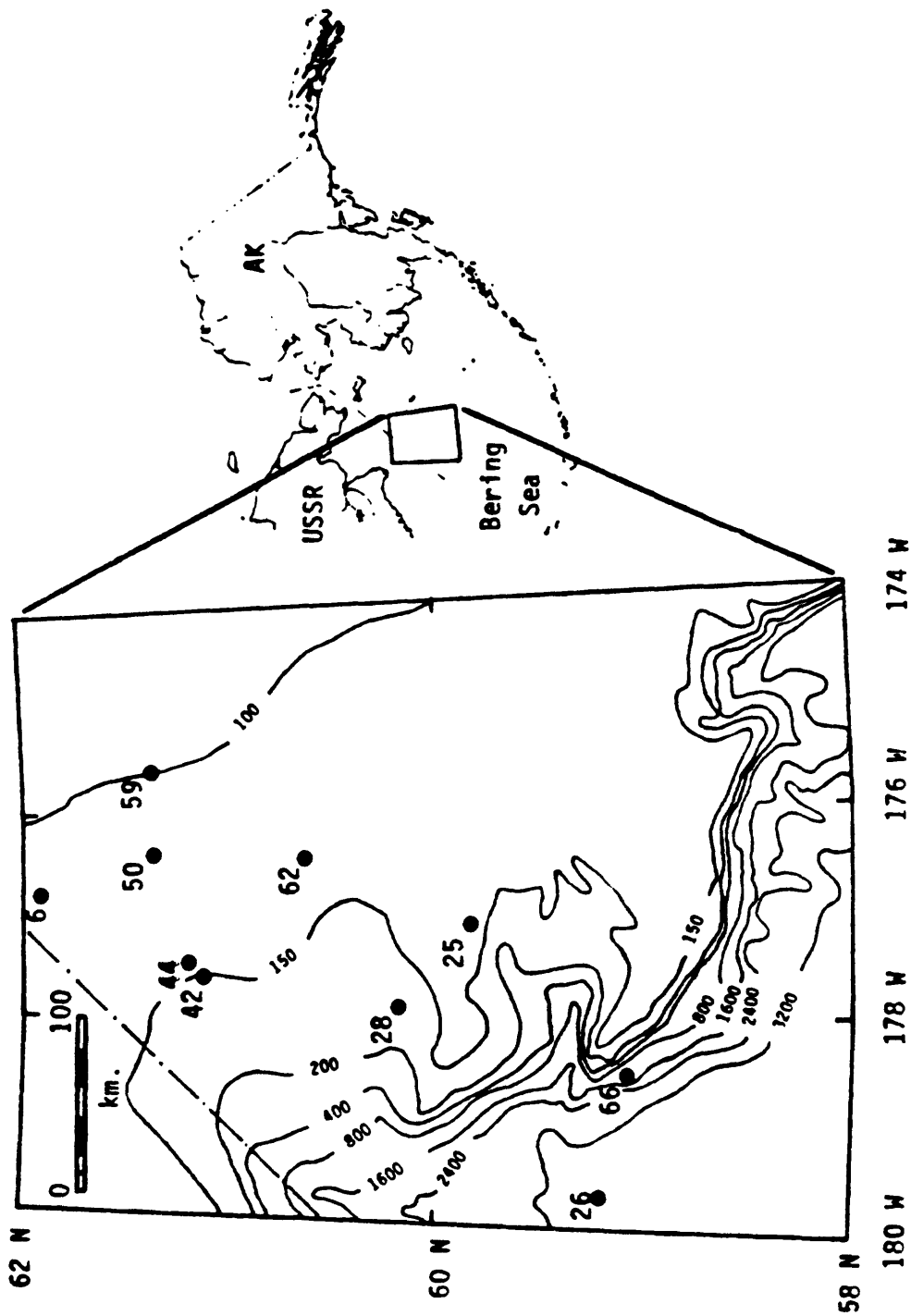


Figure 38. Location of gravity cores in the northern Navarin Basin province where fossil mollusks were studied. Bathymetry is in meters.